The Dissertation Committee for Pedro Antonio Serigos Certifies that this is the approved version of the following dissertation:

Bayesian Estimation of Finite Mixture Roughness Model

Committee:

Jorge A. Prozzi, Supervisor

Zhanmin Zhang

Robert B. Gilbert

Peter Müller

Magdy Mikhail

Bayesian Estimation of Finite Mixture Roughness Model

by

Pedro Antonio Serigos, Ingeniero, M.S.E., M.S.Stat.

Dissertation

Presented to the Faculty of the Graduate School of

The University of Texas at Austin

in Partial Fulfillment

of the Requirements

for the Degree of

Doctor of Philosophy

The University of Texas at Austin

December 2016

To my daughter Delfina,

to my wife Jacqueline,

to my parents Alejandra and Pedro,

and to my brothers Facundo and Miguel

Acknowledgements

I would like to thank my advisor Dr. Jorge A. Prozzi first for his continuous guidance and support throughout my master's and doctoral studies. His trust and advice were key to reach my academic goals and his invaluable lessons had a great impact on my formation as a researcher and as an engineer that will last throughout my career.

I would also like to thank Dr. Peter Müller, whose suggestions were essential to accomplish the technical objectives of my dissertation; Dr. Magdy Mikhail, whose inputs were fundamental to define the practical applications of my research; and to the other committee members, Dr. Zhanmin Zhang and Dr. Robert B. Gilbert, whose comments helped significantly to strengthen my dissertation.

I would like to acknowledge the Texas Department of Transportation and the Office of the Assistant Secretary for Research and Technology of the United States Department of Transportation for providing financial assistance.

In addition, I would like to thank Dr. Andre de Fortier Smit and Dr. Michael R. Murphy, with whom I had the pleasure to work with on different research projects during my graduate studies, and whose advice and guidance were very valuable to my education. I would also like to thank the many friends I made at UT Austin, who made me feel at home and helped me enjoy this journey far from my hometown.

Lastly, I'd like to especially thank my wife, Jacqueline, whose love and patience help me get through difficult times and was always by my side to enjoy the good times.

Bayesian Estimation of Finite Mixture Roughness Model

Pedro Antonio Serigos, Ph.D.

The University of Texas at Austin, 2016

Supervisor: Jorge A. Prozzi

Highway infrastructure systems provide a crucial service to society and constitute a major asset with a significant maintenance and rehabilitation cost, highway pavements comprising a major component of the total cost. The increasing need for greater capital investment, in the face of ever-decreasing federal funding to maintain highway infrastructure, highlights the importance of developing and implementing effective methods for managing pavement assets.

A key for the success of pavement management is to accurately predict the future condition of the pavements in the network. This dissertation proposes a mixture of regression models to capture the systematic differences in pavement performance not explained by variables typically available in pavement management systems. This approach assumes that the heterogeneous pavement performance, which results from the combined effect of the several unobserved factors and interactions, is manifested through a finite number of latent groups. The estimation of the proposed model allows for defining the parameters of the group-specific models while clustering the observations into the latent groups. The insights provided by the model-based clustering of performance data can also be incorporated into the design of maintenance and rehabilitation strategies, as clustering of sections according to their deterioration rate allows for identifying pavements in the network with structural deficiencies and tailoring actions in response.

The gain in model fit, along with the insights provided by the proposed methodology for the unsupervised model-based clustering of pavement performance was demonstrated using experimental data. In addition, the proposed mixture model was applied to develop a Bayesian pavement roughness model specified with variables from an existing pavement management system, plus climatic and preventive maintenance variables, and estimated using nationwide field data from the Long-Term Pavement Performance program. Lastly, the developed roughness mixture model was calibrated for Texas pavement conditions by combining both the nationwide data and data extracted from the processing and merging of various Texas Department of Transportation databases. The proposed methodology produces accurate predictions of the progression of roughness as well as robust estimates of the factor effects driving the deterioration of pavements, which, ultimately, lead to a more efficient management of highway assets.

Table of Contents

List of Tables

List of Figures

Chapter 1: Introduction

MOTIVATION

Transportation infrastructure systems provide a crucial service to society and constitute a major asset that significantly benefits local economies (Queiroz et al., 1994). Highway infrastructure assets impose a significant maintenance and rehabilitation (M&R) cost on transportation agencies, with highway pavements comprising a major component of the total cost. A challenge currently faced by local, state and federal transportation agencies is the constantly increasing traffic demand, combined with a slower increase in the availability of funds for the maintenance of the transportation infrastructure. For instance, in 2013, the American Society of Civil Engineers (ASCE) reported that 32% of America's highway infrastructure was in poor or mediocre condition and that the annual capital investment should increase from the current $91 billion to $170 billion in order to reach the proposed pavement ride quality goals for 2028 (ASCE, 2013). The increasing need for greater capital investment, in the face of ever-decreasing federal funding for transportation, highlights the importance of developing and implementing effective methods for managing transportation assets.

Given the large scale of the elements comprising the infrastructure network, the huge amount of data required to monitor the state of the infrastructure health and quality of service, and the significant M&R costs, management of the highway network presents a challenging decision problem with important implications. An infrastructure management system comprises a series of engineering and economic processes and techniques for the systematic management of the infrastructure assets making the best use of the limited available resources (Hudson et al., 1997). For instance, pavement management systems

(PMS) coordinate the processes involved in the planning, design, construction, and maintenance of pavements with the objective of optimizing the use of the available economic resources so that the utility of the highway network is maximized. PMSs employ pavement performance models to predict the future condition of the pavement network and, with that, evaluate alternatives for deciding what and when to apply possible M&R strategies, taking into account the budget, policies, and goals defined by the administration.

Pavement performance models are a key component of a PMS as their predictions directly affect decision-making processes. The performance of a pavement structure throughout its service life is affected by several factors that are uncertain due to their inherent variability or poor quality control, such as traffic, weather, and material properties. The number of variables available in PMSs for predicting the future condition of pavements is rather limited due to practical and budget constraints. For instance, network-level management databases usually do not contain information related to the materials and mixture design of each pavement section, which are expected to be significant factors in explaining the variation in pavement performance response. In the United States, PMS often do not even contain structural information. Missing relevant explanatory variables limits the model's ability to capture behavioral differences across pavement sections and time. These sources of errors, missing data, along with inaccuracies in the assessed pavement condition data (Serigos et al., 2014a, 2015 and 2016a), result in inadequate prediction of the highway infrastructure's future condition, which lead to sub-optimal budget or to a misallocation of funds (Ng et al., 2011; Saliminejad and Gharaibeh, 2013; and Serigos et al., 2014b).

Pavement performance models are usually estimated using experimental panel data —i.e., data collected from an experiment where multiple pavement sections (i.e, sectional units) are observed throughout time, such as the data collected for the American

Association of State Highway Officials (AASHO) Road Test (HRB, 1962). The simplest form of a model estimated using panel data would assume that the effect of the explanatory variables in the model does not vary across sectional units. When this assumption is not realistic, the systematic differences between the pavement sections response due to unobserved factors result in larger prediction errors and bias in the estimated parameters. This methodological issue is referred to as heterogeneity, and its consequences can be reduced by adjusting the specification of the model in order to properly capture the unobserved variation in the effect of the explanatory variables.

Heterogeneity is a critical issue to account for when estimating models from panel datasets and has been reported as significant when estimating pavement performance models by a number of studies in the literature, such as Madanat et al. (1997), Prozzi (2001), Archilla (2006), and Zhang and Durango-Cohen (2014). Furthermore, Chu and Durango-Cohen (2008) performed an empirical comparison of state-of-the-art pavement performance models using American Association of State Highway Officials (AASHO) Road Test data and concluded that the most significant improvements were achieved when accounting for heterogeneity. The AASHO Road Test consisted of a controlled experiment; therefore, the impact of not accounting for heterogeneity is expected to be much greater when estimating field data from network-level surveys, as there are more unobserved factors and interactions.

The most frequently used approaches to account for heterogeneity in pavement performance found in the literature consist of fixed and random effects models, which capture variation of effects at the individual level through a variable intercept and assume homogeneity of effects across sectional units for the explanatory variables. These approaches are methodologically sound and produce better estimates of the model parameters, as compared to when the potential heterogeneous performance across sectional

units (i.e., complete pooling of the data) is neglected. On the other hand, methods that characterize the variation of effects at the individual level offer more limited insights and less predictive power than other approaches that model heterogeneity at the group level.

The research conducted in this dissertation explores and implements advanced statistical methods for developing pavement performance models that characterize heterogeneous effects of the explanatory variables through model-based clustering of data. The proposed methodology is applied to the development of a pavement roughness model that combines nationwide and Texas data. In addition, the estimation of this model allows for the assessment of the effectiveness of preventive maintenance (PM) of flexible pavements, based on PM's impact on the progression of roughness using field data.

RESEARCH GOAL AND OBJECTIVES

The main goal of this research is to investigate advanced statistical methodologies to develop robust pavement performance models for network-level management applications. Improved modeling of pavement performance allows for more efficient planning and design of preservation strategies, which ultimately results in significant economic benefits and improved agency accountability.

The two major objectives of this research consist of:

1. Exploring and evaluating different Bayesian techniques for modeling group-level heterogeneous pavement responses not captured by variables commonly collected in pavement condition surveys, and;
2. Implementing the selected statistical methodology to develop a pavement roughness model estimated with field data extracted from pavement management information systems.

The modeling techniques evaluated to accomplish the first objective aim to overcome the methodological limitations of the approaches commonly adopted for modeling pavement performance. The proposed methodologies capture heterogeneity in pavement performance through the segmentation of data across cross-sectional units. These approaches include:

- a hierarchical model specification that model the heterogeneous effect of certain variables segmenting the population of pavement sections according to an observed factor, and
- a mixture model specification that captures systematic differences in pavement performance due to heterogeneity in effects and unobserved factors by clustering the observed data in an unsupervised manner.

For the purpose of comparison, these techniques are evaluated through the estimation of a high-quality experimental dataset and model specification that have been widely used by researchers for the demonstration of other modeling methodologies. The adopted information criterion for comparing among the different model specifications balances fit and generality. The significant gain in model fit, along with the additional insights and capabilities offered by the mixture model specification, make that specification the preferred approach to develop the pavement roughness model described as the second objective of this research.

The purpose of developing the pavement roughness mixture model as part of the second objective is two-fold:

- to accurately predict the increment in International Roughness Index values between data collection periods using variables available in the Texas Department of Transportation (TxDOT) management systems; and

- to unveil the underlying intricate relationships between site-specific pavement properties and the progression of roughness, as well as to assess the effectiveness of applying PM treatments.

The estimated pavement roughness mixture model is first estimated using nationwide pavement data and then calibrated for Texas by combining both the nationwide dataset and TxDOT data. For this, a dataset containing more than twenty years of field M&R works-related information and performance measurements from in-service flexible pavements in Texas is developed as part of this dissertation.

DISSERTATION LAYOUT

The present chapter provides a brief statement of the problem and motivations of the research carried out in this dissertation, as well as a description of the research goals and objectives.

The first section of Chapter 2 covers the main definitions and concepts of pavement management, which include a description of the major components and goals of PMSs, the types of surface condition data typically collected, and the pavement models commonly implemented in PMSs, such as the ones adopted in TxDOT's PMS. In addition, this section includes a literature review on statistical methods to address unobserved heterogeneity in pavement management data. The second part of Chapter 2 includes a description of the main objectives and techniques for pavement PM, along with a review of research efforts and methodologies implemented to assess the effectiveness of PM treatments on flexible pavement. The last part of Chapter 2 provides a methodological background and literature review of the modeling techniques proposed in this dissertation. This section includes the main concepts of Bayesian estimation of mixture models as well as a description of the

Markov chain Monte Carlo algorithms and converging criteria used for estimating the models proposed in this dissertation.

Chapter 3 contains the implementation and evaluation of two proposed modeling techniques to achieve the goals of this research. The first section of Chapter 3 describes the main characteristics of the AASHO Road Test and provides descriptive statistics of the analyzed dataset. The second section describes the basic form of the adopted pavement performance model and the expected effect of the explanatory variables. The last three sections of Chapter 3 report the Bayesian specification, results, and interpretation of the estimated models with complete pooling, hierarchical specification, and mixture specification.

Chapter 4 covers the development of a pavement roughness mixture model estimated with field data. The first section of this chapter is divided in two parts: the first covers the processing and descriptive statistics of the Long-Term Pavement Performance (LTPP) dataset used for the analyses, which includes pavements located throughout most continental states in the U.S. and some provinces in Canada; the second describes the steps carried out and criteria adopted to process different databases from various TxDOT management information systems and other sources. The second and third parts of Chapter 4 describe the proposed specifications and discuss the results from the estimation of the roughness mixture model first estimated using the nationwide dataset, and subsequently estimated combining nationwide and Texas-specific data. The analyses in this chapter also include an assessment of the effect of PM treatments on the progression of roughness.

Lastly, Chapter 5 contains the conclusions and recommendations from the estimated models and analyses conducted to achieve the objectives of this research, and discusses potential implementations of the proposed methodology in different areas of pavement management.

Chapter 2: Background on Pavement Management and Methodology

The first section of the present chapter provides background information on general pavement management concepts, definitions, and practices. The second section contains the methodological background of the statistical techniques proposed in this dissertation to model group-level heterogeneity in pavement performance data.

PAVEMENT MANAGEMENT

This section is divided into four main parts. The first part defines the major goals and components of pavement management and pavement management systems (PMS). The second part covers the indexes and measuring methods typically used to assess pavement condition in the highway networks. The third part reviews pavement performance modeling as well as previous efforts to explain unobserved heterogeneity in performance models. The last part of this section outlines Preventive Maintenance (PM) practices for flexible pavements and reviews the approaches used to assess the effectiveness of PM treatments.

Pavement Management Goals and Components

Pavement management comprises processes and methodologies for the maintenance and operation of pavement structures, with the goals of lengthening pavement life cycles and making the best use of increasingly limited resources. A PMS connects the processes involved in pavement management, unifying them and allowing for their systematic execution. The systematization of the process imparts the important benefit of increasing the consistency of solution selection and application, serving as a valuable decision support system for the decision-maker responsible for the network or facility. The implementation of a PMS is intended to transform the decision-making process into a more

rational and consistent information-based process that favors the implementation of long-term policies and strategies (Haas and Hudson, 1978).

In addition to the benefits associated with the implementation of a decision support system, other benefits resulting from the effective application of PMS processes include economic benefits, more integrated management practices and databases across divisions within the agency, and increased agency accountability, among others. Unfortunately, although the qualitative benefits of implementing a PMS have been widely recognized by pavement engineers for years, few studies in the academic literature have estimated these benefits quantitatively. In a rare example of a quantitative analysis, Smadi (2004) used condition data from the Iowa Department of Transportation's interstate network to perform a before-and-after analysis, and estimated the economic benefit of implementing a PMS as $5 million dollars over 5 years

In terms of structure, the two most important components of a typical PMS are an Attributes Database, with its associated Relational Database Management System, and a Model Base (Zhang et al., 1999). The Attribute Database has the function of storing and retrieving the data that will be used in the analyses. The data contained in this database describes the sections and elements of the pavement network. The Model Base includes all the models used by the system to accomplish the PMS's main objectives (from Haas and Hudson, 1978):

- Evaluation of the pavement network performance: the system uses indexes to determine the current condition of the pavement sections.
- Prediction of the future performance: mechanistic and empirical models are used to predict the future condition throughout time of the pavement sections in the network.

- Prioritization of candidate projects: these models define priorities to rank the candidate projects, taking into account the available budget and other constraints.
- Estimation of required budget: the future budget is estimated in order to maintain the desired level of service of the pavement network.

The diagram in Figure 2.1 illustrates the process flow of the main activities and components comprising a generic infrastructure management system, as defined by the Federal Highway Administration's (FHWA) Asset Management Primer (1999). The research work carried out for this dissertation impacts the performance forecasting step (the third box from the top of Figure 2.1), the outcomes of which have a direct influence on the subsequent processes and, therefore, on the overall success of the PMS's strategies and results.

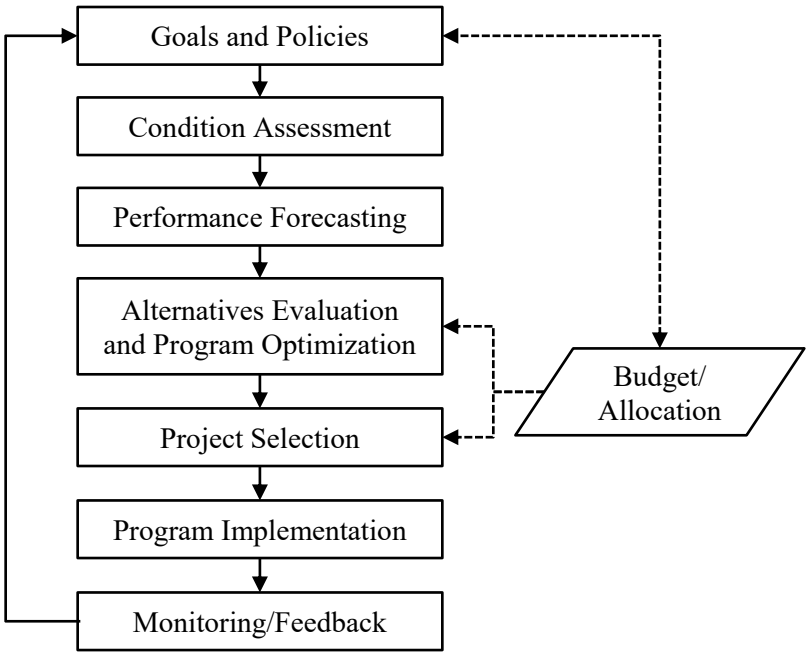

Figure 2.1: Process flow of a generic infrastructure management system (FHWA, 1999).

PMS processes can be implemented for either network- or project-level applications. At the network level the goals and objectives are set for groups of sections or projects, whereas at the project level the objectives are defined for specific sections or elements of the network. Examples of factors affecting PMS processes at the network level could include the agency's policies and goals or personnel availability, whereas factors affecting at the system at a project level are standards and specifications, among others.

Data needs differ between network- and project-level applications as well. While the data required for managing a project may include detailed data, such as mixture design, cost, quality assurance, and quality control information, conducting processing and analysis at that level of detail for the entire network might be unnecessarily demanding and expensive (Haas and Hudson, 1978; Flintsch and McGhee, 2009). The pavement performance models developed in this dissertation were estimated using data collected for network-level management applications. Therefore, the number of explanatory variables available was small in relation to the number of factors affecting the behavior of pavements, which is an inherent limitation of PMS performance models.

Pavement Condition Assessment

The condition of the pavement sections in the network is typically evaluated through the measurement of different surface distresses and surface roughness. Surface distress assessment provides information regarding the level of damage in the structural layers of the pavement whereas roughness is associated with the level of comfort that the users experience when driving on the road. These factors evolve with the accumulation of traffic, or time, and are characterized either individually or through aggregated indexes. A pavement structure fails once the level of one, or a combination, of these indexes surpasses defined tolerable limits. Depending on the quality of the pavement exceeding the expected

criteria, the failure of a pavement can be classified as a functional, structural, or safety-related failure. Failure criteria are usually multiple and vary across transportation agencies. For instance, a structural failure criterion for flexible pavements used by Texas Department of Transportation (TxDOT) District Engineers is defined as half an inch of surface rutting.

Pavement Surface Distresses

Several types of distresses are defined for the different pavement surfaces. For instance, the Long-Term Pavement Performance (LTPP) Visual Rater's Manual (Miller and Bellinger, 2003) defines 15 distresses for asphalt concrete (AC) surfaces, 16 for jointed concrete surfaces (JCP), and 15 for continuously reinforced concrete surfaces (CRCP). The two most important categories into which AC pavements' distresses are grouped are cracking and rutting. Cracking is usually measured linearly or by area, and it is classified according to the pattern and location of the cracks, as these two factors are indicators of the distressing mechanisms. As an example, *fatigue cracking* (also known as *alligator cracking*) refers to the presence of multiple interconnected cracks in the wheel-path areas and it is mainly caused by the repeated loading of traffic (Huang, 1993). *Rutting* is manifested by the formation of a depression in each wheel-path of the roadway, referred to as a rut, and it poses a safety risk as water ponded in these ruts increases the likelihood of wet-weather accidents due to hydroplaning (Horne and Dreher, 1963; Simpson, 2001). Other important distresses usually measured to assess the condition of pavements in the network include faulting, raveling, potholes, and bleeding. Refer to Smith et al. (1979), AASHTO (1989), or Roberts et al. (1996) for more details on the definitions and causal mechanisms of these and other surface distresses.

Pavement surface distress data have traditionally been collected manually. For example, a common manual method to assess rutting consists of measuring the maximum

distance between a reference straight line, which connects the two maximum points on either side of the rut, and the pavement surface using a straight-edge and a gage (ASTM E1703M-10). Manual methods are considered a reliable and inexpensive option. However, they involve time-consuming processes and require the use of traffic control, making their use inefficient for network-level data collection. These inherent limitations—the subjectivity associated with manual measurements and the small percentage of the network that can reasonably be sampled—have motivated the development of systems for the automated measurement of distress data at high speeds (Wang, 2000; Tim and McQueen, 2004).

Nowadays, several transportation agencies use, or are transitioning to, automated distress measurement systems for collecting distress data at both the project and network level. Automated distress measurement systems offer advantages such as faster and denser data surveys using non-contact sensors, while eliminating the need for traffic control (McGhee, 2004; Wang and Smadi, 2011). However, independent studies in the literature report large measurement errors and poor reproducibility of state-of-the-practice automated systems, suggesting an urgent need for the development of quality assurance and quality control (QC/QA) standards for these systems (Wix and Leschinski, 2012; Pierce et al. 2012; Serigos et al., 2014a, 2016a).

Popular sensors commercially available for automated measurements of surface distresses include, amongst others, the National Optics Institute of Canada's Laser Crack Measuring System (Laurent et al., 2012) or WayLink's PaveVision3D Ultra (Wang et al., 2015). These sensors scan the pavement surface coordinates of contiguous transverse profiles along the travelled direction through the combination of a high-resolution laser that projects a thin line onto the pavement surface and a three-dimensional (3-D) camera that captures the line image at a specific angle (Huang et at., 2009; Wang, 2011). Typically,

these systems collect more than 1,000 points in the transverse direction and at least 3,000 profiles per second. The obtained 3-D representation of the pavement surface is then used to detect and quantify surface distresses through the use of different algorithms. Refer to Peng et al. (2015) for a review of automatic pavement crack image recognition algorithms.

Pavement Surface Roughness

Roughness on a road segment is defined as the deviations of the pavement surface from a true planar plane that affect ride quality, among other aspects (ASTM E867). An associated term commonly used in the pavement engineering field is *smoothness*, which refers to the opposite of roughness. Historically, transportation agencies have prioritized measurement of surface roughness when assessing the condition of their pavements, as it affects the level of public satisfaction. Also affected by surface roughness are the user cost (through tire wear and fuel consumptions) and surface drainage (Zaniewski and Butler, 1985; Biehler, 2009).

The two most extensively used indexes to characterize pavement riding quality have been the Slope Variance (SV) and the International Roughness Index (IRI). SV precedes the development of the IRI and it is defined as the variance of the slope values collected from the pavement's longitudinal profile. The slope values are computed for each wheel-path as the difference in elevation between consecutive points spaced every one foot. Typical measuring devices used to measure the profile coordinates for estimating the SV are the CHLOE profilometer (Yoder and Witczak, 1975) or the Dipstick profiler (Face Technologies, 2016). The main limitations of the CHLOE profilometer is its slow operating speed (3–5 mph) and the inability to capture wavelengths shorter than twelve inches. The Dipstick profiler consists of a manual method that requires traffic control.

The IRI was developed by the World Bank in 1986 (Sayers et al. 1986) and it is currently the most widely used index for characterizing pavement surface roughness. This index represents the response of a single tire on a standardized vehicle suspension (Gillespie et al., 1980) travelling the pavement surface at a speed of 50 mph. The magnitude of the roughness can be interpreted as the accumulated suspension motion over a pre-established travelled distance and it is calculated from the simulation of a quarter-car model (ASTM E1170-97) using the scanned coordinates of the pavement's longitudinal profile.

The pavement longitudinal profile used to calculate the IRI of a specific wheel-path is typically measured by an inertial profiler. An inertial profiler measures the coordinates of the longitudinal profile using an accelerometer to define the reference plane, and a laser to measure the distance from the reference plane to the pavement surface (Sayers and Karamihas, 1998). The collected profile coordinates are then processed through the application of two filters: a moving average filter to remove features described by wavelengths not included in the IRI range of frequencies and, subsequently, the quarter-car filter to compute the IRI value. IRI measurements obtained from the use of standardized inertial profilers and state-of-the-practice processing software, such as ProVal (Orthmeyer, 2007), have been reported as highly repeatable and reproducible by different studies in the literature (Guerre et al. 2012; Serigos et al., 2015).

Aggregated Pavement Condition Indexes

In order to obtain an overall assessment of the pavement surface and to unify failure criteria, a number of aggregated pavement condition indexes have been formulated as a weighted function of the different surface distresses. The weight given to each individual index reflects the relative importance attributed to the specific distress by a given agency. One such example is the Pavement Serviceability Index (PSI), developed in 1960 by Carey

and Irick as part of the American Association of State Highway Officials (AASHO) Road Test (HRB, 1962), or the Pavement Condition Index (PCI), developed by the United States Army Corps of Engineers (Shahin and Khon, 1979).

As shown in Equation 2.1 the PSI is calculated as a function of the slope variance, cracking, rutting, and patching. This index was developed to correlate the surface condition measurements to the judgment of a panel of drivers that rated the ride quality of the pavement on a five-point scale, zero being impassable and five being excellent serviceability (HRB, 1962). This rating score was called Present Serviceability Rating (PSR). Since PSR measures the ride quality of the pavement, surface roughness is the most significant factor affecting the PSI value, as reflected by a number of studies that evaluated their correlation (Haas et al., 1994; Hall and Muñoz, 1999).

$$PSI = 5.03 - 1.91\log(1 + SV) - 1.38\,RD^2 - 0.01\sqrt{C + P} \quad (2.1)$$

where,

PSI: Pavement Serviceability Index

SV: average of the slope variance in the wheel-paths

RD: average rut depth, in inches

C: total cracking, in $ft^2/1000\ ft^2$

P: total patching, in $ft^2/1000\ ft^2$

TxDOT Condition Indexes

Every year TxDOT collects pavement surface distress and roughness data throughout the more than 80,000 centerline miles (one-way direction roadbed miles) of the Texas roadway network (TxDOT, 2014a). These data are processed and summarized to assess the surface condition of 0.5-mile-long pavement sections, and the findings are

recorded in the TxDOT Pavement Management Information System (PMIS). TxDOT's PMIS contains the pavement inventory data and Model Base of TxDOT's PMIS. The collected condition data for the more than 197,000 lane miles rated are used for predicting future pavement performance, estimating and allocating budget needs, and designing maintenance and rehabilitation (M&R) strategies, among other managerial decisions (Stampley et al., 1995).

The types of surface condition data collected by TxDOT are defined in the PMIS Rating Manual protocols (TxDOT, 2009). These include eight distress types for AC surfaces, five for CRCPs, and six for JCPs, in addition to the IRI measurements specified to characterize roughness. Each surface condition measurement is used to calculate a utility value, which ranges between 0 and 1 and is computed as expressed in Equation 2.2.

$$U_i = 1 - \alpha e^{-\left(\frac{\rho}{L_i}\right)^{\beta}} \tag{2.2}$$

where,

U_i: utility value for surface condition i

L_i: level of distress or ride quality loss for surface condition i, as a percentage

α, β, ρ: utility factors

The utility factors α, β, and ρ determine the horizontal asymptote, slope, and prolongation of the utility curve. These factors are tabulated in Stampley et al. (1995) as a function of the pavement type for the distress utility curves, and as a function of both the pavement type and traffic level for the ride quality utility curves.

The utility curves for the different condition indexes allow the system to weight the impact they have on the overall condition of the pavement. For instance, the impact of shallow rutting is not as significant as the impact of alligator cracking on managerial

decisions. The lower the utility value, the higher the impact on the overall condition of the pavement. Figure 2.2 shows the utility curves of the different distresses defined for the AC pavements (with surface layer thickness between 2.5 and 5.5 inches) to illustrate their relative importance. The impact assigned to each distress and ride quality measurement was defined by TxDOT based on engineering judgement.

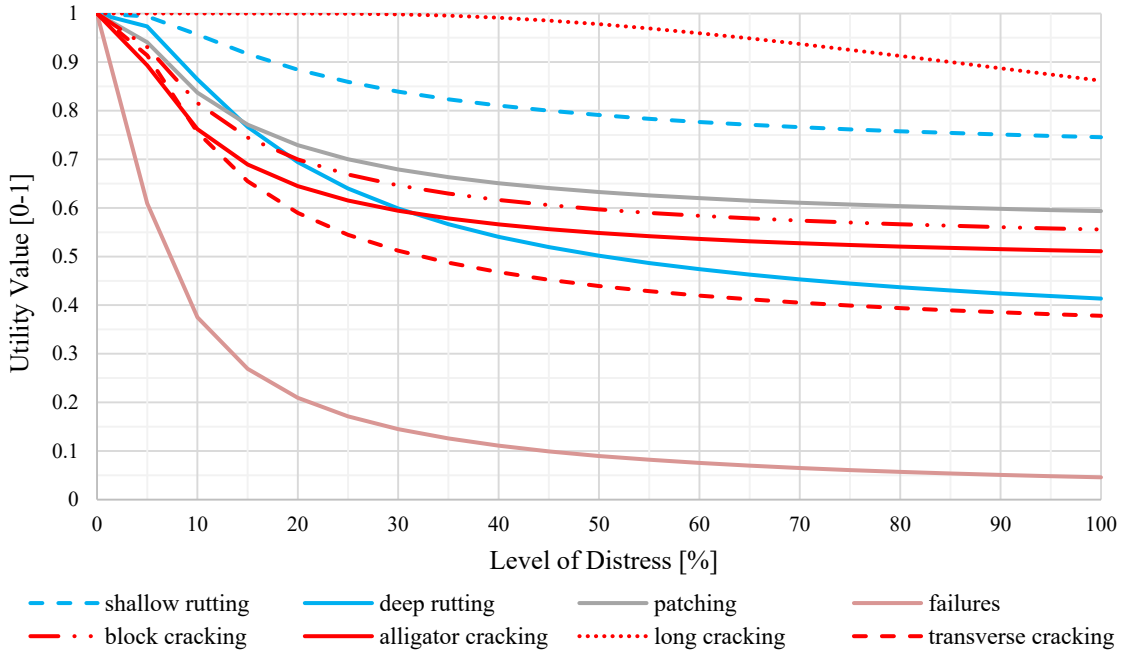

Figure 2.2: TxDOT PMIS utility curves for AC pavements with intermediate layer thickness.

The utility values of the different surface condition indexes are used to compute aggregated scores. PMIS defines two aggregated scores: the Distress Score (DS) and the Condition Score (CS). The DS describes the overall level of damage in the pavement and is calculated as a function of the distress utility values defined for the corresponding surface type, as shown in Equation 2.3.

$$DS = 100 \prod_{\forall d \epsilon P} U_d \quad (2.3)$$

where,

DS: Distress Score

U_d: utility value for distress d

P: set of distresses defined for the analyzed pavement type

The CS is calculated as a function of both the surface distresses and the ride quality (Equation 2.4) and, therefore, describes the overall condition of the pavement surface. This aggregated condition index ranges from 1 to 100, where 100 represents perfect condition of the pavement, and it is the main measurement used by TxDOT to assess the condition of the pavements at the network level. For instance, the percentage of miles in "Good" or better condition (i.e., CS $\geq$ 70) is used by TxDOT to allocate funds, monitor the performance of district 4-Year Plan M&R strategies, and make other management decisions.

$$CS = DS\, U_{RS} \quad (2.4)$$

where,

CS: Condition Score

U_{RS}: ride score utility value

Pavement Performance Modeling

The *performance* of a pavement is defined as the progression of its structural or functional condition throughout time. Factors affecting pavement performance are both internal—such as the mechanical properties of its materials or the dimensions and relative position of its layers—and external, such as the vehicle types and weights loading the pavement as well as environmental conditions. Pavement performance models seek to

describe the relationship between its condition throughout time and these influencing factors. These models are implemented to forecast the future condition of the pavement and to understand the damaging effect of specific variables.

Empirical and Mechanistic Models

The approaches implemented in the past to develop pavement performance models are usually classified into empirical and mechanistic. Put simply, their main difference is that mechanistic models are built from mechanical response laws that describe the causal relationship between variables and pavement performance, whereas empirical models aim to explain the effect of variables on the observed variation of the pavement performance using a set of data. In practice, pavement performance models typically fall in between these two categories, as mechanistic models are usually calibrated using observations and empirical models are usually specified incorporating engineering knowledge about the pavement response.

Developing a model based on empirical data presents advantages and disadvantages. The use of data allows an empirical model to estimate the reliability of its predictions as well as to be less dependent on assumptions, producing estimates based on real observations. On the other hand, the uncertainty of the predicted pavement performance from an empirical model increases significantly when extrapolating from the conditions of the data used for the estimation. In contrast, the use of physical principles (e.g., Hooke's law) for describing the causal effect of the variables allows for mechanistic models to be more general in conditions for applicability. The main limitation of mechanistic models arises from the many deviations of its assumptions from reality, which undermines the predictive power of these models.

A third group of pavement performance models, referred to as mechanistic-empirical models, was developed by combining the two approaches. Typically, one of these models employs a mechanistic model to predict strains and stresses in the pavement layers for specific traffic and climate conditions, and the results are subsequently used by an empirical model to predict the performance of the pavement in the field, where the lack of representativeness of the mechanistic model assumptions is more evident. Thus, mechanistic-empirical models make use of the main strengths of each approach, producing superior results at the cost of increased complexity.

The first pavement performance model was developed in the late 1950s using the data collected in the AASHO Road Test (HRB, 1962). The expression of this empirical model is shown in Equation 2.5, where the serviceability level at each point in time is expressed as a function of traffic and the effects of design and environmental factors are captured in the model parameters. This model assumes a monotonic non-linear relationship for traffic, the curvature of which is described by the parameter ω. In addition, the expected value of the parameter ρ provides an estimate of the cumulated traffic level required to reach the end of the pavement's service life.

$$PSI_t = PSI_o - \left(PSI_o - PSI_f\right)\left(\frac{N_t}{\rho}\right)^{\omega} \tag{2.5a}$$

$$\omega = \omega_0 \frac{\theta_0 \, (L_1+L_2)^{\theta_2}}{SN^{\theta_1} \, L_2^{\theta_3}} \tag{2.5b}$$

$$\rho = \varphi_0 \frac{SN^{\varphi_1} \, L_2^{\varphi_3}}{(L_1+L_2)^{\theta_2}} \tag{2.5c}$$

where,

PSI_t: level of serviceability at time t

PSI_o: initial level of serviceability

PSI_f: final level of serviceability

N: cumulated traffic until time t

L_1: axle load, in kips

L_2: axle type; equal to 1 for single axles and 2 for tandem axles

SN: structural number (defined as a linear combination of the layer thicknesses)

$\boldsymbol{\theta}, \boldsymbol{\varphi}, \omega, \rho$: model parameters

Another significant outcome from the AASHO Road Test was the development of an index to summarize the wide spectrum of axle types and axle loads into a unique statistic. This index was called the equivalent single-axle load (ESAL) and it is an estimate of the number of passes required for an 18-kip (80-kN) single-axle with dual wheels to produce the same damage to the pavement as caused by the different axle types and loads in traffic (Huang, 1993).

The estimated AASHO model expressed as a function of the cumulated traffic was used to specify the allowable number of ESALs for a tolerable drop in serviceability in the 1961 Interim Pavement Design Guide (HRB, 1961). This pavement design equation had the limitation of being primarily applicable to the conditions of the AASHO Road Test, which were representative of soils and climate present in the Midwestern U.S. (Prozzi, 2001) (a detailed description of the AASHO Road Test data is provided in the next chapter). In order to incorporate variations in the pavement materials, drainage condition, subgrade type, and weather, the AASHO model was updated incorporating additional variables and calibrated for wider conditions in the successive editions of the pavement design guide: 1972 Interim Guide, 1986 Guide, and 1993 Guide.

The pavement design equation corresponding to the latest edition of the American Association of State Highway and Transportation Officials (AASHTO) Guide for Design of Pavement Structures is shown in Equation 2.6, where the initial and terminal

serviceability levels were set to 4.2 and 1.5, respectively (AASHTO, 1993). The left side of Equation 2.6 represents the demand (traffic loads expressed in ESALs), whereas the right side represents the supply (structural capacity). The effect of weather is accounted for in the calculation of the effective modulus of the soil. The effect of the pavement materials, layer thicknesses, and drainage conditions are captured in the structural number. In addition, this version of the model allowed for designing the pavement for a desired reliability level using a standard deviation term to account for the overall uncertainty from the explanatory variables and error of the model (Huang, 1993).

$$log(N_{18}) = Z_R S_0 + 9.36\, log(SN+1) - .2 + \frac{log\left(\frac{4.2-PSI_f}{4.2-1.5}\right)}{.4+\frac{1094}{(SN+1)^{5.19}}} + 2.32\, log(M_R) - 8.07 \quad (2.6)$$

where,

N_{18}: allowable number of ESALs

M_R: effective resilient modulus of roadbed soil

Z_R: reliability factor

S_0: overall standard deviation (typically between 0.30 and 0.45)

The different versions of the AASHTO Guide have been widely adopted by transportation agencies in the U.S. and around the world, serving as the standard for the design of flexible pavements until the mid-2000s, when the Mechanistic-Empirical Pavement Design Guide (MEPDG) was published. This design guide was first released in 2004 (ARA, 2004) under the sponsorship of AASHTO and Federal Highway Administration (FHWA) and it is currently the most preferred method for designing and analyzing pavements.

The MEPDG allows for prediction of pavement performance for individual distresses employing mechanistic-empirical models estimated and calibrated using data

from the AASHO Road Test and the LTPP experiment. The progression of each distress is calculated bi-weekly to consider seasonal variations in traffic and environmental factors. These calculations are performed in two steps. The first step consists of calculating the pavement response in terms of strains and stresses at critical points of the pavement through mechanistic models based on multi-layer elastic theory (asphalt pavements) or finite element analysis (concrete pavements). The outcomes from the first step are then used to update the condition of the pavement surface using empirical models called "transfer functions" (ARA, 2008).

Refer to Gendreau and Soriano (1998), Prozzi (2001), Li (2005), and Chu and Durango-Cohen (2008) for further information on the models described in this section and other pavement performance models developed in the past.

Alternative Specifications for the Empirical AASHO Performance Model

A number of alternative model specifications and methodologies have been proposed to overcome limitations and enhance the capabilities of the empirical AASHO pavement performance model (Equation 2.5) since its release in 1962. Some major flaws of the original AASHO model reported in the literature are the use of an inefficient sequential estimation procedure; incorrect specification due to mismatching units (e.g., term $L_1 + L_2$ in Equation 2.5); selection bias resulting from discarding pavement sections that did not fail at the end of the experiment; and bias in the estimated parameters due to not accounting for the significant unobserved heterogeneity present in the data (Paterson, 1987; Small and Winston, 1988; Prozzi and Madanat, 2000).

An alternative modeling approach proposed by Small and Winston (1988) to address some of these issues consisted of the estimation of a Tobit model specification to properly handle the censored observations in the estimation of the pavement's service life.

This concept was further extended by Prozzi and Madanat (2000) by the estimation of the pavement's service life through a Weibull duration model specification. Another method proposed to overcome the issue of selection bias proposed by Madanat et al. (1995) consisted of the estimation of a joint discrete-continuous model of infrastructure distress initiation and progression in order to correctly incorporate the observations for which the distress has not initiated yet.

Misspecification issues of the AASHO model have been tackled by a number of studies through the specification of additional variables and alternative functional forms. An example of these is the S-shape form proposed by Garcia-Diaz and Riggins (1984) through the exponentiation of the damage function of the AASHO model (HRB, 1962) in order to better describe the double curvature in the performance curve observed for some pavement sections in the AASHO Road Test. Paterson (1987) proposed a number of incremental model specifications with the incorporation of additional variables to account for the influence of different subgrades, pavement materials, and climatic factors, among others. Archilla and Madanat (2001) and Prozzi and Madanat (2004) used a joint estimation technique for combining data from the AASHO Road Test with other data sources in order to identify parameters that are not identifiable from one data source.

A significant improvement of the AASHO empirical model was achieved by the use of specifications to account for the presence of heterogeneity. Archilla (2000) and Prozzi (2001) estimated a non-linear incremental form using the fixed-effects and random-effects estimation methods with variable intercept in order to avoid the bias in the model parameters caused by unobserved heterogeneity. The capabilities of these models were enhanced by Archilla (2006) through the estimation of a mixed-effect model specification allowing for the model to capture the heterogeneity in the data through the parameters as well, as opposed to solely through the intercept. Other studies that proposed similar

approaches to address unobserved heterogeneity in the infrastructure management literature include Madanat et al. (1997), Onar et al. (2006), and Hong and Prozzi (2010, 2014).

More recently, Zhang and Durango-Cohen (2014) proposed a cluster-wise linear regression specification for the AASHO model to capture the heterogeneity of pavement performance at the group level. This approach allows for better model fit and provides more insights to explain the systematic differences in performance among pavement sections than the previous approaches used to capture unobserved heterogeneity at the individual level (e.g., fixed, random, and mixed effects). Other studies that implemented similar approaches to capture heterogeneity in pavement performance data at the group level using other data sources include those conducted by Luo and Chou (2006) and Luo and Yin (2008).

This dissertation builds on the aforementioned research studies and contributes to the literature by proposing a methodology to capture group-level heterogeneity in performance data through the Bayesian estimation of a non-linear incremental mixture model specification estimated from the combination of multiple data sources that included experimental and in-service pavement sections, among other contributions.

TxDOT PMIS Performance Model

Transportation agencies develop and calibrate pavement performance models to be implemented in their PMS for network-level applications based on the aforementioned specifications and incorporating their engineering knowledge and expertise. These models are tailored to meet agency needs, such as specifying type of data collected and local conditions. As an example, Equation 2.7 shows the sigmoidal performance model defined

in TxDOT's PMIS to predict the level of distress, or ride quality lost, as a function of the surface's age (Stampley et al. 1995).

$$L_i = \alpha e^{-\left(\frac{\chi \epsilon \rho \sigma}{AGE_i}\right)^{\beta}} \tag{2.7}$$

where,

L_i: level of distress, or ride quality lost, for condition index i

AGE_i: pavement surface age in years

α: model parameter that controls for the maximum range of distress growth

β: model parameter that controls for the slope of the performance curve

ρ: model parameter that controls for the pavement service life

χ: traffic weighting factor

ϵ: climate weighting factor

σ: subgrade support weighting factor

The values for the parameters α, β, and ρ are tabulated in Stampley et al. (1995) for each distress index and surface type. The remaining model parameters are used to control for the effect of traffic, climate, and subgrade factors. The traffic weighting factor, χ, is computed as a function of the section's projected number of ESALs over 20 years, condition index, and pavement type. The climate weighting factor, ϵ, is defined as a function of the average county rainfall and freeze and thaw cycles; however, Stampley et al. (1995) recommended setting its value to one (i.e., not affecting the predictions) as the significance of these factors had not been clearly demonstrated by the time these models were developed. The subgrade support weighting factor, σ, controls for the characteristics of the subgrade soil and its value is defined by county, condition index, and pavement type. As an example, Figure 2.3 shows the TxDOT PMIS performance curve for the progression

of alligator cracking corresponding to an intermediate thickness AC pavement located in Travis County.

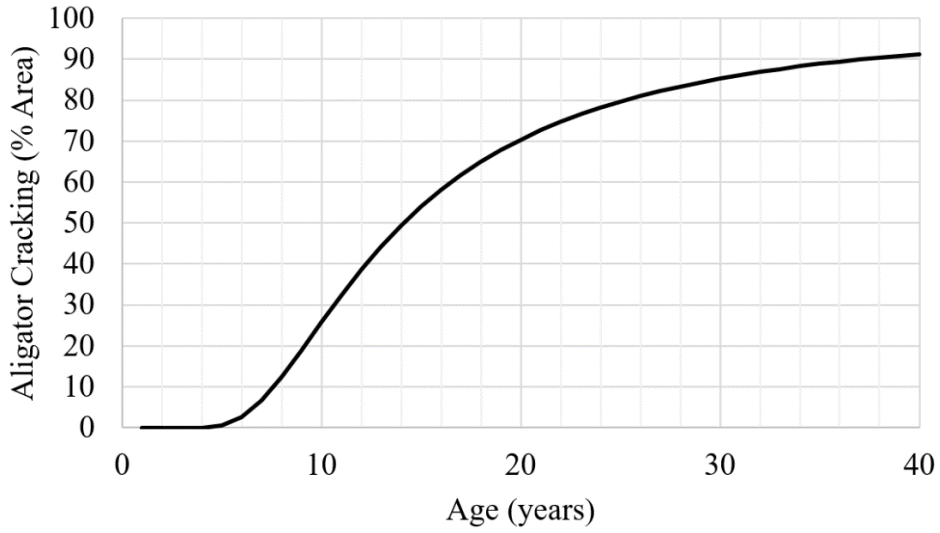

Figure 2.3: TxDOT PMIS performance curve for alligator cracking.

Preventive Maintenance of Pavements

The condition of a pavement decreases over time due to the combined effect of traffic and climate until it reaches the limit of its serviceability levels; at this point an M&R treatment is applied, suddenly increasing the serviceability level back to a high value (Figure 2.4). *Preventive maintenance* refers to a series of treatments applied to extend the service life of the pavement without necessarily increasing its structural capacity (O'Brien, 1989; Peshkin et al. 2004). These treatments are applied when the pavement surface is still in good condition in order to prevent the acceleration of damage due to the progression of distresses (e.g., cracking) and to changes in the material properties arising from wetting and freezing, among other factors.

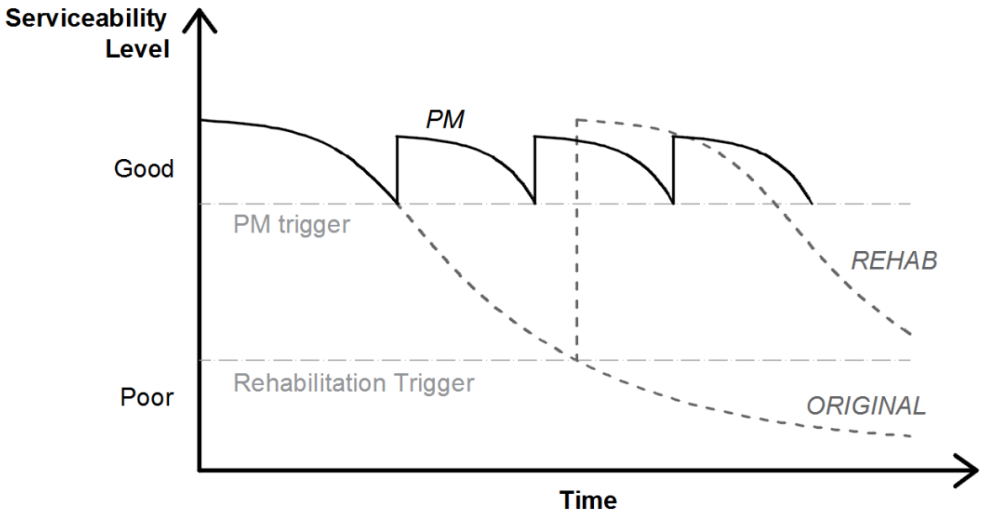

Figure 2.4: Theoretical pavement performance curve for different M&R strategies.

A number of PM treatments are available, including thin overlays (TH), chip seals (CH), microsurfacing (MS), cold in-place recycling, ultrathin friction course, fog seals, slurry seals (SS), cape seals, crack seals (CS), and scrub seals. While some of these are interim measures applied as stopgaps before full rehabilitation, others are designed to provide extended service life. In contrast to conventional rehabilitation strategies, PM treatments are used on existing pavements with low levels of distress. Therefore, these treatments will be subject to the pre-existing failure mechanisms of the underlying pavement, which may serve to accelerate deterioration and reduce the effectiveness of the PM treatment. The rate of deterioration of these treatments will vary depending on the condition or state of the underlying pavement as well as other influencing factors, such as the quality of the treatment applied and the external influences of traffic and climate.

Review of the Effectiveness of PM Treatments

Given that several local factors can affect the performance of PM treatments, many studies have sought to better understand how the various influence factors impact treatment

effectiveness. Many of these studies analyzed data collected for the LTPP Specific Pavement Study (SPS)-3 experiment, which was designed to assess the effectiveness of different PM treatments, and evaluate the optimum timing for treatment application, using performance data collected from in-service flexible pavements.

In 1998, Morian et al. applied multi-variable regression analysis to the five-year SPS-3 data to evaluate the PM treatment performance. This study modeled different performance indicators in terms of treatment type, environmental zone, age, and initial condition, among other factors. In the regression analysis, the independent variables were specified as integer indicator codes ranked from worst to best. The study concluded that TH had a significant effect in rutting and roughness reduction while the remaining PM treatments had slight or no effect. However, the researchers' assumption on the rank of each independent variable resulted in biased parameters, not capturing the true marginal effects of the different PM treatments.

One year later, Eltahan et al. (1999) conducted survival analysis to evaluate the life expectancy and the effect of the original pavement condition. The authors estimated the failure probabilities of each treatment with respect to the original condition of the test sections using the Kaplan-Meier method. The study concluded that applying treatment to sections in poor condition increased the risk of failure by two to four times, and that CH outperformed the other treatments.

In 2003, Hall et al. evaluated the initial and long-term effects of the different PM treatments on the pavement condition as well as the influence of pre-treatment condition and other experimental factors. The initial effect of the treatment was evaluated by comparing pre- and post-treatment measurements of roughness, rutting, and fatigue cracking, whereas the long-term effect was evaluated by comparing the last measurement for treated sections with the corresponding measurement for control sections. The

comparisons were carried out using two-sided multiple comparisons with the control section and paired t-tests. The study concluded that the most effective treatment in SPS-3 experiment was TH, followed by CS and SS. Only TH produced an initial reduction of and a significant long-term effect on roughness.

Another study conducted in 2003 by Chen et al. studied 14 SPS-3 test sites in Texas to investigate the effectiveness of PM treatments. The study concluded that CH was the best performer among the analyzed PM treatments, followed by TH. Although the study presents a detailed discussion of the PM treatment effects on Texas specific sites, the results from the comparison were not based on statistical methods. In addition, factors such as subgrade type, moisture, and temperature were not taken into account.

In 2010, Shirazi et al. used Friedman tests and non-parametric randomized block analysis of variance to compare the performance of the different PM treatments for different levels of temperature, precipitation, subgrade, traffic, and initial condition. The performance indicator used in this study was the weighted average of distresses normalized by the period of analysis, which allowed for comparing different data collection periods. However, the analysis did not take into account the deterioration rate and its trend. The study concluded that TH was the most effective treatment, whereas the effects of SS and CS were not statistically significant.

A more recent study, conducted by Morian et al. in 2011, applied survival analysis to twenty-year SPS-3 data to assess life expectancy of the PM treatments; it also applied Friedman tests in order to compare structural effects of the treatments. The results from the survival analysis indicated that TH performed best at high-survival probabilities, whereas CH performed best for the case of low-survival probabilities. The Friedman test results showed that the structural benefits from all treatments (except for CS) were significant.

Lastly, Haider and Dwaikat (2011) estimated the optimum timing for PM treatment by maximizing the difference between the areas below the roughness curves for pre- and post-treated pavements. The IRI value was modeled as a function of age using an exponential function. The effects of traffic, environmental, and subgrade factors were not taken into account in the analyses, and the study did not include a comparison of treatments.

METHODOLOGICAL BACKGROUND

This section of the chapter provides the background of the methodology proposed in this dissertation to model heterogeneity in pavement performance data and describes the algorithms and other aspects of the estimation of the models.

Description of Finite Mixture Models

Mixture models are defined by the combination of probability density functions. This combination is convex (i.e., its mixing proportions, or weights, are non-negative and sum to one) in order to preserve the properties of probability density functions. Finite mixture models are a special case of these for which the number of component densities is finite. The generic expression of a finite mixture model is shown in Equation 2.8, where the weight of each component density represents the probability of an individual sampled from the mixture density to belong to the specific component (McLachlan and Peel, 2004).

$$f(y_i) = \sum_{k=1}^{K} w_k \, f_k(y_i|\boldsymbol{\theta}_k) \tag{2.8}$$

where,

y_i: observed value i of random variable Y

$f(\cdot)$: mixture density

$\boldsymbol{\theta}_k$: vector of parameters of component density $f_k(\cdot)$

w_i: weight of component k

The mixture density (thick line) resulting from the combination of two- (M2) and three-component (M3) densities are shown in the plots of Figure 2.5. The component densities used in this hypothetical example are Gaussian densities with the following mean and standard deviation values: $\boldsymbol{\theta}_1 = (5.20, 1.10)$, $\boldsymbol{\theta}_2 = (7.10, 1.50)$, and $\boldsymbol{\theta}_3 = (6.50, 0.75)$, corresponding to C1, C2 and C3, respectively. The weights for the mixture with two components are $\boldsymbol{w} = (0.38, 0.62)$, and the ones for the mixture with three components are $\boldsymbol{w} = (0.38, 0.40, 0.22)$.

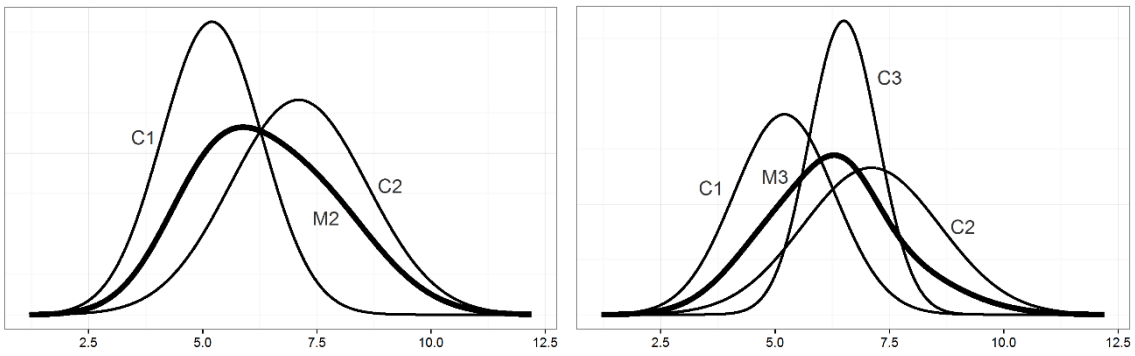

Figure 2.5: Mixture of two (left) and three (right) Gaussian densities.

The use of a mixture distribution to model the presence of heterogeneous subpopulations in data is natural, and it has been widely used in several research fields, such as in marketing (Jedidi et al., 1997; Wedel and Kamakura, 2012), biology (Do et al., 2005; Proïa et al., 2016), linguistics (Li and Yamanishi, 2003; Henderson and Lemon, 2008), and many others. An example of such application from the pavement engineering literature is the use of a mixture of two lognormal distributions to model the subpopulations of loaded and unloaded trucks from load spectrum data proposed by Timm et al. (2005).

This dissertation proposes a mixture of regression models to capture the systematic differences in pavement performance not explained by variables typically available in

pavement management databases. This approach assumes that the heterogeneous pavement performance resulting from the combined effect of the several unobserved factors and interactions is manifested through a finite number of latent groups. The estimation of the proposed model allows for defining the parameters of the group-specific densities while clustering the observations into the latent groups.

In order to illustrate this idea, the densities M2 and M3 in Figure 2.5 may represent the observed change in surface condition measured between two points in time for a sample of pavements loaded with the same traffic and exposed to the same environment, but with differences in their structural design. These differences may result in the presence of subpopulations of pavements with heterogeneous performance, whose densities are represented in the figure as C1, C2, and C3. For instance, C1 and C2 (plot in the left) may represent subpopulations of pavements with thicker and thinner surface layer thickness, respectively. Similarly, C1, C2, and C3 (plot in the right) may represent subpopulations of flexible pavements treated with different PM treatments. The estimation of a mixture model allows for capturing the underlying groups of observations with heterogeneous response, improving the fit of the model. Identifying and characterizing the underlying groups provides insights that can be further incorporated into pavement management practices.

Bayesian Estimation of Finite Mixture Models

There are a number of approaches usually used to estimate finite mixture models. These approaches include method of moments, maximum likelihood, and Bayesian approaches (McLachlan and Peel, 2004). The mixture models in this dissertation had a Bayesian specification and were estimated from Markov chain Monte Carlo (MCMC) simulations. The following subsections describe the algorithm implemented and other

aspects of the MCMC simulations performed for the estimations and analyses presented in the following chapters.

MCMC Simulations

The regression models proposed in this dissertation to predict the change in surface condition had a non-linear functional form (as will be described in Equation 3.3 and 4.3). Consequently, a full conditional distribution for the regression parameters was not available and, therefore, they were sampled from a symmetrical proposal distribution using the MCMC Metropolis-Hastings (M-H) algorithm (Metropolis et al., 1953; Hastings, 1970).

At each iteration of the M-H algorithm, the proposal values for the model parameters were sampled from a Gaussian distribution centered on the value obtained from the previous iteration. The standard deviation of the Gaussian, referred to as the scale of the proposal, was determined by trial-and-error until obtaining multiple MCMC chains—starting from different arbitrary points—that converged to the same marginal posterior distribution. Given the symmetry of the adopted proposal distribution, the probability of acceptance of the proposed values at each iteration was independent of the proposal distribution and calculated as in Equation 2.9 (Chib and Greenberg, 1995).

$$\alpha(\boldsymbol{\theta}^*, \boldsymbol{\theta}^{t-1}) = \min\{1, p(\boldsymbol{\theta}^*|\boldsymbol{y})/p(\boldsymbol{\theta}^{t-1}|\boldsymbol{y})\} \tag{2.9}$$

where,

α: acceptance probability

$\boldsymbol{\theta}^*$: vector of proposed parameters at iteration *t*

$\boldsymbol{\theta}^{t-1}$: vector of parameters from the previous iteration

$\boldsymbol{y}$: vector of observed values

$p(\boldsymbol{\theta}|\boldsymbol{y})$: posterior distribution conditional on the observed data

Therefore, to estimate a sample of the marginal posterior distribution for each individual parameter conditional on the pavement data, the following steps of the M-H algorithm were implemented:

1. Select an arbitrary initial set of values for the parameters $\boldsymbol{\theta^0}$
2. For each parameter θ_j with $j = 1..J$, and iteration t
    a. Compute $lp = \log\left[p\left(\theta_1^t,..,\theta_{j-1}^t,\theta_j^{t-1},\theta_{j+1}^{t-1},..,\theta_J^{t-1}\,|\boldsymbol{y}\right)\right]$
    b. Sample a proposal $\theta_j^{t^*}$ from $\mathrm{N}\left(\theta_j^{t-1},k\right)$; and u from $\mathrm{U}[0,1]$
    c. Compute $lp_p = \log\left[p\left(\theta_1^t,..,\theta_{j-1}^t,\theta_j^{t^*},\theta_{j+1}^{t-1},..,\theta_J^{t-1}\,|\boldsymbol{y}\right)\right]$
    d. If $lp_p - lp > \log(u)$ then $\theta_j^t = \theta_j^{t^*}$; Else $\theta_j^t = \theta_j^{t-1}$
3. Repeat steps 2 and 3 after reaching convergence of the marginal distributions.

The adjustments made to the scale of the proposal distributions during the setup of the MCMC chains were determined based on the acceptance rates obtained from the sampling of each parameter. For instance, a high acceptance rate for a specific parameter suggests that the scale of the proposal was too small and, therefore, a higher scale was tested for the next MCMC chains. Theoretically, the optimal acceptance rate in order to maximize the efficiency of the algorithm for the case of multivariate target distributions is approximately 0.23 (Roberts et al., 1997).

The M-H algorithm was implemented through a code written in R programming language (R Core Team, 2016) by the author. The packages used by the code were *snowfall* (Knaus, 2015) for running the different MCMC chains simultaneously using multiple processing cores, and *coda* (Plummer et al., 2006) to calculate the acceptance rate of each chain, summarize the MCMC outputs, and perform convergence diagnostics.

Convergence Criteria

Although the MCMC M-H algorithm will eventually converge to the target distribution for a long enough chain despite the starting position (Chib and Greenberg, 1995; Robert et al., 1997), convergence is not guaranteed for a certain simulation length. Several diagnostics and criteria are used to evaluate the convergence of MCMC chains (Cowles and Carlin, 1996). The convergence of the MCMC simulations performed in this dissertation was assessed both qualitatively and quantitatively. The quantitative component consisted of visually inspecting the trace plots and posterior distributions of each estimated parameter to ensure proper mixing (i.e., how well the random walk algorithm explored the parameter space) of the multiple chains. The quantitative component consisted of checking the potential scale reduction factor (PSRF) proposed by Gelman and Rubin (1992) as well as the multi-variate version of the PSRF (MPSRF) proposed by Brooks and Gelman (1998). The trace plots of each sampled marginal posterior distribution, as well as the values for the PSRF and the MPSRF, were calculated in R using the *coda* package (Plummer et al., 2006).

The PSRF measures the discrepancies among multiple chains obtained from over-dispersed starting points by comparing the within-chain variance to the between-chain variance. The MPSRF is an extension of the PSRF computed using the estimated within-chain and between-chain covariance matrices and, therefore, it accounts for the potential correlations across the individual chains. PSRF and MPSRF values significantly greater than 1.0 suggest important discrepancies across chains and, therefore, improper mixing. The guideline suggested by Brooks and Gelman (1998) for considering acceptable convergence of the MCMC chains is a PSRF for each individual parameter, and the MPSRF, below 1.2. This convergence criterion, commonly used in the literature, was adopted for the analyses in this dissertation.

Model Selection

The different model specifications estimated in this dissertation were selected using a penalized likelihood approach through the comparison of their deviance information criterion (DIC), shown in Equation 2.10. The DIC is commonly used to evaluate the complexity and fit of models—particularly hierarchical models in which the number of parameters is not clearly defined (Spiegelhalter et al., 2002). Models with smaller DIC values are preferred over models with larger DIC.

$$DIC = \widehat{D} + p_D \tag{2.10}$$

$$D(\boldsymbol{y}, \boldsymbol{\theta}) = -2\ log[p(\boldsymbol{y}|\boldsymbol{\theta})] \tag{2.11}$$

$$\widehat{D} = \mathrm{E}(D(\boldsymbol{y}, \boldsymbol{\theta})|\boldsymbol{y}) \tag{2.12}$$

$$p_D = 0.5\ var(D(\boldsymbol{y}, \boldsymbol{\theta})|\boldsymbol{y}) \tag{2.13}$$

where,

DIC: deviance information criterion

$\boldsymbol{y}$: vectors of observed values of random variable Y

$\boldsymbol{\theta}$: vector of model parameters

$D(\cdot)$: deviance

p_D: effective number of parameters

The DIC has two components: the expected deviance and the effective number of parameters. The deviance measures the fit of a model for a given set of data and parameters as a function of its log-likelihood, as shown in Equation 2.11, and the expected deviance (Equation 2.12) provides a point estimate of the model fit. The lower the deviance, the lower the discrepancies between data and model. The effective number of parameters

measures the complexity of the model and can be estimated as shown in Equation 2.13 (Gelman et al., 2014). The higher the effective number of parameters in a model, the greater the model's complexity. Therefore, the DIC value favors the fit of a model while penalizing for its complexity, thus allowing for a balance between fit and generality. Both the expected deviance and the effective number of parameters can be estimated using the deviance values sampled from the marginal posterior distribution obtained from the MCMC simulations.

Chapter 3: Bayesian Methods for Addressing Heterogeneity in Pavement Performance

The present chapter covers the estimation and interpretation of two Bayesian modeling techniques for specifying heterogeneity of effects in pavement performance: a hierarchical specification and a finite mixture model specification. These two specifications were estimated using experimental data from the American Association of State Highway Officials (AASHO) Road Test (HRB, 1962).

DESCRIPTION OF EXPERIMENTAL PAVEMENT PERFORMANCE DATA

AASHO Road Test

The AASHO Road Test was conducted between 1956 and 1961, and it is, to date, one of the most comprehensive experiments designed for understanding the effect of traffic characteristics and environmental factors on the deterioration of pavement structures. The data collected from this experiment were used for developing the different versions of the American Association of State Highway and Transportation Officials (AASHTO) Guide for Design of Pavement Structures (HRB, 1962; AASHTO 1972, 1986, 1993).

The AASHTO pavement design guide has been the main standard for the design of pavement structures in the US and several other countries since its development and it is still widely used. Moreover, the AASHO Road Test data have been widely used by researchers to demonstrate proposed methodologies for the modeling and analysis of pavements. Some examples of related research studies that used this dataset are Small and Winston (1988), which proposed Tobit regression in order to improve the predictions of the model used by the AASHTO design guide; Prozzi and Madanat (2003), which proposed an incremental form of the AASHTO model with variable intercept random effects to account for heterogeneity and incorporated the effect of the frost penetration gradient

(Prozzi, 2001); Hong and Prozzi (2006), which estimated a pavement performance model using a Bayesian approach; and Zhang and Durango-Cohen (2014), which estimated a cluster-wise linear regression model applying an exchange algorithm.

The AASHO Road Test was conducted in Ottawa, Illinois, and consisted of a factorial design that comprised six two-lane loops, each containing both flexible and rigid pavement test sections with different structural designs and materials (HRB, 1962). Figure 3.1 shows the general layout of the AASHO Road Test and a more detailed layout of one of the test loops. Loop 1 was used to study the effect of environmental factors on pavement deterioration and was not subjected to traffic. Loops 2 through 6 were subjected to traffic, controlling for the axle types and magnitude of loads.

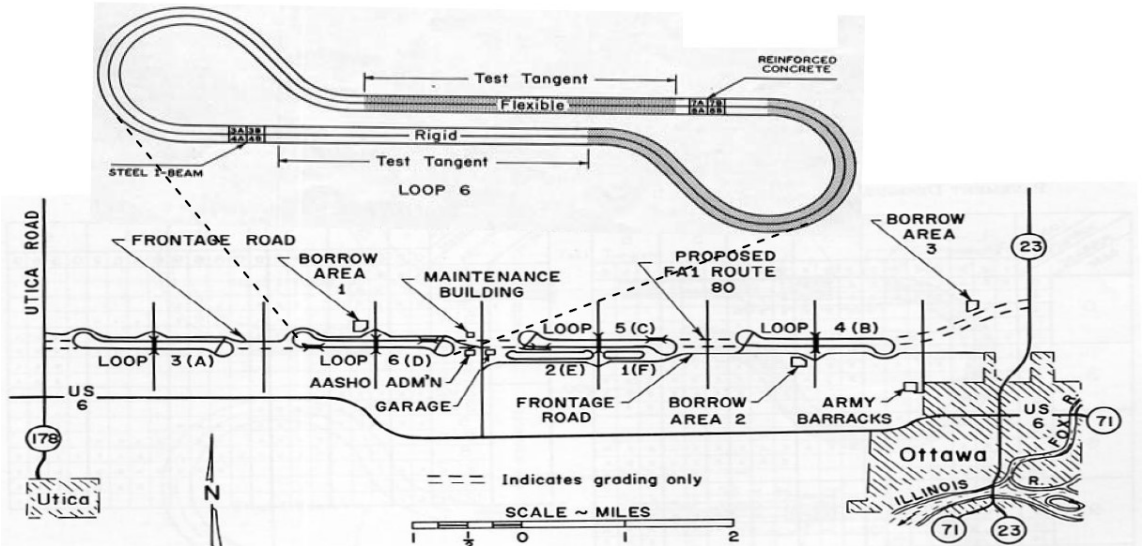

Figure 3.1: Layout of AASHO Road Test loops and schematic of Loop 6 (Pedersen, 2007).

Each loop was divided into multiple test sections with different layer thicknesses in order to control for the structural design. The structural design of flexible pavement sections was characterized by three factors:

- surface layer thickness, with six levels, ranging from 1 to 6 inches in increments of 1 inch;
- base layer thickness, with four levels, ranging from zero (no base layer) to 9 inches, in increments of 3 inches;
- and sub-base layer thickness, with five levels, ranging from zero (no sub-base layer) to 16 inches, in increments of 4 inches.

Every pavement section was tested under repeated traffic loads until reaching failure, or until the end of the experiment (two years or less). The traffic loads were applied using a series of trucks with different axle configurations and loads. Table 3.1 reports the truck configurations applied to each loop and lane; each test section was loaded with one truck configuration (HRB, 1962). As shown in Table 3.1, three axle types were included in the main factorial design: front axles, single axles, and tandem axles.

Table 3.1: Truck configuration applied to each loop and lane.

Loop	**Lane**	**Front Axle**	**Single Axle**		**Tandem Axle**		**Gross Weight**
		Kips	#	*Kips*	#	*Kips*	*Kips*
2	*1*	2.0	1	2.0	0	0.0	4.0
	2	2.0	1	6.0	0	0.0	8.0
3	*1*	4.0	2	12.0	0	0.0	28.0
	2	6.0	0	0.0	2	24.0	54.0
4	*1*	6.0	2	18.0	0	0.0	42.0
	2	9.0	0	0.0	2	32.0	73.0
5	*1*	6.0	2	22.4	0	0.0	50.8
	2	9.0	0	0.0	2	40.0	89.0
6	*1*	9.0	2	30.0	0	0.0	69.0
	2	12.0	0	0.0	2	48.0	108.0

The experiment had 836 test sections in all, of which 468 were hot-mix asphalt (HMA) pavements and 368 were Portland cement concrete pavements. Some of these sections were used for the main factorial design while the remaining sections were used for special studies, such as the comparison of different shoulder designs and surface treatments.

Descriptive Statistics of AASHO Data Used for the Analyses

The data used for the analyses in this chapter consisted of the measurements collected on the 252 flexible pavement sections corresponding to the main factorial design of the AASHO Road Test. The condition of the pavement surface at each point in time was assessed by determining the average Present Serviceability Index (PSI) of the section, computed as the mean of the PSI collected for each wheel-path every two weeks. In addition, the change in serviceability between data collection dates, ΔPSI, was computed as the difference in PSI values between consecutive measurements. The number of ΔPSI values throughout time obtained for each of the 252 pavement sections varied from 3 to 55 with an average of 28 observations per section. Thus, the data used for these analyses consist of unbalanced panel data with a total of 7,189 observations.

Figure 3.2 shows, as an example, the change in pavement condition as a function of traffic for three different pavement sections. Test section 331 (in blue) and 299 (in green) are in the same loop and lane; therefore, they were subjected to the same traffic. The slower deterioration rate observed for Section 331 is explained by the thicker surface and base layers (both sections have the same sub-base layer thickness). On the other hand, Section 446 (in red) and Section 331 have the same surface layer thickness but the latter was subjected to heavier loads, which resulted in faster deterioration.

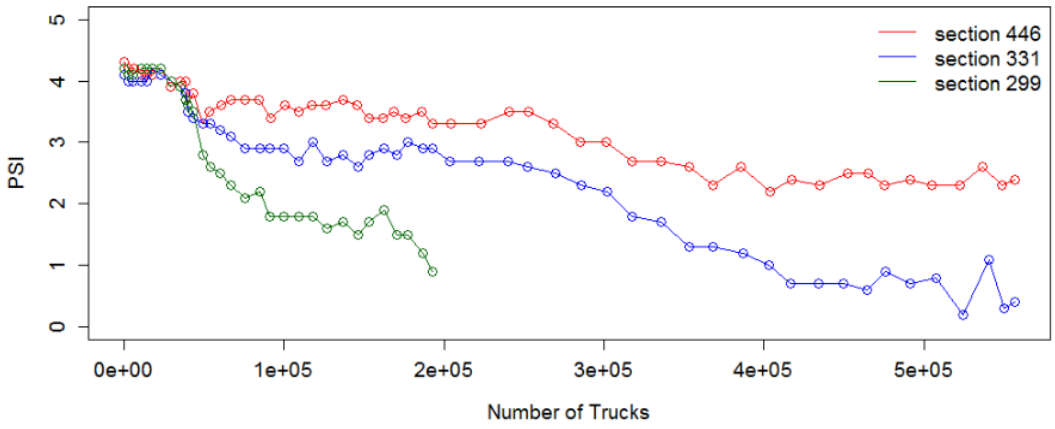

Figure 3.2: PSI as a function of traffic for test sections 446, 331, and 299.

Figure 3.3 shows the distribution of the ΔPSI values used for estimating the proposed models. From the distribution it is observed that the change in PSI values present a slight negative skew with a mean of -0.063 and a standard deviation of 0.265. The negative sign of the mean ΔPSI reflects the damaging effect of traffic and climate. Positive ΔPSI values (27.6% of the observed values) are mainly explained by measurement errors, among other factors, as pavement condition is expected to either deteriorate or remain constant with time.

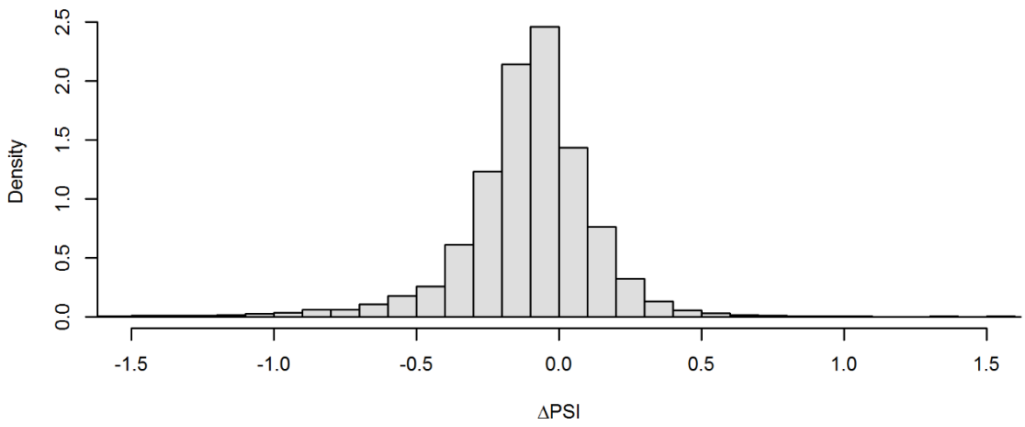

Figure 3.3: Distribution of two-week change in PSI from the analyzed data.

Table 3.2 presents the summary statistics of the experimental variables of the models estimated in this chapter. In addition, the average mean temperature during the experiment for the month of July was 24.5°C (76°F) and for January was -2.8°C (27°F), and the average annual precipitation was 837 mm (34 inches) (HRB, 1962).

Table 3.2. Descriptive statistics of main variables from AASHO Road Test database.

Variable		**unit**	**Mean**	**Std**	**Min**	**Max**
Pavement Serviceability Index	PSI	-	3.3	0.74	0.1	4.6
Two-week Change in PSI	ΔPSI	-	-0.063	0.27	-2.9	2.8
Surface Layer Thickness	H_{sur}	mm	100.5	33.21	25.4	152.4
Base Layer Thickness	H_b	mm	122.5	51.06	25.4	177.8
Sub-Base Layer Thickness	H_{sb}	mm	213.9	120.58	0.0	406.4
Frost Penetration Gradient	G	mm/day	6.3	137.4	-431.8	254.0
Accumulated Number of Trucks	N	veh	1.6E+5	1.8E+5	1.6E+2	1.1E+6
Two-Week Increment of Trucks	dN	veh	9.2E+3	6.2E+3	0E+0	9.7E+4
Load on Front Axle	FA	kips	7.0	3.27	2.0	12.0
Load on Single Axle	SA	kips	9.0	10.90	0.0	30.0
Load on Tandem Axle	TA	kips	16.3	19.72	0.0	48.0

Figure 3.4 shows the frost penetration gradient, *G*, throughout the duration of the test. This index is computed as the depth of frost penetration per unit of time and it reflects the progression of freezing or thawing that occurred during a period of analysis. Positive values correspond to periods of freezing, while negative values correspond to thawing of the subgrade. The gradient was zero during the summer months (Figure 3.4) as no frost was present in the subgrade and unbound layers. This variable has been reported in the literature as significant for explaining the seasonal variation of pavement serviceability (Prozzi, 2001).

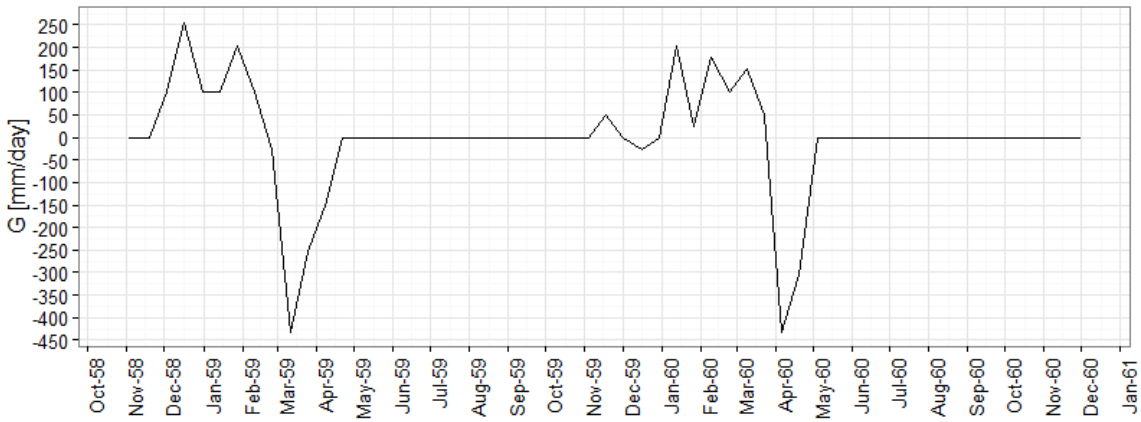

Figure 3.4: Frost penetration gradient for the duration of the AASHO Road Test.

DESCRIPTION OF PAVEMENT PERFORMANCE MODEL AND VARIABLES

The pavement performance model selected for the estimating the model specifications proposed in this chapter was adapted from the non-linear incremental model (Equation 3.3) proposed by Prozzi and Madanat (2003), which is derived from the basic form of the AASHTO design equation (HRB, 1962) expressed in Equation 3.1 (original form shown in Equation 2.5). In the model of Equation 3.1, the condition of the pavement is expressed as a function of some measurement of cumulated traffic, where the parameter a represents the initial condition of the pavement, b represents the rate of damage, and c determines the curvature of the non-linear relationship.

$$PSI = f(N) = a + bN^c \tag{3.1}$$

where,

PSI: Pavement Serviceability Index

N: cumulative measurement of traffic

a, b, c: model parameters

The incremental form of the model is approximated through first order Taylor expansion, as shown in Equation 3.2. As expressed by the authors of the original study, an incremental form of the model is convenient from a pavement management perspective since condition data are usually available on a regular basis. The typical time increment (from *t*-1 to *t*) between collections of pavement condition data in the dataset was two weeks. Three major factors that affect pavement performance are the structural design, environmental conditions, and traffic characteristics. These factors are incorporated in the model parameters *d* and *e*.

$$\Delta PSI_{t-1,t} = f'(N_{t-1})(N_t - N_{t-1}) = dN_{t-1}^{e}\Delta N_t \tag{3.2}$$

where,

$\Delta PSI_{t-1,t}$: damage from period *t*-1 to *t*

N_{t-1}: cumulated traffic up to period *t*-1

ΔN_t: increment of traffic from period *t*-1 to *t*

d, e: model parameters

The final specification of the model is presented in Equations 3.3a to 3.3c, where the model parameters are $\boldsymbol{\beta} = \{\beta_0, \beta_{sur}, \beta_b, \beta_{sb}, \beta_g, \beta_n, \beta_{FA}, \beta_{TA}, \beta_{AL},\}$ and $\boldsymbol{X} = \{H_{sur}, H_b, H_{sb}, G, n, FA, SA, TA\}$ contains the experimental data.

$$\Delta PSI_{i,t} = m(\boldsymbol{X_{i,t}}|\boldsymbol{\beta}) + \varepsilon_{i,t}$$

$$= exp(\beta_0 + \beta_{sur}H_{sur,i} + \beta_b H_{b,i} + \beta_{sb}H_{sb,i} + \beta_g G_t)\, N_{i,t-1}^{\beta_n}\Delta N_{i,t} + \varepsilon_{i,t} \tag{3.3a}$$

$$N_{i,t-1} = \sum_{l=1}^{t-1}\Delta N_{i,l} \tag{3.3b}$$

$$\Delta N_{i,l} = n_{i,l}\left\{\left(\frac{FA_i}{18\beta_{FA}}\right)^{\beta_{AL}} + A_i\left(\frac{SA_i}{18}\right)^{\beta_{AL}} + B_i\left(\frac{TA_i}{18\beta_{TA}}\right)^{\beta_{AL}}\right\} \tag{3.3c}$$

where,

$\Delta PSI_{i,t}$: drop in PSI for section i at time t

$n_{i,l}$: number of trucks on section i between period l -1 and l

$H_{sur,i}$: thickness of asphalt concrete (AC) layer for section i (mm)

$H_{base,i}$: thickness of base layer for section i (mm)

$H_{sb,i}$: thickness of sub-base layer for section i (mm)

G_t: frost penetration gradient at time period t

FA_i: front axle load magnitude (kips) on section i

SA_i: single axle load magnitude (kips) on section i

TA_i: tandem axle load magnitude (kips) on section i

A_i: number of single axles per vehicle on section i

B_i: number of tandem axles per vehicle on section i

$\varepsilon_{i,t}$: error term for observation at section i, period t

The response variable ΔPSI in the model represents the drop in serviceability between data collection dates and, therefore, it was computed as the negative value of the observed change in PSI between consecutive measurements (negative of the values reported in Figure 3.3). Thus, the effect of each explanatory variable is interpreted in relation to a decrease in serviceability.

The structural capacity of each pavement section is represented by weighed sum of the thickness of each layer. It is assumed that these thicknesses are constant throughout the experiment; therefore, variables $H_{sur,i}, H_{b,i}$ and $H_{sb,i}$ do not have a sub-index for time. Since serviceability is expected to decrease at a slower pace for thicker structural layers, the model parameters $\beta_{sur}, \beta_b \; and \; \beta_{sb}$ are expected to have a negative sign.

The effect of environmental factors is captured in the model by the frost penetration gradient, which is defined as the rate of change in frost penetration depth per unit of time. Considering that all test sections were subjected to essentially the same environmental conditions (i.e., air temperature, precipitation, humidity), and assuming the same subgrade characteristics, the variable G_t varies with time but not between test sections. The pavement structure will deteriorate faster during thawing periods due to the loss in strength of the unbounded structural layers; therefore, β_g is expected to have a negative sign.

Equation 3.3c shows the expression used to normalize the different loads and axle types applied to each test section. Each term in the summation of Equation 3.3c is used to estimate the number of passes required for a generic axle type and load to cause the same deterioration to the pavement as one pass of a single axle loaded with 18 kips—i.e., the number of equivalent single-axle loads (ESALs). The parameters β_{FA} and β_{TA} are used to convert the damaging effect of front axles and tandem axles respectively, whereas β_{AL} is used to convert the damaging effect of the load magnitude.

BAYESIAN ESTIMATION OF PAVEMENT PERFORMANCE MODEL

The incremental non-linear model described in the previous section (Equation 3.3) is first estimated in this study using a Bayesian specification with the objective of obtaining a distribution of the model parameters and estimating baseline statistics for comparison with the model specifications estimated in the next sections of this chapter.

Bayesian Model Specification

The formulation for the posterior distribution of the model parameters is shown in Equation 3.4, which expresses that the posterior distribution of the vector of parameters is proportional to the likelihood of the observed data times the prior distribution of the parameters (Gelman et al., 2014).

$$p(\boldsymbol{\beta}, \sigma^2|\Delta\boldsymbol{PSI}) = \frac{p\left(\Delta\boldsymbol{PSI}\middle|\boldsymbol{\beta}, \sigma^2\right)p(\boldsymbol{\beta},\sigma^2)}{\int p\left(\Delta\boldsymbol{PSI}\middle|\boldsymbol{\beta}, \sigma^2\right)p(\boldsymbol{\beta},\sigma^2)d(\boldsymbol{\beta},\sigma^2)} \propto p(\Delta\boldsymbol{PSI}|\boldsymbol{\beta}, \sigma^2)p(\boldsymbol{\beta}, \sigma^2) \quad (3.4)$$

where,

$p(\boldsymbol{\beta}, \sigma^2|\Delta\boldsymbol{PSI})$: posterior joint distribution of model parameters and error term variance given the observed drop in PSI

$p(\Delta PSI|\boldsymbol{\beta}, \sigma^2)$: likelihood of the observed drop in PSI given the parameters

$p(\boldsymbol{\beta}, \sigma^2)$: prior joint distribution of model parameters and error term variance

The error term of the model in Equation 3.3a is assumed to follow a normal distribution with zero expected value (Equation 3.5). Therefore, the drop in PSI is normally distributed and centered on the predicted ΔPSI, as expressed in Equation 3.6. Since each test section in the AASHO Road Test was loaded with one truck configuration and load magnitude throughout the experiment, the expression for the predicted change in PSI presented in Equation 3.3a to 3.3c can be re-written as in Equation 3.7, which simplifies the computations.

$$\varepsilon_{i,t} \sim N(0, \sigma^2) \quad (3.5)$$

$$\Delta PSI_{i,t} \sim N(\widehat{\Delta PSI_{i,t}}, \sigma^2) \quad (3.6)$$

$$\widehat{\Delta PSI_{i,t}} = exp\left(\beta_0 + \beta_{sur}T_{sur,i} + \beta_b T_{b,i} + \beta_{sb}T_{sb,i} + \beta_g G_t\right)\left\{\left(\frac{FA_i}{18\beta_{FA}}\right)^{\beta_{AL}} + A_i\left(\frac{SA_i}{18}\right)^{\beta_{AL}} + B_i\left(\frac{TA_i}{18\beta_{TA}}\right)^{\beta_{AL}}\right\}^{\beta_n+1}\left(\sum_{l=1}^{t-1} n_{i,l}\right)^{\beta_n} n_{i,t} \quad (3.7)$$

where,

$\widehat{\Delta PSI_{i,t}}$: predicted drop in PSI for section i at time t

σ^2: variance of error term

Given the Gaussian distribution of the drop in PSI, and assuming independence between consecutive observations, the likelihood function of the model is presented in Equation 3.8. It should be noted that the number of observations per section was not constant because some sections were removed from the experiment before others.

$$p(\Delta \boldsymbol{PSI}|\boldsymbol{\beta}, \sigma^2) = \prod_{i=1}^{S} \prod_{t=1}^{T_i} \sqrt{\frac{1}{2\pi\sigma^2}}\, e^{\frac{-1}{2\sigma^2}\left(\Delta PSI_{i,t} - m\left(\boldsymbol{X_{i,t}}|\boldsymbol{\beta}\right)\right)^2} \propto$$

$$\left(\frac{1}{\sigma^2}\right)^{T/2} exp\left(\frac{-1}{2\sigma^2} \sum_{i=1}^{S} \sum_{t=1}^{T_i} \left(\Delta PSI_{i,t} - m\left(\boldsymbol{X_{i,t}}|\boldsymbol{\beta}\right)\right)^2\right) \quad (3.8)$$

where,

$m\left(\boldsymbol{X_{i,t}}|\boldsymbol{\beta}\right)$: incremental model (Equation 3.7)

S: total number of test sections

T_i: total number of observations at section i

T: total number of test sections in the experiment

Selection of Prior Distributions

Assuming independence among the marginal prior distributions, the joint prior distribution takes the form shown in Equation 3.9.

$$p(\boldsymbol{\beta}, \sigma^2) = \prod_{j=1}^{J} p\left(\beta_j\right) p(\sigma^2) \quad (3.9)$$

where,

$p\left(\beta_j\right)$: marginal prior distribution for the model parameter β_j

$p(\sigma^2)$: marginal prior distribution for the variance of the error term

J: total number of parameters in vector $\boldsymbol{\beta}$

The marginal prior distribution adopted for each model parameter β_j consisted of non-informative normal distributions (Equation 3.10) with zero mean and high variance

(i.e., 1.0E6), resulting in essentially flat distributions with an unrestricted domain from -∞ to ∞. Since the variance of the error term has to be positive, its prior (Equation 3.11) was defined as an inverse gamma distribution with both parameters equal to 0.001 (i.e., non-informative). These vague distributions were adopted to reflect the lack of previous experimental data similar to that collected for the AASHO Road Test.

$$p(\beta_j) = N\left(\mu_{\beta_j} = 0, \sigma^2_{\beta_j} = 10^6\right) \propto \sigma^{-1}_{\beta_j} exp\left(-\left(\beta_j - \mu_{\beta_j}\right)^2 / 2{\sigma_{\beta_j}}^2\right) \quad (3.10)$$

$$p(\sigma^2) = IG(a = 10^{-3}, b = 10^{-3}) \propto (\sigma^2)^{(-a-1)} exp\left({-b}/{\sigma^2}\right) \quad (3.11)$$

where,

μ_{β_j} and σ_{β_j}: fixed mean and standard deviation of the prior distribution for β_j

a and b: fixed shape and scale of inverse gamma prior distribution for σ^2

Joint Posterior Distribution

Equation 3.12 shows the resulting form of the posterior joint distribution of the model parameters and the variance of the error term given the observed data, corresponding to the incremental pavement performance model.

$$p(\boldsymbol{\beta}, \sigma^2 \,|\Delta\boldsymbol{PSI}) \propto \prod_{j=1}^{J} p(\beta_j)\, p(\sigma^2) p(\Delta\boldsymbol{PSI}|\boldsymbol{\beta}, \sigma^2) \propto$$

$$(\sigma^2)^{(-a-1)} exp\left(\frac{-b}{\sigma^2}\right) exp\left(\frac{-1}{2{\sigma_{\beta_j}}^2}\sum_{j=1}^{J}\left(\beta_j - \mu_{\beta_j}\right)^2\right)\left(\frac{1}{\sigma^2}\right)^{\frac{T}{2}} exp\left(\frac{-1}{2\sigma^2}\sum_{i=1}^{S}\sum_{t=1}^{T_i}\left(\Delta PSI_{i,t} - m\left(\boldsymbol{X_{i,t}}|\boldsymbol{\beta}\right)\right)^2\right) \quad (3.12)$$

Setup of Markov chain Monte Carlo (MCMC) Chain

The MCMC simulation for estimating this model specification was performed in duplicate, using both a code written by the author in R programming language (R Core Team, 2016) and in WinBUGS14 (Lunn, et al., 2009) in order to corroborate the results.

Two chains per simulation were run starting from different initial values. The initial value of each model parameter for each chain was randomly drawn from a normal distribution centered on an initial estimate for the posterior modes of the parameters and a coefficient of variation of 20%. The initial estimates for the posterior modes of the parameters were $[\boldsymbol{\beta_{in}}, \sigma_{in}^2] = [-5.500, -0.020, -0.006, -0.006, -0.005, -0.250, 0.750, 2.200, 3.500, 0.100]$. These values were selected as a combination of maximum likelihood estimates (MLE) reported in similar studies (Prozzi, 2001; Huang, 1993; Hong and Prozzi, 2006) and values selected based on the author's engineering judgment.

Different scales of the proposal distribution for each estimated parameter were tried in an iterative process until reaching an acceptable convergence for the simulated chains; i.e., until the converging criteria described in Chapter 2 were satisfied. The simulated chains obtained after setting up the MCMC algorithm showed acceptable convergence for the parameters' posterior distributions after 50,000 iterations. The "burn-in" number of iterations was set to 15,000 and the thinning interval was set to 5 iterations in order to reduce the autocorrelation of the sampling. Therefore, the resulting number of samples for each posterior distribution was 7,000.

Results from Estimation of Pavement Performance Model

Table 3.3 and Figure 3.5 present the summary statistics and the estimated posterior marginal densities of the model parameters from the MCMC simulations. The mean values for the posterior distributions are similar to the MLE estimates reported in related studies that used the same dataset (Prozzi, 2001; Hong and Prozzi, 2006). This observation is expected, as non-informative priors were assigned to each parameter. The Bayesian estimation of this model allows for obtaining the distribution of the estimated parameters

as opposed to only a point estimate. As observed from Figure 3.5, the posterior densities of all parameters are essentially symmetrically distributed around its mean except for β_{FA} and β_{TA}, which present positively skewed distributions.

The last three columns of Table 3.3 show the median and the boundaries of the 95% credible interval for each parameter. From the credible intervals it is observed that all the parameters were significant in explaining the change in PSI with more than 95% confidence. In addition, the mean of the posterior distribution for the variance of the error term was 0.067; therefore, the standard error of the pavement performance model in Equation 3.6 is estimated as $\sigma = 0.259$.

Table 3.3. Summary statistics of posterior marginal distribution of model parameters for the Bayesian specification.

Parameter	**Mean**	**Std**	**2.5%**	**Median**	**97.5%**
β_0	-4.86E+00	2.24E-01	-5.28E+00	-4.86E+00	-4.39E+00
β_{sur}	-2.03E-02	1.99E-03	-2.43E-02	-2.03E-02	-1.67E-02
β_b	-4.27E-03	5.63E-04	-5.40E-03	-4.27E-03	-3.19E-03
β_{sb}	-5.20E-03	5.02E-04	-6.22E-03	-5.20E-03	-4.24E-03
β_g	-3.78E-03	1.68E-04	-4.11E-03	-3.78E-03	-3.45E-03
β_n	-3.32E-01	1.76E-02	-3.64E-01	-3.32E-01	-2.96E-01
β_{FA}	6.37E-01	2.57E-01	3.90E-01	5.48E-01	1.42E+00
β_{TA}	2.41E+00	4.83E-01	1.96E+00	2.27E+00	3.71E+00
β_{AL}	2.97E+00	2.39E-01	2.51E+00	2.96E+00	3.45E+00
σ^2	6.70E-02	1.12E-03	6.49E-02	6.70E-02	6.92E-02
Deviance	9.69E+02	4.40E+00	9.62E+02	9.68E+02	9.79E+02

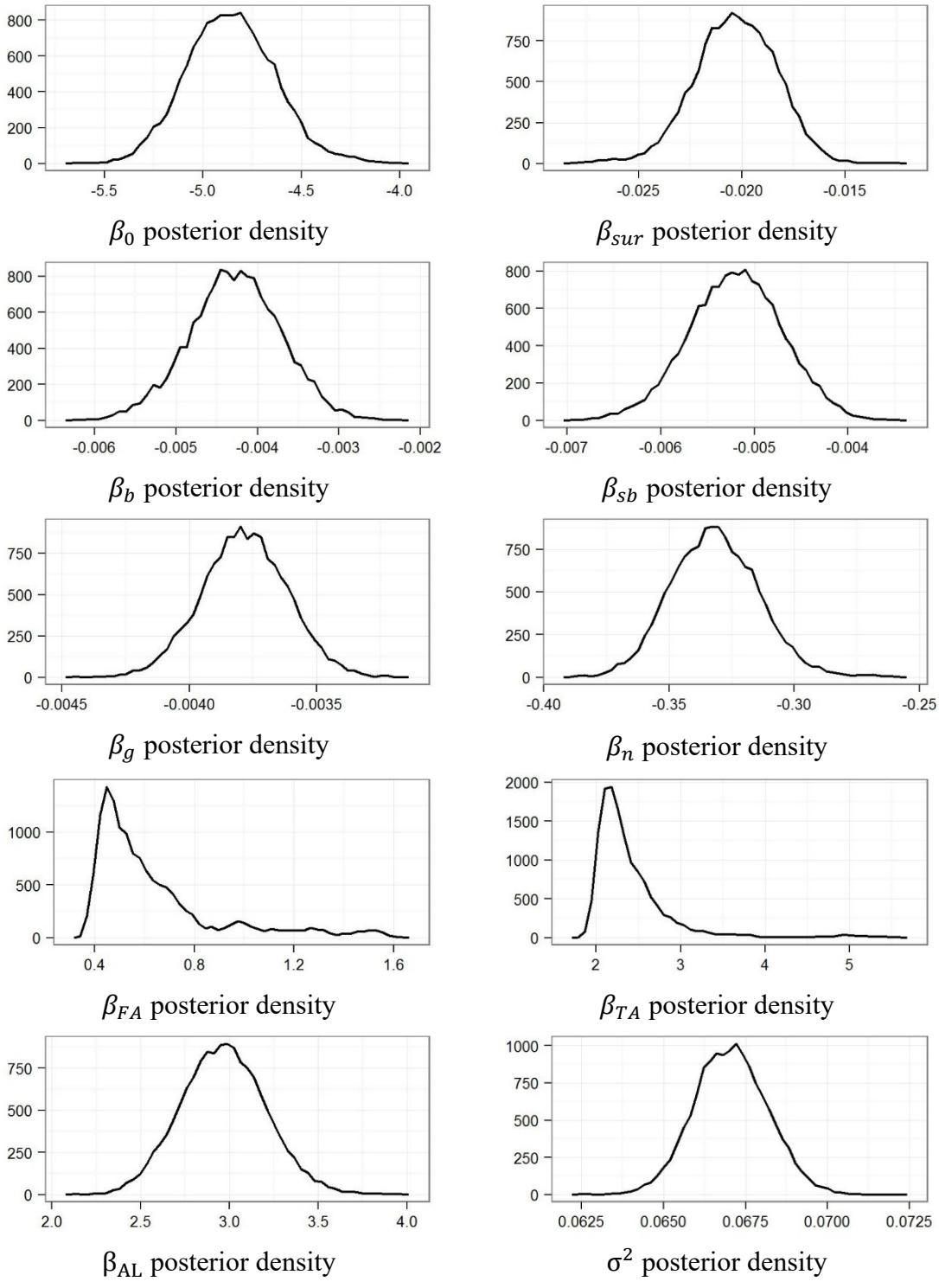

Figure 3.5: Posterior densities of estimated performance model parameters.

The summary statistics of the deviance distribution presented in Table 3.3 were used to compute the effective number of parameters and the deviance information criterion (DIC) of the model using Equations 2.13 and 2.10. Therefore, the Bayesian specification of the pavement performance model had an effective number of parameters, p_D, equal to 9.32 and a DIC equal to 975.77. These values were used to evaluate the impact of implementing the proposed specifications for capturing heterogeneity of effects in the next sections of this chapter.

BAYESIAN ESTIMATION OF PAVEMENT PERFORMANCE HIERARCHICAL MODEL

The Bayesian specification proposed in the previous section assumes homogenous effects for the different variables of the model across all pavement sections in the database. In order to relax this assumption given the observed over-dispersion of some of the model parameters, a hierarchical model specification is proposed. A hierarchical specification allows for estimating the parameters of particular subpopulations through partial pooling of the dataset where subpopulation estimates borrow strength from the rest of the data (Gelman et al., 2014). The combined sub-models can better capture systematic differences in the pavement performance response, obtaining more reliable estimates and improving the fitting of the model.

In order to demonstrate the use of a hierarchical specification for addressing possible heterogeneous effects in pavement data, the AASHO dataset was divided into two subpopulations for analysis:

- "thinner" structures, for the sections with AC layer (H_{sur}) thinner than 100 mm (i.e. 1 to 3 inches); and
- "thicker" structures, for the sections with an AC layer thicker than 100 mm (i.e., 4 to 6 inches).

The parameters estimated following a hierarchical structure were those related to environmental factors and the characterization of traffic loads and axle types, i.e., β_g, β_n, β_{FA}, β_{TA}, and β_{AL}. A hierarchical estimation of the traffic characteristics according to these two subpopulations allows for testing whether certain axle types and loads are more damaging for thinner pavement structures or not, and to quantify their different deterioration rates.

Hierarchical Model Specification

The joint posterior distribution of the model parameters with hierarchical specification is expressed in Equation 3.13, where the posterior distribution is proportional to the likelihood times the prior times the hyper-priors as derived from the Bayes's theorem (Gelman et al., 2014).

$$p(\boldsymbol{\beta}, \sigma^2|\Delta\boldsymbol{PSI}) \propto p(\Delta\boldsymbol{PSI}|\boldsymbol{\beta}, \sigma^2)p(\boldsymbol{\beta}, \sigma^2|\boldsymbol{\lambda})p(\boldsymbol{\lambda}) \quad (3.13)$$

where,

$p(\Delta\boldsymbol{PSI}|\boldsymbol{\beta}, \sigma^2)$: likelihood of the observed drop in PSI given the parameters

$p(\boldsymbol{\beta}, \sigma^2|\boldsymbol{\lambda})$: prior joint distribution of parameters given the hyper-parameters

$p(\boldsymbol{\lambda})$: prior joint distribution of model hyper-parameters

The likelihood function of this model is as specified in Equation 3.8 but incorporates the sub-index s for β_{g_s}, β_{n_s}, β_{FA_s}, β_{TA_s}, and β_{AL_s} into the incremental model (Equation 3.7). The sub-index s is equal to one for pavement sections with thinner AC layers and two for those with thicker AC layers.

Selection of Prior Distributions

The prior distribution for each of the model parameters with non-hierarchical structure $(\beta_0, \beta_{sur}, \beta_b \; and \; \beta_{sb})$ was specified as in Equation 3.9; i.e., a non-informative

normal distribution. The prior distributions for β_{g_s}, β_{n_s}, β_{FA_s}, β_{TA_s}, and β_{AL_s} were defined as normally distributed with a random mean and low variance (Equation 3.14). The parameters without corresponding hyper-parameters are referred to with the sub-index j, whereas the parameters with hierarchical structure are referred to with the sub-index r.

Equation 3.15 shows the hyper-prior for each hyper-parameter, which was also defined as non-informative normal with mean zero and low precision in order to reflect the lack of previous information.

$$p(\beta_r) = N(\mu_r = \lambda_r, \sigma_r^2 = 10^6) \propto \sigma_r^{-1} exp(-(\beta_r - \lambda_r)^2 / 2{\sigma_r}^2) \tag{3.14}$$

$$p(\lambda_r) = N\left(\mu_r = 0, \sigma_{\lambda_r}^2 = 10^3\right) \propto \sigma_{\lambda_r}^{-1} exp\left(-\lambda_r^2 / 2\sigma_{\lambda_r}^2\right) \tag{3.15}$$

where,

$p(\beta_r)$: prior distribution of parameters with hierarchical structure

$p(\lambda_r)$: prior distribution of hyper-parameters

λ_r: hyper-parameter for the mean of β_r

σ_r^2: fixed standard deviation of the prior distribution for β_r

μ_r and σ_r: fixed mean and standard deviation of the hyper-prior distribution

Joint Posterior Distribution

Equation 3.16 presents the final form of the posterior joint distribution of the model parameters, hyper-parameters, and error term variance given the observed data, corresponding to the hierarchical specification (Equation 3.12) of the incremental pavement performance model.

$$p(\boldsymbol{\beta}, \sigma^2, \boldsymbol{\lambda}_r \,|\Delta \boldsymbol{PSI}) \propto \prod_{j=1}^{J} p\left(\beta_j\right) \prod_{r=1}^{R} p(\beta_r) \prod_{r=1}^{R} p(\lambda_r)\, p\left(\frac{1}{\sigma^2}\right) p(\Delta \boldsymbol{PSI} | \boldsymbol{\beta}) \propto$$

$$\left(\frac{1}{\sigma_j^2}\right)^{\frac{J}{2}} exp\left(\sum_{j=1}^{J}\frac{-{\beta_j}^2}{2{\sigma_j}^2}\right)\left(\frac{1}{\sigma_r^2}\right)^{\frac{R}{2}} exp\left(\sum_{r=1}^{R}\frac{-(\beta_r-\lambda_r)^2}{2{\sigma_r}^2}\right)\left(\frac{1}{\sigma_{\lambda_r}^2}\right)^{\frac{R}{2}} exp\left(\sum_{r=1}^{R}\frac{-\lambda_r^2}{2\sigma_{\lambda_r}^2}\right)$$

$$(\sigma^2)^{(-a-1)} exp\left(\frac{-b}{\sigma^2}\right)\left(\frac{1}{\sigma^2}\right)^{T/2} exp\left(\frac{-1}{2\sigma^2}\sum_{i=1}^{S}\sum_{t=1}^{T_i}\left(\Delta PSI_{i,t} - m(\boldsymbol{X_{i,t}}|\boldsymbol{\beta})\right)^2\right) \quad (3.16)$$

where,

$p\left(\boldsymbol{\beta}, \frac{1}{\sigma^2}, \boldsymbol{\lambda}_r \middle| \Delta \boldsymbol{PSI}\right)$: joint posterior distribution of parameters, hyper-parameters, and error term variance

J: total number of model parameters without hyper-parameters

R: total number of model parameters with hyper-parameters

Results from Estimation of Hierarchical Model

Table 3.4 presents the results from the MCMC simulations carried out to estimate the posterior marginal distribution of the parameters from the model with hierarchical specification (Equation 3.12). The sub-index $s = 1$ refers to the subpopulation of pavement sections with surface layer thinner than 100 mm, whereas $s = 2$ refers to the subpopulation with thicker surface layers. The MCMC algorithm was set up to reach acceptable convergence for the model parameters for the two 50,000-iteration long simulated chains run simultaneously.

The effective number of parameters and the DIC for the hierarchical specification of the pavement performance model were computed using the summary statistics of the deviance in Table 3.4, obtaining a $p_D = 11.92$ and a $DIC = 944.35$. The DIC of the hierarchical specification was lower than that of the non-hierarchical specification despite the greater number of parameters, showing an improved fit of the observed data. In addition, the hierarchical model specification had the advantage of allowing for making inferences about the different damaging effects of traffic characteristics and frost penetration gradient between thin and thick pavements.

Table 3.4. Summary statistics of posterior marginal distribution of model parameters for hierarchical specification.

Parameter	Mean	Std	2.5%	Median	97.5%
β_0	-4.82E+00	1.51E-01	-5.14E+00	-4.79E+00	-4.57E+00
β_{sur}	-2.11E-02	1.54E-03	-2.41E-02	-2.11E-02	-1.81E-02
β_b	-4.82E-03	5.15E-04	-5.60E-03	-4.87E-03	-3.64E-03
β_{sb}	-6.10E-03	5.54E-04	-7.25E-03	-6.07E-03	-5.00E-03
$\beta_{g_{s=1}}$	-4.43E-03	2.06E-04	-4.86E-03	-4.41E-03	-3.95E-03
$\beta_{g_{s=2}}$	-3.12E-03	1.86E-04	-3.48E-03	-3.11E-03	-2.66E-03
$\beta_{n_{s=1}}$	-3.14E-01	1.96E-02	-3.48E-01	-3.17E-01	-2.78E-01
$\beta_{n_{s=2}}$	-2.95E-01	2.26E-02	-3.37E-01	-2.97E-01	-2.57E-01
$\beta_{FA_{s=1}}$	4.20E-01	2.17E-02	3.75E-01	4.20E-01	4.63E-01
$\beta_{FA_{s=2}}$	9.72E-01	1.27E-01	7.78E-01	9.62E-01	1.23E+00
$\beta_{TA_{s=1}}$	3.31E+00	2.50E-01	2.81E+00	3.34E+00	3.75E+00
$\beta_{TA_{s=2}}$	1.96E+00	7.41E-02	1.81E+00	1.97E+00	2.08E+00
$\beta_{AL_{s=1}}$	3.89E+00	1.40E-01	3.67E+00	3.87E+00	4.15E+00
$\beta_{AL_{s=2}}$	3.14E+00	1.26E-01	2.91E+00	3.13E+00	3.43E+00
σ^2	6.67E-02	1.10E-03	6.45E-02	6.67E-02	6.85E-02
Deviance	9.32E+02	4.88E+00	9.24E+02	9.32E+02	9.44E+02

Table 3.4 indicates that all of the parameters are different than zero with more than 95% confidence; therefore, all of the model parameters are significant in explaining the change in pavement condition. Comparing the effects between the subpopulations of thinner and thicker pavements reveals a significant overlap between the 95% credible intervals for β_{n_s}. This observation indicates that the effect of the truck traffic count in terms

of structural damage does not vary across the thin and thick pavement subpopulations. On the other hand, the 95% credible intervals for all other parameters with hierarchical structure do not overlap between subpopulations; therefore, their effect differs significantly between thinner and thicker pavements. Furthermore, the parameter β_{g_s} was greater in magnitude for the subpopulation of thinner pavements, which indicates that thinner pavements were more susceptible to the frost penetration gradient. Similarly, $\beta_{TA_{s=1}} > \beta_{TA_{s=2}}$ and $\beta_{AL_{s=1}} > \beta_{AL_{s=2}}$, which indicates that the damaging effect that tandem axles and load magnitude have on thin pavements is greater than on thick pavements. This observation might be explained by the wider stress bulb, and consequently lower strains, that occur on thicker HMA layers.

BAYESIAN ESTIMATION OF PAVEMENT SERVICEABILITY MIXTURE MODEL

This section presents the estimation results of the pavement serviceability model using a finite mixture specification in order to account for heterogeneity of effects at a group level, further improving the estimation of each variable's effect and the model fit. A finite mixture model specifies the likelihood of the data as a convex combination of density functions and allows for assigning the different observations into a finite number of latent classes through the estimation of the posterior marginal densities of the model parameters given the observed data. Thus, the clustering of the cross-sectional units is driven by the data in an unsupervised manner and captures unobserved factors. As a result, the estimation of this model specification provides a finite number of models. These models capture systematic differences in pavement performance response that cannot be sufficiently explained by the individual model variables, along with the probability of the different observations belonging to each class.

Finite Mixture Model Specification

Equation 3.17 shows the proposed finite mixture model specification where the probability of observing the drop in serviceability between data collection dates is a weighted sum of $K = 2$ normal distributions. Two model parameters were specified to vary across clusters, the intercept, $\beta_{0,k}$, and the effect of the number of ESALs, $\beta_{n,k}$. Thus, the proposed model specification allows for capturing heterogeneous effects due to unobserved factors and interactions, allowing for the parameters on the traffic variables to change across clusters. The effect of the remaining variables are assumed to be homogeneous across observations and, therefore, specified as constant across clusters.

$$p\left(\Delta PSI_{i,t} \middle| \boldsymbol{w}, \boldsymbol{\beta}, \boldsymbol{\sigma^2}\right) = \sum_{k=1}^{K=2} w_k \, N(\Delta\widehat{PSI_{i,t,k}}, \sigma_k^2) \tag{3.17}$$

$$\Delta\widehat{PSI_{i,t,k}} = exp\left(\beta_{0,k} + \beta_{sur} T_{sur,i} + \beta_b T_{b,i} + \beta_{sb} T_{sb,i} + \beta_g G_t\right)\left\{\left(\frac{FA_i}{18\beta_{FA}}\right)^{\beta_{AL}} + A_i\left(\frac{SA_i}{18}\right)^{\beta_{AL}} + B_i\left(\frac{TA_i}{18\beta_{TA}}\right)^{\beta_{AL}}\right\}^{\beta_{n,k}+1}\left(\sum_{l=1}^{t-1} n_{i,l}\right)^{\beta_{n,k}} n_{i,t} \tag{3.18}$$

where,

$\Delta\widehat{PSI_{i,t,k}}$: predicted drop in PSI for section i at time t and cluster k

$\beta_{j,k}$: model parameter j for model corresponding to cluster k

σ_k: variance of error term for model corresponding to cluster k

w_k: weight of cluster k, where $\sum_{k=1}^{2} w_k = 1$

As shown in Equation 3.19, the likelihood function of the model was specified to assign the observations within cross-sectional units to the same class. Thus, the estimated model was used to capture heterogeneous effects across pavement sections.

$$p(\Delta \boldsymbol{PSI} | \boldsymbol{w}, \boldsymbol{\beta}, \boldsymbol{\sigma}^2) = \prod_{i=1}^{S} \sum_{k=1}^{2} w_k \left(\prod_{t=1}^{T_i} \sqrt{\frac{1}{2\pi\sigma_k^2}} e^{\frac{-1}{2\sigma_k^2}\left(\Delta PSI_{i,t} - \Delta\widehat{PSI_{i,t,k}}\right)^2} \right) \tag{3.19}$$

Selection of Prior Distributions

The adopted prior distributions for all model parameters $\beta_{j,k}$ and for the error term variance σ_k^2 for each cluster were non-informative, as was the case for the specification with one cluster previously estimated. These priors consisted of flat Gaussian distributions for each model parameter $\beta_{j,k}$ (Equation 3.10) and vague inverse-gammas for each error term variance σ_k^2 (Equation 3.11).

The prior distribution adopted for the weights w_k consisted of a Dirichlet distribution (Equation 3.20) with its vector of parameters set to $\boldsymbol{\alpha} = [1,1]$. Thus, the prior for the weights of the K clusters was non-informative to reflect the lack of previous information on the proportion of pavement sections belonging to each latent class.

$$p(\boldsymbol{w}) = Dir(\boldsymbol{\alpha}) \propto \prod_{k=1}^{K} w_k^{\alpha_k - 1} \tag{3.20}$$

where,

$p(\boldsymbol{w})$: prior distribution for the vector of weights of the K clusters

$\boldsymbol{\alpha}$: vector of parameters of Dirichlet distribution

Joint Posterior Distribution

The joint posterior distribution of model parameters, weights, and error term variance is derived from the specified likelihood function and the adopted prior distributions as shown in Equation 3.21.

$$p(\boldsymbol{w}, \boldsymbol{\beta}, \boldsymbol{\sigma^2} | \Delta \boldsymbol{PSI}) \propto \prod_{k=1}^{K} \prod_{j=1}^{J} p(\boldsymbol{w}) p(\beta_{j,k})\, p(\sigma_k^2) p(\Delta \boldsymbol{PSI} | \boldsymbol{w}, \boldsymbol{\beta}, \boldsymbol{\sigma}^2) \propto$$
$$\prod_{k=1}^{2} \left((\sigma_k^2)^{(-a-1)} exp\left(\frac{-b}{\sigma_k^2}\right) \right) exp\left(\frac{-1}{2\sigma_{\beta_{j,k}}{}^2} \sum_{k=1}^{2} \sum_{j=1}^{J} \left(\beta_{j,k} - \right. \right.$$
$$\left. \left. \mu_{\beta_{j,k}} \right)^2 \right) \prod_{i=1}^{S} \sum_{k=1}^{2} w_k \left(\prod_{t=1}^{T_i} \frac{1}{\sigma_k} \exp\left(\frac{-1}{2\sigma_k^2} \left(\Delta PSI_{i,t} - \Delta \widehat{PSI_{\iota,t,k}} \right)^2 \right) \right) \tag{3.21}$$

Results from Estimation of Finite Mixture Model

Table 3.5 shows the summary statistics of the marginal posterior distributions estimated from the MCMC simulations. From the credible intervals, it is observed that all the parameters were significant in explaining the change in PSI with more than 95% confidence. In addition, the DIC of the mixture model specification, computed as in Equation 2.10, was equal to 18.66. The significant difference in DIC between the model specified with complete pooling of observations (Equation 3.6) and the mixture of two clusters shows the large unobserved heterogeneity present in the data, as suggested by other studies in the literature (Archilla, 2000; Prozzi, 2001; Hong and Prozzi, 2010). The difference in DIC also reflects the significant gain in model fit achieved by properly specifying the heterogeneous response of pavement subpopulations through the group-level clustering technique proposed in this study.

About 65% of the pavement sections were assigned to Cluster 1 and the remaining 35% were assigned to Cluster 2. These weights are estimates of the probability of an unobserved pavement section belonging to each cluster. The significant differences between the model parameters for each cluster attest to the different pavement performance response for the two heterogeneous subpopulations. The model parameters estimated for Cluster 1 show a smaller effect of cumulated traffic, β_{n_1}, and a smaller baseline parameter β_{0_1}; therefore, Cluster 1 captured the sections with lower deterioration rate after controlling for all the observed variables in the model. Since all pavement sections included in the AASHO Road Test were designed and built with the same materials and specifications, unobserved factors that may explain these difference may be related to local variations in the compaction of the pavement layers and subgrade or the presence of voids in the soil, among others possible explanations.

Table 3.5. Summary statistics of posterior marginal distribution of model parameters for the mixture model specification.

Parameter	Mean	Std	2.5%	Median	97.5%
β_{0_1}	-6.75E+00	4.33E-01	-7.59E+00	-6.77E+00	-5.87E+00
β_{0_2}	-4.51E+00	3.09E-01	-5.14E+00	-4.50E+00	-3.89E+00
β_{sur}	-1.77E-02	2.52E-03	-2.26E-02	-1.76E-02	-1.30E-02
β_b	-3.50E-03	8.44E-04	-5.15E-03	-3.51E-03	-1.90E-03
β_{sb}	-5.79E-03	7.67E-04	-7.26E-03	-5.78E-03	-4.36E-03
β_g	-3.63E-03	2.04E-04	-4.03E-03	-3.63E-03	-3.24E-03
β_{n_1}	-2.28E-01	4.35E-02	-2.91E-01	-2.37E-01	-1.29E-01
β_{n_2}	-3.85E-01	2.60E-02	-4.29E-01	-3.84E-01	-3.33E-01
β_{FA}	3.42E-01	3.33E-02	2.85E-01	3.38E-01	4.28E-01
β_{TA}	2.57E+00	8.77E-01	1.67E+00	2.26E+00	4.90E+00
β_{AL}	3.11E+00	2.47E-01	2.66E+00	3.12E+00	3.61E+00
w_1	65.1%	3.7%	57.7%	65.1%	72.0%
w_2	34.9%	3.7%	28.0%	34.9%	42.3%
σ_1^2	4.27E-02	1.25E-03	4.04E-02	4.27E-02	4.53E-02
σ_2^2	1.54E-01	8.97E-03	1.38E-01	1.53E-01	1.72E-01
Deviance	-2.64E+01	9.49E+00	-4.15E+01	-2.75E+01	-3.59E+00

The different performance response for the two clusters is illustrated in Figure 3.6. These curves were computed as shown in Equation 3.23, for which the values for the remaining independent variables were set to be constant across clusters for the purpose of comparison. The pavement layer thicknesses in this example were set to the mean values reported in Table 3.2, the axle loads were those corresponding to the truck configuration assigned to Loop 4 and Lane 2 (Table 3.1), and the frost penetration gradient was set to zero across time. As shown in Figure 3.6, the difference of predicted drop in PSI between clusters decreases with the number of ESALs.

$$ESAL_l = \sum_{l=1}^{t-1} n_l \left\{ \left(\frac{FA_i}{18\beta_{FA}} \right)^{\beta_{AL}} + A_i \left(\frac{SA_i}{18} \right)^{\beta_{AL}} + B_i \left(\frac{TA_i}{18\beta_{TA}} \right)^{\beta_{AL}} \right\} \quad (3.22)$$

$$\widehat{\Delta PSI_{t,k}} = E\left[\Delta PSI_{t,k} | k, \boldsymbol{\beta_k}\right] = \begin{cases} C\ exp(-6.75)\ ESAL_t^{-0.228}, & k = 1 \\ C\ exp(-4.51)\ ESAL_t^{-0.385}, & k = 2 \end{cases} \quad (3.23)$$

where,

$\widehat{\Delta PSI_k}$: predicted drop in PSI at time t and cluster k

$ESAL_t$: cumulated ESAL at time t

C: constant across clusters for fixed layer thicknesses, weather, and traffic increment

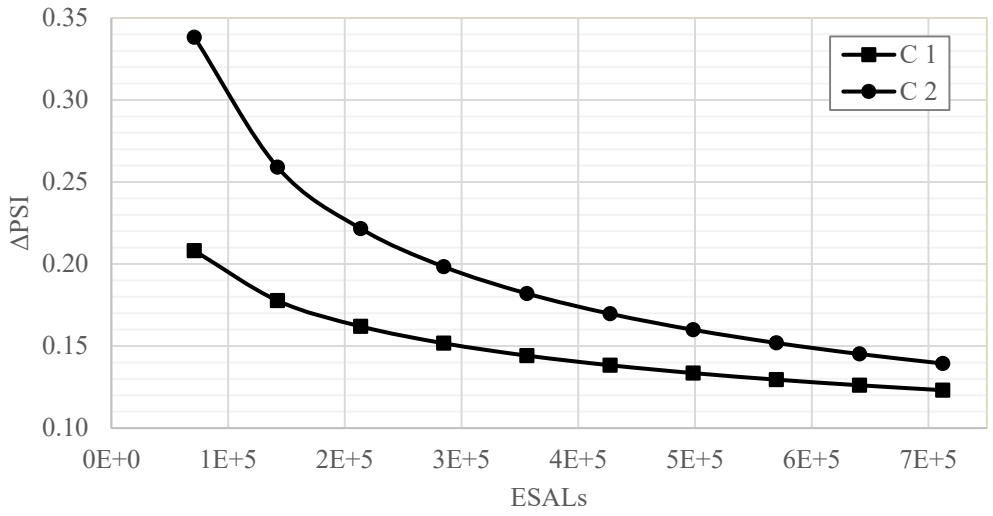

Figure 3.6: Drop in PSI as a function of cumulated ESALs for the two estimated clusters.

In addition, Figure 3.7 shows the different performance curves predicted by each of the two clusters in the example, as well as for the weighted mixture of clusters. The performance curve was computed as shown in Equation 3.24, assuming an initial PSI of 3.20. For instance, adopting a terminal serviceability of 3.0, the representative pavement

section of this case scenario would reach the end of life approximately 1.9E+05 ESALs earlier if it follows the behavior described by the Cluster 2 model. This simple example shows the significant practical implications of properly modeling the heterogeneous performance response of subpopulations of pavements due to unobserved factors in management applications.

$$\widehat{PSI_{t,k}} = E\left[PSI_{t,k}|k, \boldsymbol{\beta_k}\right] = PSI_0 - \sum_{l=1}^{t} E\left[\Delta PSI_{t,k}|k, \boldsymbol{\beta_k}\right] \quad (3.24)$$

$$\widehat{PSI_t} = E[PSI_t|k, \boldsymbol{w}, \boldsymbol{\beta}] = PSI_0 - \sum_{l=1}^{t} \sum_{k=1}^{K} w_k E\left[\Delta PSI_{l,k}|k, \boldsymbol{\beta_k}\right] \quad (3.25)$$

where,

$\widehat{PSI_{t,k}}$ =: predicted PSI at time t and cluster k

$\widehat{PSI_t}$ =: predicted PSI at time t from mixture of clusters

PSI_0: PSI value at beginning of service life

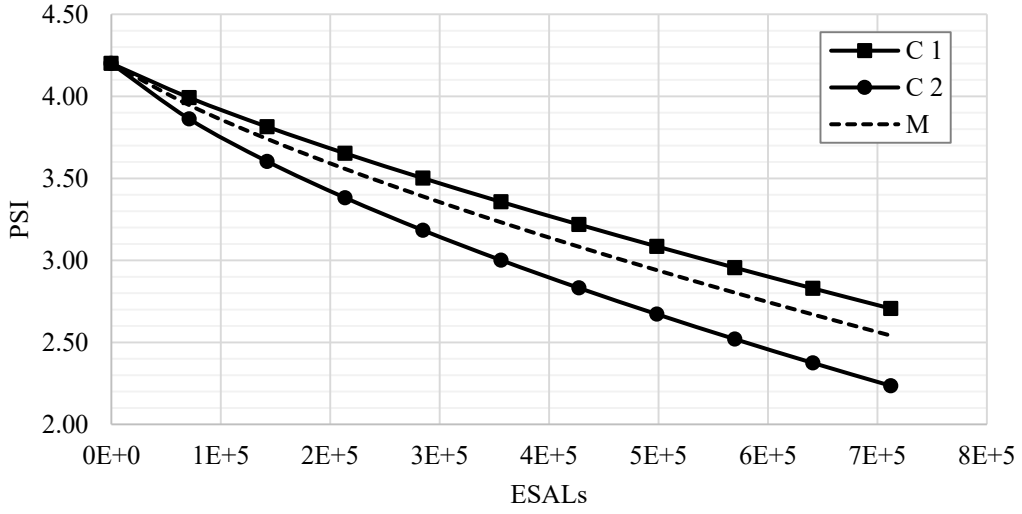

Figure 3.7: PSI as a function of cumulated ESALs for the two estimated clusters (C1 and C2) and for the mixture of clusters (M).

Sensitivity of timespan of collected data to pavement section clustering

An additional analysis was conducted to evaluate how the number of years of data used to estimate the model affects the clustering of pavement sections. For this, the mixture model specification was estimated using data from the first half of the duration of the AASHO Road Test (i.e., data from the first year) and the resulting clustering of pavement sections was compared to the one resulting from estimating all the available data.

Table 3.6 shows the summary statistics of the posterior marginal distributions of the model parameters estimated using only data from the first year. The estimated scale parameter, β_{0_k}, and traffic parameter, β_{n_k}, show that the first cluster captured the pavement sections with slower deterioration rate, as observed in the model estimated using all the available data. The estimated parameters for the remaining explanatory variables were similar to the ones estimated using all data.

Table 3.6. Summary statistics of posterior marginal distribution of parameters for the mixture model estimated using data from the first year of the experiment.

Parameter	Mean	Std	2.5%	Median	97.5%
β_{0_1}	-6.49E+00	4.65E-01	-7.61E+00	-6.46E+00	-5.61E+00
β_{0_2}	-5.84E+00	5.26E-01	-6.93E+00	-5.80E+00	-4.83E+00
β_{sur}	-1.40E-02	3.14E-03	-2.06E-02	-1.40E-02	-7.87E-03
β_b	-1.62E-03	8.38E-04	-3.22E-03	-1.63E-03	1.11E-06
β_{sb}	-4.34E-03	7.61E-04	-5.81E-03	-4.35E-03	-2.89E-03
β_g	-3.65E-03	2.81E-04	-4.19E-03	-3.65E-03	-3.07E-03
β_{n_1}	-3.89E-01	2.39E-02	-4.35E-01	-3.89E-01	-3.44E-01
β_{n_2}	-2.91E-01	3.45E-02	-3.59E-01	-2.92E-01	-2.22E-01
β_{FA}	2.96E-01	1.93E-01	6.86E-02	2.41E-01	8.79E-01
β_{TA}	2.09E+00	1.20E-01	1.91E+00	2.07E+00	2.41E+00
β_{AL}	3.08E+00	2.31E-01	2.66E+00	3.08E+00	3.53E+00

For comparison purposes, Table 3.7 presents the number of pavement sections assigned to each of the two clusters from the estimation of the mixture model using the data from the first year of the experiment cross-tabulated with the number of sections assigned to each cluster when using all data. For instance, 126 pavement sections were assigned to the first cluster (C1) from the estimation of the model using each dataset, whereas 34 pavement sections that were assigned to the second cluster (C2) when using data from the first year only were assigned to C1 when using all data. 84% of the 252 pavement sections of the AASHO Road Tests were clustered in the same group, having a larger number of sections switching from C1 to C2 when considering all the available data in the estimation.

Table 3.7. Comparison of number of sections assigned to each of the two clusters from the estimation using data from the first year and using all data.

		all data		
		C1	**C2**	
first year	**C1**	126	7	*53%*
	C2	34	85	*47%*
		63%	*37%*	

In addition, Table 3.7 shows the proportion of pavement sections assigned to each of the two clusters (values in italics) from the estimation of each dataset. Thus, approximately 47% of the sections were assigned to the cluster with faster deterioration rate (i.e., to C2) when using data from the first year only, whereas this percentage decreased to 37% when using all the available data. Data from the second year contains observations for higher levels of cumulated traffic, which are related to smaller observed changes in serviceability. Incorporating the smaller changes in serviceability to the estimation results in flatter performance curves. When the flattening of the performance curve was large

enough, the corresponding pavement section switched from C2 to C1 when considering all data.

Chapter 4: Estimation of Pavement Roughness Mixture Model

This chapter covers the development of a pavement roughness mixture model using field performance data from a nationwide database and further calibrated for Texas highway conditions by combining the nationwide and the Texas Department of Transportation (TxDOT) data. The first part of this chapter provides information on the data sources from which data were extracted and describes the processing and filtering criteria applied. The second and third sections describe the model specifications and results from the estimation of both the nationwide and Texas data.

DESCRIPTION OF PAVEMENT ROUGHNESS FIELD DATA

Nationwide field roughness data were obtained from the Long-Term Pavement Performance (LTPP) database; more specifically, from measurements collected for the Specific Pavement Study (SPS)-3 experiment "Preventive Maintenance of Flexible Pavements". The database containing roughness measurements from Texas was developed from a number of data sources, including various TxDOT information systems and the National Oceanic and Atmospheric Administration (NOAA).

Nationwide Pavement Roughness Field Data

The LTPP SPS-3 experiment was designed to assess the effectiveness of PM treatments on flexible pavements and to evaluate the optimum timing to apply the treatments. This experiment considered four different preventive maintenance (PM) treatments: thin hot-mix asphalt overlay (TH), slurry seal, chip seal (CH), and crack seal. These PM treatments were applied to consecutive 500-ft-long sections (Figure 4.1) of existing in-service roads along with non-treated (control) sections at 81 sites located in 33 states and Canada during the early 1990s. Thus, each site consisted of five consecutive sections all subject to the same traffic loads, structure, and environmental conditions.

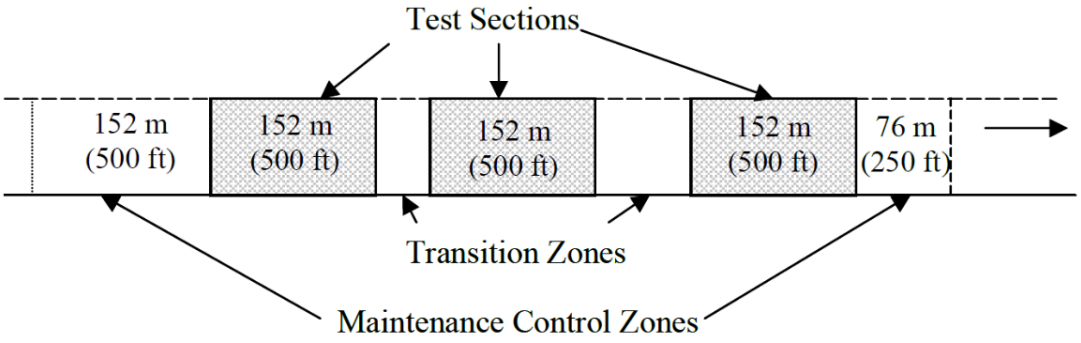

Figure 4.1: Layout of control and treated sections on a generic site of the LTPP SPS-3 experiment (Elkins et al., 2003).

Some of the design factors considered for the experiment included four climatic regions (all combinations of freeze and no-freeze areas and wet and dry areas); two subgrade types (fine grained or coarse grained soils); two traffic levels (low and high); and three existing pavement conditions (good, fair, and poor) (Elkins et al., 2003). The combinations of treatments were not considered in the experimental design.

A number of studies have used data from the LTPP SPS-3 experiment to assess the effectiveness of PM treatments, adopting different performance indices and implementing methodologies that included multiple regression analysis (Morian et al., 1998), survival analysis (Eltahan et al., 1999; Morian et al. 2011), and various statistical comparison techniques (Hall et al., 2003; Shirazi et al., 2010; Morian et al., 2011). Although the previous studies provide information on the relative effectiveness of treatments, the approach proposed in this dissertation overcomes limitations of previous studies in that it allows for comparing the treatment effectiveness for particular experimental factors while controlling for the remaining factors and producing more robust estimates of the treatment's marginal effect. In addition, the proposed model specifications accounts for

more variables and incorporates more realistic assumptions than the previous models found in the literature (refer to the literature review in Chapter 2).

Processing of LTPP SPS-3 Data

The LTPP SPS-3 experiment data used for estimating the proposed pavement roughness mixture model was obtained from the Standard Data Release version 29 (LTPP InfoPave 2015). The main filtering criteria applied to the original dataset consisted of considering only the pavement sections containing at least one computed annual number of equivalent single-axle loads (ESAL) during the years for which the SPS-3 experiment was conducted. The computed annual number of ESALs was obtained from the "TRF_ESAL_COMPUTED" table, and was estimated from monitored axle data (Elkins et al. 2003). Traffic data estimated from other sources was filtered out in order to make use of only the best quality data available for estimating the model.

The change in International Roughness Index (IRI) values for each point in time, ΔIRI, was computed as the difference between consecutive IRI measurements between data collection dates. Therefore, only sections with at least two roughness measurements collected during the SPS-3 experiment were considered for the analyses in this chapter. After applying the two filters mentioned, the resulting dataset included data from 64 SPS-3 sites (each site containing multiple pavement sections); Figure 4.2 maps these locations. As Figure 4.2 depicts, the filtered SPS-3 sites covered a variety of climatic regions in the study.

Figure 4.2: Location of LTPP SPS-3 sections used for estimating the model.

The increments of traffic values, $\Delta N_{i,\Delta t}$, were estimated as the sum of all annual number of ESALs corresponding to section i, weighted by the proportion of time falling within the period of analysis Δt. The annual number of ESALs for the years with missing traffic data were estimated as the mean value for the corresponding pavement section and period of analysis. Lastly, the values for accumulated traffic until the period of analysis, $N_{i,\Delta t}$, were computed as the sum of all preceding increments of traffic ($\Delta N_{i,\Delta t}$) for the corresponding pavement section.

The climatic variables were extracted from the "Climate Summary Data" tables, providing the temperature, freezing index, and precipitation values for each site. Temperature values consisted of the annual average of daily mean air temperatures; precipitation values consisted of annual total precipitation; and the freezing index was computed as the negative sum of all daily mean air temperatures below 0°C in a year (Elkins et al. 2003). The values for each of these climatic variables assigned to each

observation were computed as the average of their yearly values weighted by the proportion of time falling within data collection dates.

The subgrade type of each site was characterized with an indicator variable equal to one for coarse soils and zero otherwise. The pavement layer thicknesses for each section were computed as the sum of the layer thicknesses corresponding to the sub-base, base, and surface layer, respectively. In addition, two indicator variables were computed as a function of the pavement layer thicknesses in order to incorporate the pavement type categories for flexible pavements defined in TxDOT's Pavement Management Information System (PMIS): PavType_05 was equal to one when the surface layer was ≤ 5.5 inches and ≥ 2.5 inches, and zero otherwise; and PavType_06 was equal to one when the surface layer was <2.5 inches and zero otherwise.

Summary Statistics of LTPP SPS-3 Data

The processed dataset used for these analyses had a total of 1,076 observations. These observations were collected from 211 test sections grouped in 62 sites. The average number of observations throughout time per test section was 5.1, ranging from 2 to 14 IRI measurements per section. In addition, the average time between data collection dates was 464 days.

Figure 4.3 shows the distribution of the observed change in IRI value between data collection dates from the analyzed dataset. The mean change in IRI was equal to 0.068 m/km. Negative changes in IRI value are explained by measurement errors or as a result of factors not observed in the dataset and comprise 31.3% of the observations.

Table 4.1 shows the summary statistics for some of the continuous explanatory variables considered for estimating the models presented in the next sections of this chapter. The climatic variables, as well as the increment of number of ESALs and the

change in IRI value consist of the representative values for the period between data collection dates.

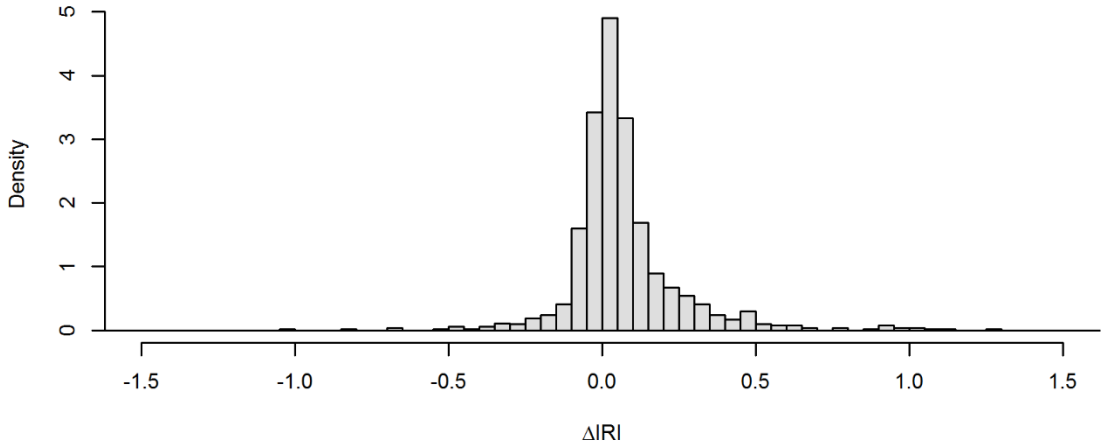

Figure 4.3: Distribution of change in IRI between data collection dates from the analyzed set of LTPP SPS-3 data.

Table 4.1. Descriptive statistics of main continuous explanatory variables from the analyzed LTPP SPS-3 data.

Variable		**unit**	**Mean**	**Std**	**Min**	**Max**
International Roughness Index	IRI	m/km	1.37	0.48	0.62	4.51
Change in IRI	ΔIRI	m/km	0.068	0.208	-1.718	2.391
Surface Layer Thickness	H_{sur}	mm	146.5	78.8	35.6	348.0
Base Layer Thickness	H_b	mm	199.4	98.9	0.0	472.4
Sub-Base Layer Thickness	H_{sb}	mm	188.4	250.2	0.0	1905.0
Mean Daily Average Temperature	Tmp	°C	11.2	6.1	0.8	23.3
Mean Daily Temperature Range	Trg	°C	12.8	1.8	9.4	19.0
Mean Annual Freezing Index	FI	°C	476.4	543.1	0.0	2171.9
Mean Total Annual Precipitation	Prp	mm	873.9	418.4	93.8	2265.1
Cumulated Number of ESALs	$ESAL$	#	7.8E+5	1.3E+6	5.1E+3	1.9E+7
Increment of Number of ESALs	$\Delta ESAL$	#	2.2E+5	4.6E+5	4.9E+1	6.1E+6

Regarding the discrete variables used in the model specifications: 61% of the sections had a subgrade classified as coarse while the remaining sections were classified as having fine soils; 57% of the test sections received PM treatments (either TH or CH were included in the analysis) while the remaining 43% were treated as control sections; and the pavement types, according to the TxDOT PMIS definitions, were distributed in the data as 49% Type 4, 36% Type 5, and 15% Type 6.

Texas Pavements Field Data

This section describes the development of a database containing maintenance and rehabilitation (M&R) work information and performance measures of flexible pavements throughout Texas for estimating the proposed model specifications. Obtaining these data required the processing and merging of a number of existing databases extracted from TxDOT's various information systems, such as the Design and Construction Information System (DCIS), SiteManager, the Maintenance Management Information System (MMIS), Compass, and the PMIS.

Processing of TxDOT Data

TxDOT databases containing M&R project-related information can be divided into two groups regarding data formatting and content. The first group, which includes DCIS and SiteManager, contains data from contracted projects, while the second, which includes MMIS and Compass, contains data from internal or in-house projects performed by TxDOT personnel. Data from the first group was used as the primary source as it contains more accurate and detailed information.

DCIS has "as designed" information for contracted projects, as well as cost-tracking information; SiteManager has "as constructed" information. Both databases contain information relevant to the purpose of this study and complement each other. For

instance, DCIS contains information regarding the design of the work, such as the selected materials, that is not included in SiteManager. On the other hand, SiteManager data were used in this work to confirm that a project appearing in DCIS has been completed and obtain more detailed information regarding the completion date. Compass includes information regarding TxDOT internal M&R projects from FY 2012 to the present. Information from previous years is archived in MMIS databases.

The main objective of processing the aforementioned databases consisted of extracting location, date, and design-related information for pavement sections with and without PM treatments applied. The following sections describe the main criteria applied to extract these pieces of information from the M&R works data, as well as the processing of other databases to extract information regarding external factors.

Location

Every TxDOT-contracted M&R work is assigned a unique number referred to as the Control Section Job (CSJ). A CSJ consists of a nine-digit number, where the first six digits correspond to the Control Section (CSec) in which the job was performed and the last three digits identify the job. Each CSec, assigned for maintenance purposes, refers to a unique segment of roadway in the TxDOT highway network. As an example, Figure 4.4 shows a number of CSecs (colored lines) located near the town of Refugio, Texas. CSec 0047-04 (blue line) is located on State Highway 202, between U.S. Route 183 and the Bee County line.

In most cases, the M&R work does not extend over the entire CSec. Therefore, the location of each contracted work is defined by the CSec and by a beginning and an ending point located within the CSec. The location of both limiting points for each CSJ is contained in DCIS in descriptive language (in the majority of cases), such as “0.7 mi S of

LP 256 in Palestine" or "Begin curb and gutter in Frankston", or as defined by the distance to a highway reference marker (RM), such as "210+0.21," which indicates that the limiting point of the job is located 0.21 miles after RM 210 on the highway's direction of travel. Having location information of the CSJ in descriptive language requires manual processing of the data, which is not practical considering the size of the databases. Therefore, the analysis included CSecs that have all their CSJs with distance-to-RM information. It should be mentioned that the final dataset contained distance-to-RM information of approximately 300 CSJs manually determined using the descriptive sentence-form location data in order to increase the number of PM projects.

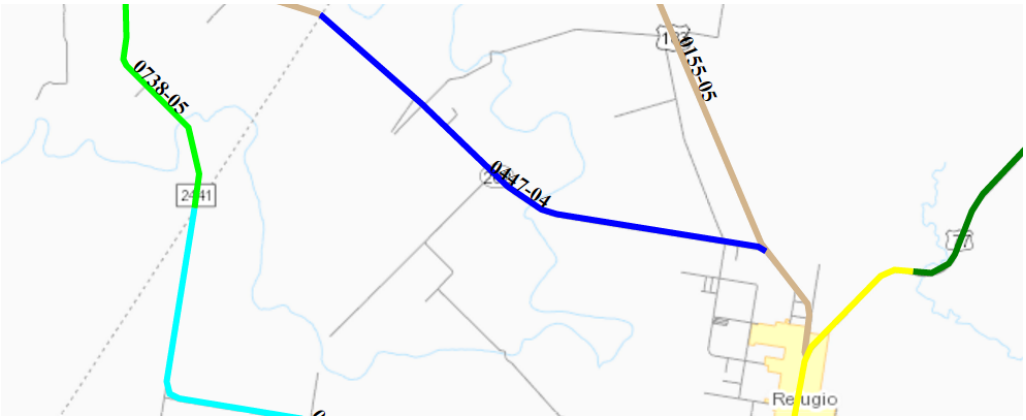

Figure 4.4: Screenshot of TxDOT Statewide Planning Map (TxDOT, 2016).

The location of a CSJ might overlap, at least partially, other CSJs applied at different points in time, resulting in segments of the roadway with different M&R history. Figure 4.5 illustrates this situation where the black lines show the location limits of three CSJs applied within the same CSec in 1998, 2006, and 2012, respectively. The overlapping segments of these three M&R works results in five different stretches of road with a different number of treatments applied (e.g., the segment between 212-0.56 and 216+0.10

had two M&R works while the segment between 216+0.10 and 218-0.18 had three). Therefore, the criteria applied to segment all CSec resulted in pavement segments with homogenous M&R work history, as shown in Figure 4.5.

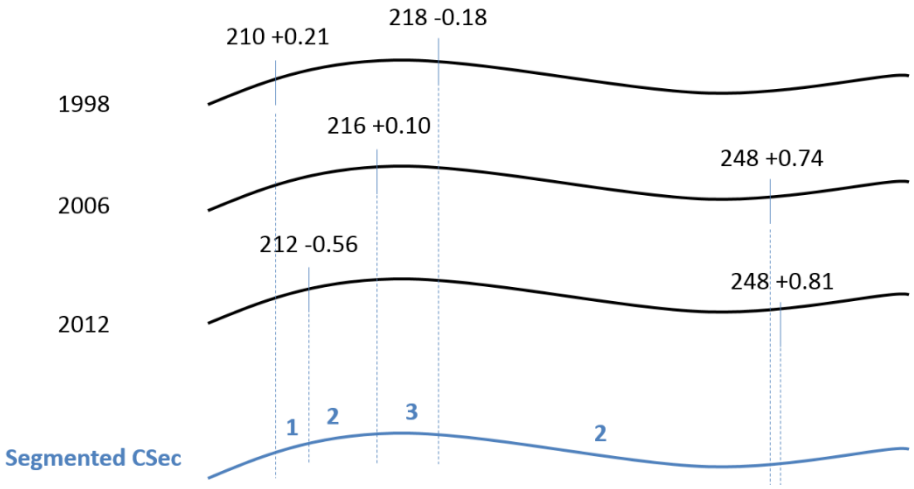

Figure 4.5: Segmenting of TxDOT Control Sections.

Timeline

The starting time of a PM-treated surface was defined as the date at which the surface treatment was completed and opened to traffic. The completion date for each CSJ was directly extracted from a SiteManager database. Similarly, the ending time of the PM treatment life span (if observed) was defined as the completion date of the next M&R job applied to the same pavement surface.

Once the starting and ending times for each CSJ were extracted from the databases with contracted projects, each ending time was corrected, if necessary, using information from internal works data. For this, M&R information extracted from MMIS databases was used to check if internal works were performed during the service life of each treated section and, if there were, to correct the ending date of the corresponding CSJ as the earliest

internal M&R work applied during the PM treatment's life span. Therefore, the extracted data for analysis include information from both contracted and internal works.

The last processing step regarding the beginning and ending dates of each pavement surface consisted of verifying that the dates extracted from the processed databases corresponded to the expected improvement in pavement condition. For this, the performance curve of each pavement section was visually inspected and corrected when the processed dates were within two years apart from the observed improvement in condition. For instance, Figure 4.6 shows the mean and most critical Condition Score (CS), Distress Score (DS), and IRI values throughout time for a flexible pavement located in the main lane of US70 at the CSec 014506 in Floyd County between miles 320 and 337.93. The processed M&R information for this pavement segment shows two PM treatments applied: a CH in late 2004 and another CH in late 2011, and a non-PM M&R work applied in early 2014. The performance curve shows a significant increase in pavement condition just before the CH was applied in late 2014. Therefore, the estimated application date of this PM treatment was corrected a few months to reflect the improvement between data collection dates performed in 2013 and 2014. Therefore, the data used for estimating the proposed models was manually assessed to ensure the highest possible quality.

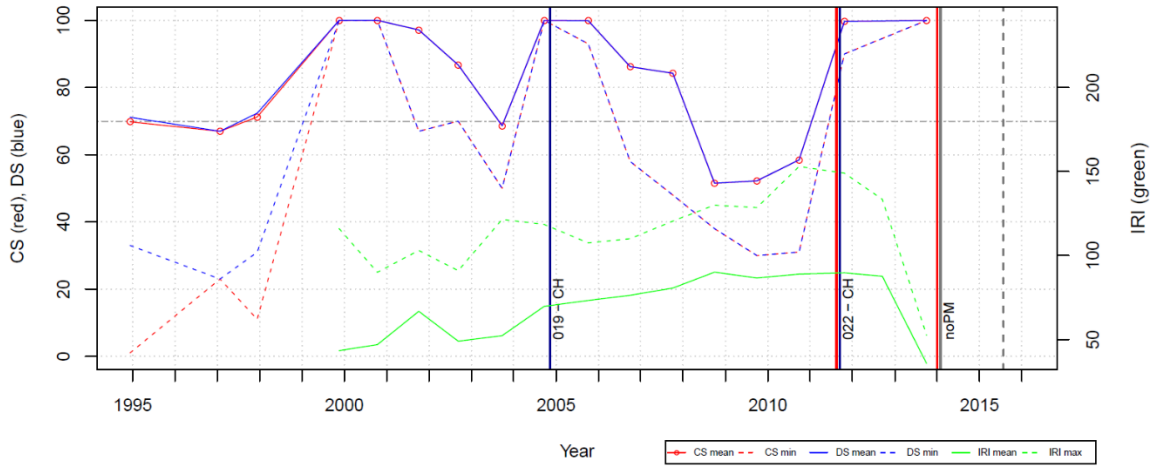

Figure 4.6: Individual performance curves with processed M&R works dates before manual inspection.

Work Type

The next piece of information to extract after the date and location information of each CSJ was the type of M&R work applied in order to differentiate between PM and non-PM works. Every CSJ in DCIS comprises one or multiple items, each of them related to a TxDOT standard specification (SS). As an example, Table 4.2 shows fields from a DCIS database, including the SS and the specification year of each item for four different CSJs. The analyzed dataset included TxDOT SSs corresponding to the specifications from 1982, 1993, 1995, 2004, and 2014. TxDOT SSs related to PM treatments are, for example, 316 for CH, 315 for Fog Seals, 350 for Micro-surfacing, and 247 for TH (TxDOT, 2014b), in addition to a large number of special specifications and provisions.

The work type of each CSJ was determined by analyzing the assigned SSs, as well as the job descriptions. For instance, both the SS number (316) and the description of the single item assigned to CSJ 047907004 indicate that the job consisted of applying a CH. This example illustrates a case for which defining the treatment type was straightforward. Potential complications arose when multiple items were assigned to the same CSJ or when

the information provided in the job description was not clear enough to determine the work type. An example where the item information suggests that the work type does not correspond to a PM treatment is given by CSJ 039901009. As shown in Table 4.2, this CSJ has seven items assigned, which include SSs corresponding to a surface treatment, a prime coat, a dense-graded hot-mix asphalts (HMA), and a milling job; its description indicates that the job consisted of road widening. In this case, the seal coat is placed beneath the HMA layer, per TxDOT standard practice, to provide an impermeable barrier to prevent moisture ingress into the underlying flexible base layer and to improve adhesion between the HMA and granular base layers. It was important to distinguish these rehabilitation projects from those where the seal coat is placed on the surface as a PM treatment.

Table 4.2: Standard specification number and other information used to determine the CSJ's work type.

csj	descr	compdate	SS	spec_yr
039901009	CCSJ: 020202015 | WORK: WIDEN ROADWAY | FROM:...	20090917	316	4
039901009	CCSJ: 020202015 | WORK: WIDEN ROADWAY | FROM:...	20090917	316	4
039901009	CCSJ: 020202015 | WORK: WIDEN ROADWAY | FROM:...	20090917	316	4
039901009	CCSJ: 020202015 | WORK: WIDEN ROADWAY | FROM:...	20090917	310	4
039901009	CCSJ: 020202015 | WORK: WIDEN ROADWAY | FROM:...	20090917	316	4
039901009	CCSJ: 020202015 | WORK: WIDEN ROADWAY | FROM:...	20090917	340	4
039901009	CCSJ: 020202015 | WORK: WIDEN ROADWAY | FROM:...	20090917	354	4
047907005	CCSJ: 000501094 | WORK: SEAL COAT PROGRAM | FR...	20020924	316	93
047907005	CCSJ: 000501094 | WORK: SEAL COAT PROGRAM | FR...	20020924	316	93
047907004	CCSJ: 007502020 | WORK: SEAL COAT | FROM: PECOS...	19950907	316	95

Explanatory Variables

The explanatory variables extracted from the various TxDOT's information systems included pavement type, and traffic variables. Temperature and precipitation data were extracted from the latest release of the NOAA's 30-year Climate Normals (NOAA,

2016). Climate Normals consist of 30-year averages of climatological values (Arguez et al. 2012). The temperature and precipitation values assigned to each pavement section consisted of the average Normals of all weather stations for the corresponding county. The average climatic values computed for each county in Texas are presented in Figure 3.4. The mean annual temperatures range from 55°F (12.8°C) to 75°F (23.9°C) (north-to-south) and the annual total precipitations range from 10 to 60 inches per year (west-to-east).

The effect of traffic was incorporated through the average number of ESALs applied to the pavement section during the surface's observed lifespan. This information was extracted from a PMIS database and its processing consisted of identifying and averaging the PMIS sections located within the analyzed treated section for the corresponding period of analysis.

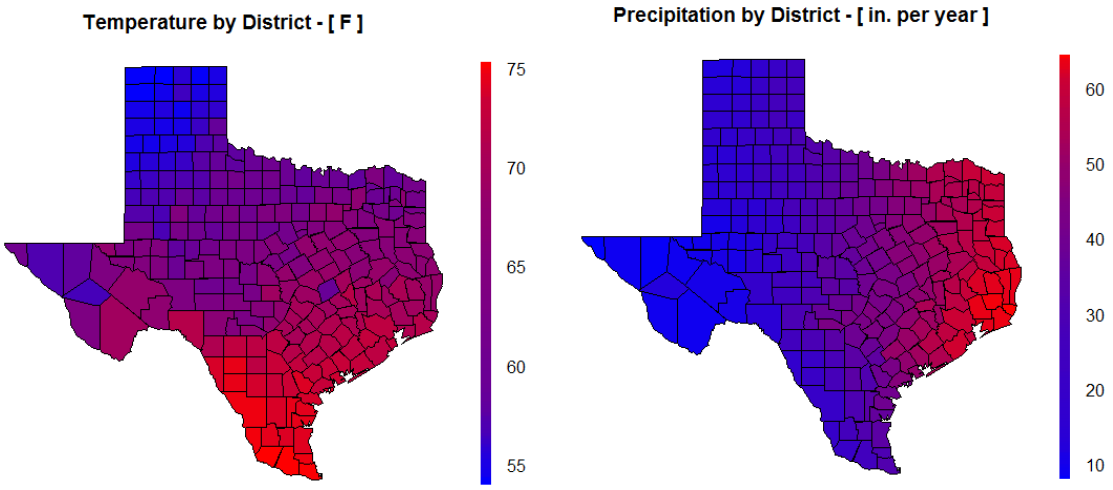

Figure 4.7: Counties' temperature (on the right) and precipitation (on the left) extracted from NOAA's Climate Normals database (NOAA, 2016).

The information related to the pavement type in PMIS is restricted to a ten-group category system, from which three categories are assigned to HMA surfaces: "Type 04: Thick Asphaltic Concrete (over 5.5")", "Type 05: Medium Thickness Asphaltic Concrete

(2.5 - 5.5")", and "Type 06: Thin Asphaltic Concrete (under 2.5")". Therefore, these three categories were used to characterize the pavement structural design in our model. Since there were multiple 0.5-mile-long PMIS sections (each with its own pavement type) located within the extent of the analyzed pavement surfaces, the pavement type assigned to each segment was the one corresponding to the most predominant category; i.e., the category with more than 95% of occurrences. It should be noted that all PMIS sections within a segment of analysis presented a unique category in the large majority of cases.

Summary Statistics of Texas Data

The data used for estimating the roughness mixture model consisted of a subset of the data obtained from processing the various TxDOT information systems. The objective of selecting a subset of the data was to increase the number of thick pavements for the estimation (from the less than 2% observed in the original data) while covering the different climatic regions in Texas and a wide range of traffic levels.

The seven TxDOT Districts selected for the analysis were Amarillo, Lubbock, Fort Worth, Dallas, Lufkin, San Antonio, and Corpus Christi. These Districts included the three pavement types defined in PMIS for HMA surfaces and contained data in 50 counties that covered the different climatic regions in Texas, as shown in Figure 4.9. The original dataset contained data in 152 counties distributed in 19 Districts.

The set of data used for analysis included a total of 1,008 observations from 233 pavement sections, which had a median length of 2.9 miles. Of this set, 43% were rural highways (Farm to Road and Road to Market highways), 47% were US and State highways, and the remaining 10% were Interstate Highways.

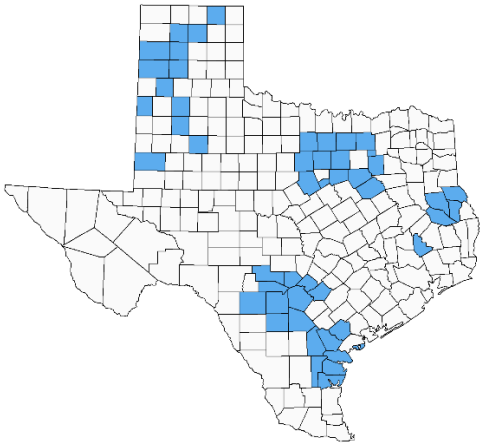

Figure 4.8: Map of Texas counties from which pavement data were extracted for estimating the roughness mixture model.

Figure 4.10 shows the distribution of the change in IRI value between data collection dates observed in the analyzed dataset. The mean change in IRI was 0.0674 m/km, and the proportion of negative observations was 38.4%.

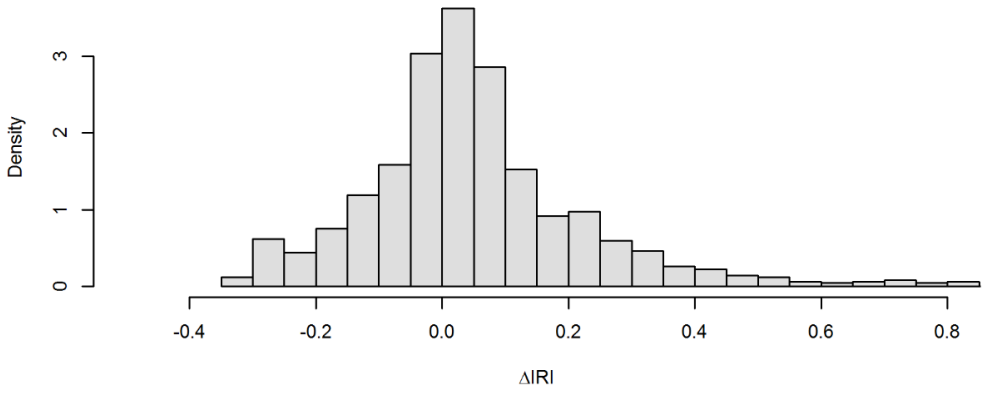

Figure 4.9: Distribution of the observed change in IRI between data collection dates from the analyzed set of TxDOT data.

Table 4.3 shows the summary statistics of some of the continuous variables in the data. Regarding the discrete variables in the model, 73% of the sections received a PM

treatment while the remaining sections consisted of non-treated HMA surfaces; the distribution of pavement types were 8% Type 4, 65% Type 5, and 27% Type 6.

Table 4.3. Descriptive statistics of main continuous variables from the Texas dataset.

Variable		unit	Mean	Std	Min	Max
International Roughness Index	IRI	m/km	1.81	0.58	0.86	6.40
Change in IRI	ΔIRI	m/km	0.067	0.258	-0.321	3.370
Mean Daily Average Temperature	Tmp	C	19.0	2.0	12.9	22.6
Mean Total Annual Precipitation	Prp	mm	914.5	215.5	455.7	1376.7
Cumulated Number of ESALs	$ESAL$	-	1.7E+4	3.3E+4	2.7E-2	2.8E+5
Increment of Number of ESALs	$\Delta ESAL$	-	3.6E+3	3.9E+3	4.1E+0	2.4E+4
Annual Average Daily Traffic	$AADT$	-	5.6E+3	6.3E+3	1.3E+1	4.9E+4
Percentage of Trucks	$\%Tr$	%	16.0	8.4	3.2	46.2

NATIONWIDE PAVEMENT ROUGHNESS MIXTURE MODEL

This section covers the development of a pavement roughness mixture model estimated from the nationwide field data described in the previous section of the chapter. Additional analyses conducted on the same dataset to assess the relative effectiveness of different PM treatments using censored regression are included in Serigos et al. (2016b).

Description of Roughness Model Specification

The basic expression of the estimated pavement roughness model adopts the form of the model estimated in Chapter 3 for the incremental change in PSI (Equation 3.1). Therefore, pavement roughness, as measured by the IRI value, is expressed as a function of cumulated traffic throughout time while accounting for structural design and climatic factors. The progression of PSI and surface roughness are expected to follow a similar trend given the strong relationship between these two measures, as documented in several studies (Carey and Irick, 1960; HRB 1962; Haas et al., 1994; Hall and Correa Muñoz, 1999).

Equation 4.1 shows the adopted model for the increment of IRI value between data collection dates where the model parameter λ takes a natural exponential form as a function of factors related to climate and structural design, as shown in Equation 4.2.

$$\Delta IRI_{t-1,t} = \lambda N_{t-1}^{\gamma} \Delta N_t \tag{4.1}$$

$$\lambda = exp(\boldsymbol{X_{SD\&CL}}' \boldsymbol{\beta_{SD\&CL}}) \tag{4.2}$$

where,

$\Delta IRI_{t-1,t}$: increment of IRI value from time *t*-1 to *t*, in m/km

λ, γ: model parameters

$\boldsymbol{X_{SD\&CL}}$: explanatory variables related to the structural design and climate

$\boldsymbol{\beta_{SD\&CL}}$: vector of parameters for $\boldsymbol{X_{SD\&CL}}$

The model estimated from the nationwide dataset was subsequently calibrated using data from pavements in Texas. Therefore, the explanatory variables to consider for estimating the nationwide roughness model were constrained to variables available in TxDOT's PMIS and other information systems, such as the ones described in the previous section of this chapter. Data collected for pavement management purposes is less detailed and includes fewer variables than data obtained from an experiment such as LTPP, mainly due to budget and practical limitations. For instance, LTPP data includes the thickness of each pavement layer whereas TxDOT PMIS data related to the structural design of HMA pavements is limited to a three-category classification system determined solely by the asphalt concrete (AC) surface layer thickness and does not consider base and sub-base layer information.

The final specification for the model estimated using the nationwide dataset is shown in Equation 4.3, where the error term is normally distributed with zero mean;

pavement type, subgrade, and treatment variables vary across sections; and climatic and traffic variables vary across sections and time. The explanatory variables included in the specification were chosen carefully based on a rigorous model development process. Model refinement was carried out through exclusion of statistically insignificant variables by following standard step-wise procedures and statistical tests.

$$\Delta IRI_{i,t} = \widehat{\Delta IRI_{i,t}} + \varepsilon_{i,t} \tag{4.3a}$$

$$\widehat{\Delta IRI_{i,t}} = exp\big(\beta_0 + \beta_{Ty5} Ty5_i + \beta_{Ty6} Ty6_i + \beta_{SG} SG_i + \beta_{PM} PM_i + \beta_{FI} FI_{i,t}\big)\, ESAL_{i,t-1}^{\beta_{ESAL}} \Delta ESAL_{i,t} \tag{4.3b}$$

$$\varepsilon_{i,t} \sim N(0, \sigma^2) \tag{4.3c}$$

where,

$\Delta IRI_{i,t}$: observed change in IRI value for section i at time t, in m/km

$\widehat{\Delta IRI_{i,t}}$: estimated change in IRI value for section i at time t, in m/km

β_j: model parameter j

$Ty5_i$: Pavement Type 5, equal to 1 if AC_i is ≤ 5.5" and ≥ 2.5", 0 otherwise

$Ty6_i$: Pavement Type 6, equal to 1 if AC_i is < 2.5", 0 otherwise

SG_i: subgrade type, equal to 1 for coarse soils and 0 for fine soils

PM_i: preventive maintenance, equal to 1 for treated surfaces and 0 otherwise

$FI_{i,t}$: annual average freezing index for section i at time t, in °C degree-days

$\Delta ESAL_{i,t}$: increment of traffic for section i at time t, in ESALs

$ESAL_{i,t-1}$: cumulated traffic for section i up to time t-1, in ESALs

Among the climatic variables included in LTPP, the annual average freezing index (FI) was the most significant at explaining the variation of the change in IRI. Other variables considered were the annual average temperature and the annual total

precipitation. Temperature and freezing index were not included simultaneously during the development of the model specification in order to avoid multi-collinearity issues given their high correlation. The effect of freezing index, captured by the parameter β_{FI}, is expected to be positive as cycles of freezing and thawing of the subgrade relate to higher deterioration rates.

The parameters on the two indicator variables related to the pavement structural design, β_{Ty5} and β_{Ty6}, capture the effect of "intermediate" and "thin" HMA surface layer pavements relative to "thick" HMA surface layer pavements. Therefore, β_{Ty6} is expected to be larger than β_{Ty5}, and both positive, as thinner pavements provide less structural capacity. Contrarily, the effect of coarse subgrade relative to fine subgrade type, β_{SG}, is expected to be negative as coarser soils provide a better foundation to the pavement structure (among other advantages) and, therefore, a lower damage rate.

As shown in Equation 4.3c, one indicator variable representing all PM-treated surfaces was specified in the model, as opposed to assigning a unique indicator variable to each of the four different PM treatments tested in the LTPP SPS-3 experiment. This approach was chosen based on the findings from a preliminary study conducted by the author (Serigos et al., 2016b), which showed that, although all four PM treatments presented slower deterioration rates relative to non-treated sections, the differences in performance among treatments were not statistically significant. In addition, historical information available from the TxDOT information systems regarding the type of PM treatment applied does not provide the adequate level of detail to accurately differentiate among PM treatment types.

Bayesian Estimation of Nationwide Mixture Model Specification

Equation 4.4 shows the finite mixture model specification proposed for the pavement roughness mixture model to be estimated using nationwide field data, where the probability of observing the increment of IRI value is a weighted sum of K normal distributions. In this specification, the number of clusters is fixed, and determined by evaluating the gain in deviance information criterion (DIC) as a function of the number of clusters, in order to avoid over-fitting. The model was estimated multiple times by increasing the number of clusters until the gain in fit was compensated by the larger number of parameters.

$$p\left(\Delta IRI_{i,t} \middle| \boldsymbol{w}, \boldsymbol{\beta}, \boldsymbol{\sigma^2}\right) = \sum_{k=1}^{K} w_k \, N(\Delta\widehat{IRI_{\iota,t,k}}, \sigma_k^2) \tag{4.4}$$

$$\Delta\widehat{IRI_{\iota,t,k}} = exp\left(\beta_{0,k} + \beta_{Ty5} Ty5_i + \beta_{Ty6} Ty6_i + \beta_{SG} SG_i + \beta_{PM} PM_i + \beta_{FI} FI_{i,t}\right) ESAL_{i,t-1}^{\beta_{ESAL,k}} \Delta ESAL_{i,t} \tag{4.5}$$

where,

$\Delta\widehat{IRI_{\iota,t,k}}$: predicted change in IRI for section i at time t and cluster k

As shown in Equation 4.5, two model parameters were specified to vary across clusters and time: the baseline parameter, $\beta_{0,k}$, and the parameter on the number of ESALs, $\beta_{ESAL,k}$. Thus, the proposed specification captures the group-level heterogeneity in the effect of traffic and the baseline parameter due to unobserved factors and interactions through the unsupervised clustering of observations. The effect of the remaining explanatory variables are assumed to be homogeneous across observations and, therefore, specified as constant across clusters.

Equation 4.6 shows the likelihood function for the vector of observed change in IRI values given the parameters of the mixed model specification. As reflected in the equation,

the model assumes independence across time and test sections as observations of a given pavement section are not expected to be affected by observations from another section. Also, the number of observations throughout time varied across test sections as indicated by the sub-indexes of the equation (previously defined in Equation 3.8).

$$p(\Delta \boldsymbol{IRI}|\boldsymbol{w}, \boldsymbol{\beta}, \sigma^2) = \prod_{i=1}^{S} \prod_{t=1}^{T_i} \sum_{k=1}^{2} w_k \sqrt{\frac{1}{2\pi\sigma_k^2}} e^{\frac{-1}{2\sigma_k^2}\left(\Delta IRI_{i,t} - \widehat{\Delta IRI_{i,t,k}}\right)^2} \quad (4.6)$$

The likelihood function of the model was specified to assign the individual observations to a specific cluster. Thus, a given pavement section may have observations assigned to different clusters, allowing for the model to capture heterogeneous effects across pavement sections and time.

Selection of Prior Distributions

The prior distributions for each model parameter and variance of the error term were specified as non-informative. The prior for the parameters on each independent variable, β_j, consisted of a flat Gaussian with zero mean and low precision, as shown in Equation 3.10, whereas the prior for the variance of the error, σ^2, consisted of an inverse-gamma distribution with both parameters, a and b, equal to 0.001 (Equation 3.11). The prior distribution for the weights of the *K* clusters consisted of a Dirichlet distribution (Equation 3.20) with α_k=1 for all *k*.

Joint Posterior Distribution

The joint posterior distribution of the mixed model parameters given the observed change in IRI values from the nationwide dataset is shown in Equation 4.7. The posterior marginal distributions for each model parameter and number of clusters were estimated from multiple Markov chain Monte Carlo (MCMC) simulations and presented in the next sections of this chapter.

$$p(\boldsymbol{w}, \boldsymbol{\beta}, \sigma^2 | \Delta \boldsymbol{IRI}) \propto \prod_{k=1}^{K} \prod_{j=1}^{J} p\left(\beta_{j,k}\right) p(\sigma_k^2) p(\boldsymbol{w}) p(\Delta \boldsymbol{IRI} | \boldsymbol{w}, \boldsymbol{\beta}, \boldsymbol{\sigma}^2) \propto$$
$$\prod_{k=1}^{K} \left((\sigma_k^2)^{(-a-1)} exp\left(\frac{-b}{\sigma_k^2}\right) \right) exp\left(\sum_{k=1}^{K} \frac{-1}{2{\sigma_{\beta_{j,k}}}^2} \sum_{j=1}^{J} \left(\beta_{j,k} - \right. \right.$$
$$\left. \left. \mu_{\beta_{j,k}} \right)^2 \right) \prod_{i=1}^{S} \prod_{t=1}^{T_i} \sum_{k=1}^{K} \left(\frac{w_k}{\sigma_k} \exp\left(\frac{-1}{2\sigma_k^2} \left(\Delta IRI_{i,t} - \widehat{\Delta IRI_{i,t,k}} \right)^2 \right) \right) \quad (4.7)$$

Results from Estimation of Nationwide Model Specification with Complete Pooling

The summary statistics of the estimated marginal distributions for the parameters of the mixture model specification with one cluster (i.e., complete pooling) are presented in Table 4.4. In addition, the deviance information criterion (DIC) value computed for this model specification was equal to -353.0. These results were obtained from the simulated MCMC chains that reached acceptable convergence according to the criteria described in Chapter 2. Each of the two chains used for estimating the marginal distributions had a length of 50,000 iterations, a "burn-in" period of 15,000 iterations, and a thinning interval of 5 iterations.

The signs of the estimated model parameters show that the effect of each explanatory variable was as expected. The 95% credible intervals indicate that the change in IRI values for pavements with intermediate layer thickness (Type 5) was not significantly different, on average, than for pavements with thick surface layer (Type 4); in contrast, thinner pavements presented a higher deterioration rate. Similarly, the difference in effect between coarser and finer soils was not statistically significant. Even though the estimation of LTPP SPS-3 data did not show a significant effect for these two variables, they were kept in the model specification for the estimation with multiple clusters due to their role in explaining the pavement response variation based on engineering knowledge.

Pavement surfaces with a PM treatment presented, on average, a smaller increment of IRI value than sections that did not receive a PM treatment, after controlling for the

climate, traffic, and type of pavement structure. Therefore, applying the PM treatment to the test pavement surfaces led to a modified performance curve, with a slower progression of roughness. In addition, the estimated parameter on the traffic variable indicates that the increment of roughness decreases with cumulated traffic, as observed for the estimated model using AASHO data.

Table 4.4. Summary statistics of posterior marginal distributions for the model parameters of the nationwide model specification with complete pooling.

Parameter	Mean	Std	2.5%	Median	97.5%
β_0	-5.45E+00	5.84E-01	-6.80E+00	-5.40E+00	-4.36E+00
β_{Ty5}	2.71E-01	3.26E-01	-3.03E-01	2.51E-01	9.63E-01
β_{Ty6}	1.06E+00	3.52E-01	4.78E-01	1.02E+00	1.86E+00
β_{SG}	2.46E-02	2.60E-01	-4.69E-01	1.66E-02	5.53E-01
β_{PM}	-9.19E-01	2.34E-01	-1.40E+00	-9.12E-01	-4.79E-01
β_{FI}	8.47E-04	1.64E-04	5.38E-04	8.39E-04	1.19E-03
β_{ESAL}	-5.08E-01	6.52E-02	-6.36E-01	-5.10E-01	-3.66E-01
σ^2	4.20E-02	1.81E-03	3.86E-02	4.19E-02	4.57E-02
Deviance	-3.64E+02	4.59E+00	-3.70E+02	-3.64E+02	-3.52E+02

Results from Estimation of Nationwide Mixture Model Specification

This section presents the results from the estimation of the roughness mixture models specified to capture the group-level heterogeneous performance response of pavements using nationwide data. As shown in Equations 4.4 and 4.5, the proposed specification captures unobserved heterogeneity through the varying effect of cumulated traffic and the baseline parameter, β_0, across clusters.

Tables 4.5 and 4.6 show the results from the estimated models specified with two and three clusters, respectively. The model specified with two clusters had a DIC of -985.2 and the one specified with three clusters had a DIC of -987.1. The significant gain in fit—

reflected by the large reduction in DIC value from the model specified with complete pooling of observations to the one with mixture specification—shows the significant heterogeneity present in the data. Moreover, the relatively small difference in DIC value between the model with two clusters and the one with three clusters suggests that the heterogeneous response of pavements due to unobserved factors is properly captured by the modeling of two main subpopulations. The estimated weights of the clusters for each model reinforces this observation, as the model specified with three clusters has the vast majority of the data (94%) clustered in two groups.

Assessment of the estimated parameters of the model specified with two clusters indicates that the effect of the cumulated traffic was higher for the Cluster 1 model, whereas the baseline factor was higher for the Cluster 2 model. Therefore, the data grouped in Cluster 1 follows a performance curve with a faster progression of roughness and the difference in response between the two clusters increases with cumulated traffic. The probability of an observation belonging to Cluster 1 was 0.73 and the variance of the predictive error for this group was lower than the one obtained from complete pooling of the data, even considering the lower sample size.

Table 4.5. Summary statistics of posterior marginal distribution of model parameters for the nationwide mixture model specification with two clusters.

Parameter	Mean	Std	2.5%	Median	97.5%
β_{0_1}	-4.73E+00	1.12E+00	-6.92E+00	-4.78E+00	-2.66E+00
β_{0_2}	-1.31E+00	1.15E+00	-3.75E+00	-1.24E+00	7.58E-01
β_{Ty5}	5.15E-01	6.73E-01	-4.67E-01	5.73E-01	1.36E+00
β_{Ty6}	4.78E-01	4.39E-01	-4.61E-01	5.07E-01	1.27E+00
β_{SG}	-5.06E-01	3.54E-01	-1.25E+00	-4.86E-01	1.61E-01
β_{PM}	-4.34E+01	9.19E+00	-5.60E+01	-4.42E+01	-2.24E+01
β_{FI}	-1.86E-04	4.67E-04	-1.14E-03	-1.39E-04	5.71E-04
β_{ESAL_1}	-5.88E-01	1.66E-01	-8.99E-01	-5.80E-01	-2.83E-01
β_{ESAL_2}	-8.91E-01	1.63E-01	-1.22E+00	-8.88E-01	-5.73E-01
w_1	73%	3%	68%	73%	78%
w_2	27%	3%	22%	27%	32%
σ_1^2	5.23E-03	6.08E-04	4.18E-03	5.19E-03	6.53E-03
σ_2^2	1.49E-01	1.81E-02	1.19E-01	1.48E-01	1.89E-01
Deviance	-1.04E+03	1.02E+01	-1.05E+03	-1.04E+03	-1.01E+03

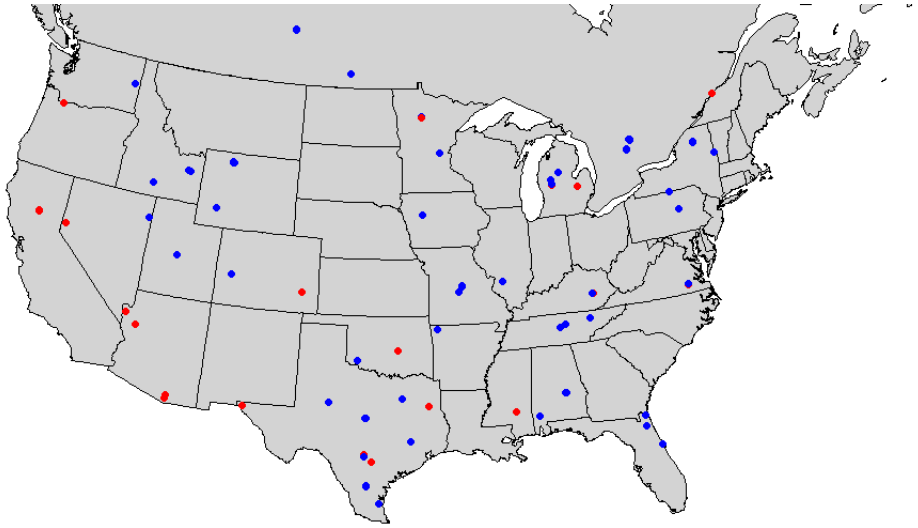

Figure 4.10: Geographical distribution of test sections grouped into Cluster 1 (blue points) and Cluster 2 (red points) by the mixture model.

Table 4.6. Summary statistics of posterior marginal distribution of model parameters for the nationwide mixture model specification with three clusters.

Parameter	Mean	Std	2.5%	Median	97.5%
β_{0_1}	-5.96E+00	9.63E-01	-7.84E+00	-5.86E+00	-4.22E+00
β_{0_2}	2.93E+00	1.35E+01	-2.96E+01	9.66E-01	2.85E+01
β_{0_3}	-2.41E+00	1.66E+01	-3.76E+01	-2.55E+00	3.23E+01
β_{Ty5}	2.81E-02	2.14E+00	-8.23E+00	5.43E-01	1.46E+00
β_{Ty6}	7.60E-01	5.36E-01	-5.07E-02	6.94E-01	2.09E+00
β_{SG}	-4.65E-01	3.54E-01	-1.11E+00	-4.79E-01	2.54E-01
β_{PM}	-1.46E+01	1.12E+01	-3.64E+01	-1.36E+01	-5.23E-01
β_{FI}	-6.16E-04	4.19E-03	-2.36E-03	-1.93E-04	5.65E-04
β_{ESAL_1}	-4.04E-01	1.34E-01	-6.62E-01	-4.14E-01	-1.27E-01
β_{ESAL_2}	-7.95E+00	8.19E+00	-2.96E+01	-5.73E+00	-2.00E-01
β_{ESAL_3}	-1.43E+01	8.82E+00	-2.86E+01	-1.53E+01	-6.47E-01
w_1	63%	3%	56%	63%	69%
w_2	6%	3%	2%	5%	12%
w_3	31%	4%	24%	32%	38%
σ_1^2	3.84E-03	4.38E-04	3.07E-03	3.82E-03	4.78E-03
σ_2^2	5.42E-01	2.10E-01	2.19E-01	5.17E-01	1.02E+00
σ_3^2	5.56E-02	1.09E-02	3.54E-02	5.52E-02	7.80E-02
Deviance	-1.08E+03	1.36E+01	-1.11E+03	-1.08E+03	-1.06E+03

Figure 4.10 shows the geographical distribution of test sections from the LTPP SPS-3 experiment grouped in Cluster 1 (blue points) and Cluster 2 (red points) according to the highest probability of belonging to each cluster. The probability of each pavement section falling into a particular cluster was estimated as the joint likelihood of the section's multiple observations belonging in a particular cluster. The main purpose of mapping the test sections according to their most likely cluster is to detect the unobserved factors

causing the systematic differences in pavement performance. Unfortunately, there are no clear patterns or information detectable from the map to help reveal the factors explaining the heterogeneous subpopulations. Many potential unobserved factors and interactions can cause the heterogeneous behavior, considering the limited data collected for pavement management purposes relative to the various variables that affect the performance of a pavement structure.

Regarding the effect of the variables specified as constant across clusters, it is observed that most of the variation of the observed change in IRI values is explained by the PM treatment variable as opposed to what was observed from the estimation of the model with complete pooling, where a larger number of variables had a significant effect. Test sections that have received a PM treatment presented a slower progression of roughness compared to control sections in both specifications.

Assessment of PM Treatment Effectiveness through Model-Base Clustering of Data

An additional specification for the roughness mixture model was estimated with the objective of analyzing the possible heterogeneous effect of the PM treatment variable across sections and time. To that end, a new expression for the predicted increment of IRI value between data collection dates was specified as shown in Equation 4.8. This model allows for the parameter on the PM variable and the baseline parameter, β_0, to change across clusters, thus capturing the heterogeneity in effects for these two variables due to unobserved factors. The remaining components of the Bayesian specification of this model were specified as in the mixture model estimated in the previous section of this chapter.

$$\widehat{\Delta IRI_{\iota,t,k}} = exp\big(\beta_{0,k} + \beta_{Ty5}Ty5_i + \beta_{Ty6}Ty6_i + \beta_{SG}SG_i + \beta_{PM,k}PM_i + \beta_{FI}FI_{i,t}\big)\, ESAL_{i,t-1}^{\beta_{ESAL}} \Delta ESAL_{i,t} \quad (4.8)$$

Results from the Estimation of Mixture Specification for PM Treatment Effectiveness

The mixture model specified with the predicted increment of IRI value as shown in Equation 4.8 was estimated for a different number of clusters. The DIC values estimated from the converging MCMC chains of each estimated model are shown in Figure 4.11. The curve in the figure attests that the reduction in DIC value became relatively small after specifying three clusters; therefore, the model with four clusters was selected for analysis.

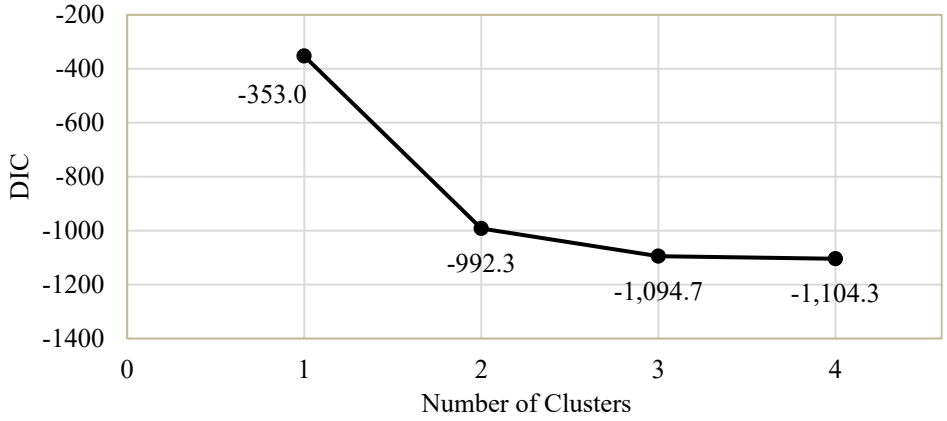

Figure 4.11: DIC as a function of the number of clusters for the mixture model specification to address the effectiveness of PM treatments.

Table 4.17 shows the summary statistics of the posterior marginal distributions of the model parameters with four clusters. Judging by the estimated parameters on the PM treatment variable, about 60% of the observations showed a significant reduction in the progression of roughness for the sections where a PM treatment was applied. Thirty-three percent presented a non-significant difference between treated and control test sections, whereas the remaining 7% presented a faster deterioration rate for the case of treated surfaces. Also, the models corresponding to the clusters where the application of PM treatments resulted in either a slower or non-modified progression of roughness presented a smaller variance of the error term, even considering the smaller sample size.

Table 4.7. Summary statistics of posterior marginal distribution of model parameters for the nationwide mixture model specification with four clusters for analysis of PM treatment effectiveness.

Parameter	Mean	Std	2.5%	Median	97.5%
β_{0_1}	-5.98E+00	4.78E-01	-7.21E+00	-5.89E+00	-5.32E+00
β_{0_2}	-7.13E+00	6.94E-01	-8.91E+00	-7.00E+00	-6.20E+00
β_{0_3}	-1.65E+01	5.75E+00	-2.68E+01	-1.57E+01	-8.36E+00
β_{0_4}	-2.92E+01	7.57E+00	-4.10E+01	-3.14E+01	-1.62E+01
β_{Ty5}	2.15E-01	2.99E-01	-4.53E-01	2.58E-01	6.82E-01
β_{Ty6}	6.96E-01	2.17E-01	1.55E-01	7.10E-01	1.06E+00
β_{SG}	7.47E-02	1.71E-01	-2.54E-01	7.45E-02	4.39E-01
β_{PM_1}	-3.61E+01	6.64E+00	-4.74E+01	-3.64E+01	-2.47E+01
β_{PM_2}	2.68E-01	3.70E-01	-4.48E-01	2.58E-01	1.02E+00
β_{PM_3}	-4.26E+01	4.74E+00	-4.93E+01	-4.37E+01	-3.31E+01
β_{PM_4}	1.16E+01	4.07E+00	3.13E+00	1.17E+01	1.80E+01
β_{FI}	1.31E-03	2.56E-04	9.71E-04	1.24E-03	2.04E-03
β_{ESAL}	-3.69E-01	5.42E-02	-4.73E-01	-3.77E-01	-2.32E-01
w_1	29.4%	6.4%	15.3%	29.6%	37.5%
w_2	33.2%	2.9%	28.5%	32.9%	41.3%
w_3	30.4%	5.4%	18.1%	29.2%	40.3%
w_4	7.0%	2.0%	3.6%	6.5%	11.1%
σ_1^2	3.56E-03	8.72E-04	2.15E-03	3.43E-03	5.54E-03
σ_2^2	3.54E-02	7.25E-03	2.35E-02	3.47E-02	5.04E-02
σ_3^2	3.23E-03	7.17E-04	2.11E-03	3.14E-03	4.77E-03
σ_4^2	3.92E-01	5.42E-02	2.83E-01	3.89E-01	5.09E-01
Deviance	-1.16E+03	1.02E+01	-1.17E+03	-1.16E+03	-1.13E+03

TEXAS PAVEMENT ROUGHNESS MIXTURE MODEL

The Texas database developed from various TxDOT and NOAA data sources was used to estimate a roughness mixture model that incorporated the nationwide data through the prior distribution of the model parameters. This section describes the model specification and the results from the estimation of the model with complete pooling and with clustering of observations in order to account for group-level heterogeneity.

Model Specification

Equation 4.9 shows the model specified for predicting the increment of IRI between data collection dates for pavements in Texas using explanatory variables available in TxDOT's PMIS, with the addition of climatic variables. As opposed to the specification for the nationwide model (Equation 4.3), which had the freezing index as the most significant climatic variable to explain the increment of roughness, the climatic variables selected for modeling Texas data were the mean daily average temperature and the mean total annual precipitation. This difference in specification is due to the insignificant freezing index values observed in Texas.

$$\Delta IRI_{i,t} = \widehat{\Delta IRI_{i,t}} + \varepsilon_{i,t} \tag{4.9a}$$

$$\widehat{\Delta IRI_{i,t}} = exp\big(\beta_0 + \beta_{Ty5} Ty5_i + \beta_{Ty6} Ty6_i + \beta_{PM} PM_i + \beta_{Tmp} Tmp_{i,t} + \beta_{Prp} Prp_{i,t}\big)\, ESAL_{i,t-1}^{\beta_{ESAL}} \Delta ESAL_{i,t} \tag{4.9b}$$

$$\varepsilon_{i,t} \sim N(0, \sigma^2) \tag{4.9c}$$

where,

$Tmp_{i,t}$: mean daily average temperature for section i at time t, in degrees Celsius

$Prp_{i,t}$: mean total annual precipitation for section i at time t, in mm

Selection of Prior

The prior distributions for the Texas model parameters were specified to incorporate the information from the estimation of nationwide data. To that end, the model in Equation 4.9 was estimated using the nationwide dataset and adopting a Bayesian specification with non-informative priors. The estimated marginal posterior distributions from the nationwide dataset were then used to specify the prior distribution for the Texas model parameters, adjusting for the differences between datasets.

Table 4.8 shows the summary statistics of the posterior marginal distributions for the model parameters in Equations 4.9 estimated using LTPP SPS-3 data. The DIC value of this model was -348.4. The obtained DIC value is slightly higher than the one obtained from the estimation of the model in Equation 4.5 using the same data, which reflects the higher significance of the freezing index variable for explaining the progression of roughness compared to the other climatic variables. It should be noted that the effect of subgrade type was not statistically significant (Table 4.4).

Table 4.8. Summary statistics of posterior marginal distributions used to specify the prior distributions for the Texas model parameters.

Parameter	Mean	Std	2.5%	Median	97.5%
β_0	-5.78E+00	7.96E-01	-7.48E+00	-5.73E+00	-4.42E+00
β_{Ty5}	6.95E-01	3.20E-01	1.15E-01	6.76E-01	1.35E+00
β_{Ty6}	1.49E+00	3.75E-01	8.61E-01	1.47E+00	2.26E+00
β_{Tmp}	-9.38E-02	2.11E-02	-1.33E-01	-9.28E-02	-4.65E-02
β_{Prp}	2.91E-04	2.79E-04	-2.62E-04	2.94E-04	8.08E-04
β_{ESAL}	-3.35E-01	7.42E-02	-4.71E-01	-3.37E-01	-1.96E-01
β_{PM}	-5.75E-01	2.55E-01	-1.06E+00	-5.75E-01	-8.76E-02
σ^2	4.22E-02	1.82E-03	3.89E-02	4.21E-02	4.59E-02
Deviance	-3.58E+02	4.27E+00	-3.64E+02	-3.58E+02	-3.47E+02

The prior distributions specified for each parameter β_j in the Texas roughness model consisted of Gaussian distributions centered on the corresponding mean value reported in Table 4.4. The standard deviation for these prior distributions was specified as two times the corresponding standard deviation from the estimation of nationwide data (Table 4.4). The standard deviation of the prior distributions was inflated in order to reflect the uncertainty in the model parameters issuing from the discrepancies between datasets. For instance, the quality and design of PM treatments applied in the LTPP SPS-3 study, as well as the pavement materials and construction standards used, may significantly differ from the analyzed pavements and treatments in Texas, potentially resulting in more different effects.

The prior distribution for the variance of the error term and for the weights of the mixture specification were non-informative and specified as in Equation 3.11 and 3.20. Both parameters of the inverse-gamma distribution for the variance of the error term, a and b, were equal to 0.001, whereas the parameters for the Dirichlet distribution, α_k, specified for the weights of the K clusters were all set to 1.

Joint Posterior Distribution

The resulting joint posterior distribution of the Texas roughness mixture model had the same form as that of the model used to estimate nationwide data (Equation 4.7). The main difference between these two is given by the use of informative prior parameters. The marginal posterior distributions of the model parameters were estimated from multiple MCMC simulations, implementing the algorithms and converging criteria described in Chapter 2.

Results from Estimated Roughness Model

The Texas roughness model was first estimated assuming homogeneity of effects (complete pooling of observations) and then accounting for group-level heterogeneity of pavement performance through the estimation of a mixture model with multiple clusters. This section covers the reporting and interpretations of the results from the Bayesian estimation of these two model specifications.

Estimation of Model with Complete Pooling of Data

Table 4.9 presents the summary statistics of the marginal posterior distributions of the Texas model estimated with complete pooling of observations. The converging MCMC chains were 50,000-iteration long, had a "burn-in" phase of 25,000 observations, and a thinning interval of 5 iterations. In addition, the DIC value computed from the estimated deviance distribution was equal to 202.8.

Table 4.9. Summary statistics of posterior marginal distributions for the Texas model parameters with complete pooling.

Parameter	Mean	Std	2.5%	Median	97.5%
β_0	-6.66E+00	1.08E+00	-8.84E+00	-6.69E+00	-4.54E+00
β_{Ty5}	7.90E-01	5.99E-01	-3.89E-01	7.89E-01	1.96E+00
β_{Ty6}	7.05E-01	6.93E-01	-6.38E-01	7.01E-01	2.12E+00
β_{Tmp}	2.58E-02	1.37E-01	-2.94E-01	4.17E-02	2.54E-01
β_{Prp}	-2.84E-03	1.78E-03	-6.52E-03	-2.72E-03	4.12E-04
β_{ESAL}	-4.44E-01	1.74E-01	-7.69E-01	-4.50E-01	-6.90E-02
β_{PM}	-1.00E+00	5.68E-01	-2.05E+00	-1.04E+00	1.54E-01
σ^2	7.01E-02	3.13E-03	6.42E-02	6.99E-02	7.65E-02
Deviance	1.78E+02	5.47E+00	1.69E+02	1.78E+02	1.91E+02

The effect of cumulated traffic on the increment of roughness was statistically significant and negative; i.e., the increment of IRI value decreased with cumulated traffic, as observed from the estimated models using AASHO and LTPP data. In addition, the probability of the parameter β_{PM} being equal to or greater than zero, given the observed LTPP and TxDOT data, was less than 0.05; therefore, the effect of applying a PM treatment on the increment of IRI value was statistically significant with more than 95% confidence. The predicted increment of IRI value was, on average, 37% smaller for those pavements that received a PM treatment.

The sign of the estimated parameters related to the pavement type show that the increment of IRI value between data collection dates was larger for thinner pavements, as expected. However, the difference in effect for thin and intermediate pavements was not statistically significant in relation to thicker pavements and when compared among each other. Lastly, neither of the two climatic variables presented a statistically significant effect for the model specified with complete pooling of data.

Estimation of Model with Multiple Clusters

The Texas mixture model was estimated for a different number of clusters in order to evaluate the gain in model fit while accounting for the increasing number of parameters. The DIC values for the models with two and three clusters were -537.2 and -573.0, respectively; whereas the DIC value for the model with one cluster was equal to 202.8. The significant gain in model fit when clustering the observations shows the significant amount of unobserved heterogeneity present in the data. The number of clusters finally selected for the mixture model specification was three, given the relatively small reduction in DIC value from the model specified with two clusters.

Tables 4.10 shows the summary statistics of the marginal posterior distributions for the parameters of the model estimated with three clusters. As observed from the weights of each cluster, the vast majority of the observations (96%) were assigned to two clusters, and both of these two clusters presented a variance of the model error lower than that generated by the model estimated with complete pooling of the data. Furthermore, the variance of the error assigned to 37% of the observations (Cluster 1) was an order lower, despite the smaller sample size. The estimated weights for the model specified with two clusters were 93% and 7%, and the respective error variances were 2.04E-02 and 7.12E-01.

The parameters on the cumulated traffic variable corresponding to the first and third cluster had a probability of being greater than or equal to zero lower than 0.10 and 0.01, respectively. Therefore, the effect of cumulated traffic was statistically significant (with more than 90% confidence) and negative for 96% of the observations, but was not statistically significant for the remaining 4%. In addition, the increment of roughness for pavements with PM treatments was, on average, 48% smaller than for non-treated pavement surfaces and this difference was statistically significant, with more than 90% confidence.

Lastly, the pavement type and precipitation variables were not statistically significant at explaining the increment of IRI value, whereas temperature was statistically significant and presented a negative effect. These observations are contrary to expectations and are possibly explained by randomness due to unobserved variables, measurement errors, an unbalanced number of observations, and other issues related to the use of field data.

Table 4.10. Summary statistics of posterior marginal distributions for the Texas model parameters with complete pooling.

Parameter	Mean	Std	2.5%	Median	97.5%
β_{0_1}	-5.88E+00	1.04E+00	-7.88E+00	-5.95E+00	-3.80E+00
β_{0_2}	-2.71E+00	1.09E+00	-4.63E+00	-2.78E+00	-3.98E-01
β_{0_3}	1.53E+00	8.55E-01	-1.70E-01	1.53E+00	3.23E+00
β_{Ty5}	-1.17E-01	1.91E-01	-4.90E-01	-1.20E-01	2.67E-01
β_{Ty6}	1.03E-04	2.31E-02	-4.59E-02	-5.42E-04	4.51E-02
β_{Tmp}	-2.39E-01	8.57E-02	-4.31E-01	-2.35E-01	-5.71E-02
β_{Prp}	-3.41E-04	5.26E-04	-1.33E-03	-4.22E-04	7.77E-04
β_{ESAL_1}	-1.61E-01	1.11E-01	-3.70E-01	-1.65E-01	8.97E-02
β_{ESAL_2}	-2.83E-02	2.42E-02	-7.72E-02	-2.81E-02	1.86E-02
β_{ESAL_3}	-5.85E+00	1.28E+00	-8.53E+00	-5.76E+00	-3.56E+00
β_{PM}	-7.44E-01	5.26E-01	-1.80E+00	-7.27E-01	2.93E-01
w_1	37%	6%	26%	36%	51%
w_2	4%	1%	2%	4%	6%
w_3	59%	6%	47%	60%	70%
σ_1^2	3.65E-03	1.07E-03	1.90E-03	3.56E-03	6.08E-03
σ_2^2	1.35E+00	4.66E-01	7.16E-01	1.28E+00	2.57E+00
σ_3^2	3.97E-02	6.02E-03	3.09E-02	3.86E-02	5.51E-02
Deviance	-6.12E+02	8.81E+00	-6.24E+02	-6.13E+02	-5.87E+02

Intraclass Correlation of Texas Mixture Model

The intraclass correlation coefficient (ICC) was calculated for the estimated model in order to measure the expected correlation between observations assigned to the same group. The ICC is calculated as the fraction of the overall variance explained by the variation between clusters, as shown in Equation 4.10. Largely separated clusters result in high ICC values while low ICC values correspond to large overlap between clusters.

$$ICC = \frac{\sigma^2_{\bar{y}_k}}{\sigma^2_{\bar{y}}} = \frac{\sum_k^K w_k(\bar{y}_k - \bar{y})^2}{\sum_k^K w_k[(\bar{y}_k - \bar{y})^2 + \sigma_k^2]} \quad (4.10)$$

where,

ICC: intraclass correlation coefficient

$\sigma^2_{\bar{y}_k}$: variation between clusters

$\sigma^2_{\bar{y}}$: variance of the mixture distribution

$\bar{y}_k$: mean observed value for cluster k

$\bar{y}$: mean observed value for the mixture distribution

Equation 4.11 shows the expression and resulting value for the ICC corresponding to the mixture model with three clusters estimated using field data from both nationwide and Texas pavements. The observed ICC value indicates that 44% of the total variance is explained by the variation between clusters, which suggests a mild correlation for the observations within clusters.

$$ICC_{Texas} = \frac{\sum_k^K w_k\left(E\left[\widehat{\Delta IRI}_k\right] - E\left[\widehat{\Delta IRI}_M\right]\right)^2}{\sum_k^K w_k\left[\left(E\left[\widehat{\Delta IRI}_k\right] - E\left[\widehat{\Delta IRI}_M\right]\right)^2 + \sigma_k^2\right]} = \frac{6.07\text{E}{-02}}{1.39\text{E}{-01}} = 0.44 \quad (4.11)$$

Although this coefficient provides valuable information to measure the overall separation between groups relative to the total variance of the mixture distribution, it is worth noting that even in the case of large overlapping of clusters, the modeling of subpopulations according to heterogeneous performance allows for a deeper understanding of the different factor effects. For instance, the estimation of the mixture model specification may result in two clusters with similar means but different variances. Even though the corresponding ICC value would be low, the estimated individual parameters for the different clusters provide valuable insights for characterizing the hidden heterogeneous subpopulations present in the data.

Chapter 5: Conclusions

This chapter describes the contributions and conclusions from the estimated models and analyses conducted to achieve the objectives of this research, along with recommendations for the implementation of the proposed model specifications in different areas of pavement management.

SUMMARY AND CONCLUDING REMARKS

The present section summarizes the work performed to achieve the two main objectives of this dissertation and discusses possible applications of the investigated methodologies.

Bayesian Estimation of Methodologies for Explaining Group-level Heterogeneity in Pavement Performance Data

The estimation of the different model specifications proposed for explaining group-level heterogeneity of effects in pavement performance data resulted in a significant improvement of the model fit compared to the models specified with complete pooling of the data. This improvement was observed from the estimation of each of the different datasets used, which included both experimental and field data. Enhancements in the modeling and prediction of pavement performance led to a more accurate description of the effect of the factors driving the deterioration of pavements in the network, which facilitates a more successful management of the highway assets.

The improvement in model fit achieved by the Finite Mixture Model specification was much larger than the one obtained by the Hierarchical Mixture Model specification. An important characteristic that explains the superior performance of the former is the way each method assigns the observations to the estimated sub-models: the mixture model specification clusters the data in an unsupervised manner whereas the hierarchical model

specification requires assigning the estimated data into subpopulations according to pre-established criteria. The data-driven segmentation of observational units into sub-models carried out by the estimation of the mixture model specification optimizes the fitting of heterogeneous subpopulations in the data, leading to a better description of the systematic differences in pavement performance response caused by unobserved factors.

The segmenting of observations across pavement sections, or across pavement sections and time, into groups with different performance response offers valuable insights, revealing the unobserved factors that cause the heterogeneity. For instance, the geographical location of a certain cluster of pavements may correlate to specific regions where a particular maintenance practice or material is more commonly applied by local engineers. Once an unobserved factor is found to be significant in explaining the heterogeneity of effects, it can be incorporated in the model specification as an additional explanatory variable. Unfortunately, the large number of relevant factors and interaction effects not captured by the variables available in pavement management databases make it difficult to identify the unobserved causes. The insights provided by the model-based clustering of performance data can also be incorporated into the design of M&R strategies, as the clustering of sections according their deterioration rate allow for identifying pavements in the network with structural deficiencies and taking tailored actions in response.

Estimated Pavement Performance Models Using Experimental Data

A Bayesian mixture model specification as well as a hierarchical specification were estimated and evaluated using experimental data, and the results were compared to those from the estimated model, assuming homogeneity of effects. The basic form of the estimated model was adapted from Prozzi and Madanat (2003) and the data was obtained

from the American Association of State Highway Officials (AASHO) Road Test main factorial design (HRB, 1962); both have been widely used in the literature to demonstrate other modeling methodologies. A slight reduction in the deviance information criterion (DIC) value was observed from the estimation of the model with hierarchical specification compared to the one specified with complete pooling of data—this reduction was significantly large for the mixture model specification, despite the larger number of parameters.

The hierarchical model was specified in order to capture the different damaging effects that environmental factors and traffic characteristics have on two pavement subpopulations: thinner (1 to 3 inches) and thicker (4 to 6 inches) asphalt surface layers. The parameters of the sub-models estimated through partial pooling of data showed that the damaging effects of climatic factors (captured by the Frost Penetration Gradient), as well as the damages related to axle types and load magnitudes, were higher for the population with thinner surface layer. On the other hand, the difference between the effects that the cumulated ESALs had on the pavement deterioration for the subpopulations with thinner or thicker asphalt surface layers was not statistically significant.

The Finite Mixture Model with two clusters estimated using experimental data was specified to capture group-level heterogeneity in pavement performance across sections through the estimation of the varying effects of traffic and baseline parameters. Ceteris paribus, the pavement sections of the AASHO Road Test clustered into the first group, which comprised about 65% of the sections, exhibited a significantly lower deterioration rate. The difference in predicted change in serviceability between the two heterogeneous subpopulations decreased with cumulated traffic. Since all pavement sections in the analyzed dataset were designed and built with the same materials and specifications, unobserved factors that may explain the difference in performance between clusters may

be related to local deficiencies, possibly related to localized differences in subgrade properties or differences in compaction of untreated layers, among others possible explanations.

Estimated Pavement Roughness Mixture Models Using Field Data

The significant improvements achieved by the estimation of the unsupervised model-based clustering of pavement performance using data from a controlled experiment showed the potential of this methodology for pavement management performance models, as the number of unobserved factors in field data at the network level is much greater. In order to implement this methodology in a more practical application, a pavement roughness mixture model specified with variables commonly available in state transportation agencies' pavement management systems (PMS) was estimated using field data from different in-service flexible pavements. The model was first estimated using nationwide data from the LTPP Specific Pavement Study (SPS)-3 experiment and subsequently calibrated for Texas highway conditions by combining nationwide and TxDOT PMIS data.

The number of clusters for each mixture model specification estimated using field data was determined as the smallest number for which the reduction in DIC value was relatively small. The improvement in model fit achieved by the modeling of group-level heterogeneity of effects was significant for all the proposed model specifications. The final number of clusters specified for the nationwide mixture models estimated to explain group-level heterogeneity of effects for the traffic and PM treatment variables were determined as two and four clusters, respectively. The final number of clusters specified for the Texas mixture model to characterize the heterogeneous subpopulations in pavement performance data was determined to be three.

Both clusters of the nationwide roughness mixture model specified to capture group-level heterogeneity in the effects of traffic showed a statistically significant and negative effect. The cluster comprising the majority of observations (73%) captured the cases where roughness developed at a faster rate; i.e., the pavement deteriorated more rapidly. Also, the difference in predicted response between the two clusters of the model increased with cumulated traffic. The results from the estimation of the nationwide mixture model specified to characterize the heterogeneous effect of PM treatments showed that, ceteris paribus, the increment of International Roughness Index (IRI) value for treated surfaces was smaller than for non-treated pavements with a probability of 60%, while the opposite effect was observed with a frequency of only 7%. The observations for which treated surfaces exhibited a slower progression of roughness were further clustered into two almost equally likely subpopulations, one presenting a higher susceptibility to the cumulated traffic variable. The fourth cluster captured the remaining cases, for which the difference in predicted increment of IRI between treated and non-treated surfaces was not statistically significant.

An unobserved factor that potentially explains part of the heterogeneity in PM effectiveness is the pre-existing condition of the surface when the PM treatment was applied. As described in Chapter 2, PM treatments are expected to be more effective at delaying the deterioration of pavements if applied when the pavement is still in good condition. Furthermore, a potential factor to explain the difference in effectiveness between the two clusters for which PM resulted in improved performance is the type of treatment applied. For instance, thin overlays are expected to have a higher effect on performance than chip seals. Incorporating these variables into the model specification are expected to reduce the heterogeneity of effects.

From the estimation of the Texas roughness mixture model, it was observed that the vast majority of observations (96%) were assigned to two clusters, whose estimated models had a variance of error lower than that of the model estimated with complete pooling of the data, despite the smaller sample size. Cumulated traffic was statistically significant and had a negative effect for the two clusters with the majority of data, whereas it was not significant for the third cluster. Examples of unobserved factors that explain, in part, the observed heterogeneous performance not captured by the variables in the model include the mixture design of the asphalt surface layer, the thickness and materials used on the base and sub-base layers, as well as the type of soil present in the subgrade. In addition, the increment of IRI value for treated pavements was, on average, 48% smaller than for non-treated pavements. The remaining variables were not statistically significant or had an effect contrary to expectations, possibly as a consequence of issues related to the estimation of field data, such as measurement errors and unbalanced number observations.

RESEARCH CONTRIBUTIONS

The first objective of this research effort was to investigate Bayesian methodologies to model the heterogeneity of effects in pavement performance data at a group level, focusing on the estimation of Bayesian mixture specifications for the model-based clustering of observations. The second objective was to implement this methodology to estimate a pavement roughness model using field data available in existing pavement management databases. Following are the main contributions from the work carried out for this dissertation:

- Demonstration of the benefits and capabilities of a Bayesian methodology for the unsupervised model-based clustering of pavement performance data.

- Estimation and interpretation of an incremental pavement performance model using data from a controlled experiment implementing two statistical techniques: a Bayesian Hierarchical Model specification and Finite Mixture Model specification.
- Development of a database containing more than twenty years of maintenance and rehabilitation (M&R) work history and performance data of in-service flexible pavements located throughout Texas from the processing and merging of various Texas Department of Transportation (TxDOT) management information systems and other data sources.
- Development of a pavement roughness mixture model estimated using nationwide field data from the Long-Term Pavement Performance (LTPP) experiment that allowed for explaining the group-level heterogeneity of effects for the traffic and preventive maintenance (PM) treatment variables.
- Calibration of the pavement roughness mixture model specified with explanatory variables from the TxDOT Pavement Management Information System (PMIS) plus additional climatic variables, and estimated by combining both the nationwide field data and the developed Texas dataset.
- Model-based assessment of the effectiveness of PM treatments using performance data from in-service flexible pavements.

References

AASHTO (1972) “Interim Guide for Design of Pavement Structures – 1972.” American Association of State Highway and Transportation Officials, Washington, D.C.

AASHTO (1986, 1993) “Guide for Design of Pavement Structures.” American Association of State Highway and Transportation Officials, Washington, D.C.

AASHTO (1989) “Report of the AASHTO Joint Task Force on Rutting.” American Association of State Highway and Transportation Officials, Washington, D.C.

Applied Research Associates (ARA) (2004) *Mechanistic-Empirical Design of New and Rehabilitated Pavement Structures*. National Cooperative Highway Research Program, NCHRP Project 1-37A, National Research Council, Washington, D.C.

Applied Research Associates (ARA) (2008) *Mechanistic-Empirical Pavement Design Guide, Interim Edition: A Manual of Practice*. ISBN Number: 1-56051-423-7.

Archilla, A. (2000) *Development of Rutting Progression Models by Combining Data from Multiple Sources*. Doctoral dissertation. University of California Berkeley, Berkeley, CA.

Archilla, A. and S. M. Madanat (2001) “Estimation of Rutting Models by Combining Data from Different Sources.” *Journal of Transportation Engineering*, (ASCE)0733-947X(2001)127:5(379): 379–389.

Archilla, A. (2006) “Repeated Measurement Data Analysis in Pavement Deterioration Modeling.” *Journal of Infrastructure Systems*, 10.1061/(ASCE)1076-0342(2006)12:3(163): 163–173.

Arguez, A., S. Applequist, R. S. Vose, I. Durre, M. F. Squires, and X. Yin (2012) *NOAA’s 1981–2010 Climate Normals: Methodology of Temperature-related Normals*. National Climatic Data Center Report. Asheville, N.C.

ASCE (2013) "2013 Report Card for America's Infrastructure." American Society of Civil Engineers. Available online at: http://www.infrastructurereportcard.org/ (last accessed on 04/27/15).

ASTM E867 (2012) "Standard Terminology Relating to Vehicle-Pavement Systems." American Society for Testing Materials Standards.

ASTM E1170 (2012) "Standard Practices for Simulating Vehicular Response to Longitudinal Profiles of Traveled Surfaces." American Society for Testing Materials Standards.

ASTM E1703/E1703M-10 (2015) "Standard Test Method for Measuring Rut-Depth of Pavement Surfaces Using a Straightedge." American Society for Testing Materials Standards.

Biehler, A. (2009) "Rough Roads Ahead: Fix Them Now or Pay for Them Later." American Association of State Highway and Transportation Officials, Washington, D.C.

Brooks, S. P. and A. Gelman (1998) "General methods for monitoring convergence of iterative simulations." *Journal of computational and graphical statistics*, 7(4), pp.434-455.

Carey, W. N. and P. E. Irick (1960) "The pavement serviceability – performance concept." Highway Research Board Bulletin 250.

Chen, D. H. (2003) "Effectiveness of Preventative Maintenance Treatments Using Fourteen SPS-3 Sites in Texas." *Journal of Performance of Constructed Facilities*, 17(3), 136–143.

Chib, S. and E. Greenberg (1995) "Understanding the Metropolis-Hastings Algorithm." *The American Statistician*, vol. 49, no. 4, pp. 327-335.

Chu, C. and P. Durango-Cohen (2008) "Empirical Comparison of Statistical Pavement Performance Models." *Journal of Infrastructure Systems*, 10.1061/(ASCE)1076-0342(2008)14:2(138): 138–149.

Cowles, M. K. and B. P. Carlin (1996) "Markov chain Monte Carlo convergence diagnostics: a comparative review." *Journal of the American Statistical Association*, 91(434), pp.883-904.

Do, K. A., P. Müller, and F. Tang (2005). "A Bayesian mixture model for differential gene expression." *Journal of the Royal Statistical Society: Series C (Applied Statistics)*, 54(3), pp.627-644.

Elkins, G. E., P. Schmalzer, T. Thompson, and A. Simpson (2003) *Long-Term Pavement Performance Information Management System, Pavement Performance Database User Guide*. Report No. FHWA-RD-03-088. Federal Highway Administration, Office of Infrastructure Research and Development, Washington, D.C.

Eltahan, A., J. Daleiden, and A. Simpson (1999) "Effectiveness of Maintenance Treatments of Flexible Pavements." *Transportation Research Record,* 1680: 18–25.

Face Technologies (n.d.) "Dipstick Road Profiler." Available online at: http://www.dipstick.com/road-profiler-info/ (last accessed on 04/27/16).

Federal Highway Administration (FHWA) (1999) "Asset Management Primer." Federal Highway Administration's Office of Asset Management, Washington, D.C.

Flintsch, G. W. and K. K. McGhee (2009) "Quality management of pavement condition data collection." National Cooperative Highway Research Program (NCHRP) Synthesis 401, Washington, D.C.

Garcia-Diaz, A. and M. Riggins (1984) "Serviceability and distress methodology for predicting pavement performance." *Transportation Research Record,* 997: 56–61.

Gelman, A. and D. B. Rubin (1992) "Inference from iterative simulation using multiple sequences." *Statistical science*, pp.457-472.

Gelman, A., J. B. Carlin, H. S. Stern, and D. B. Rubin (2014) *Bayesian data analysis.* Second Edition. Boca Raton, FL, USA: Chapman & Hall/CRC.

Gendreau, M. and P. Soriano (1998) "Airport pavement management systems: An appraisal of existing methodologies." *Transportation Research Part A: Policy and Practice*, 32(3): 197–214.

Gillespie, T. D., M. W. Sayers, and L. Segel (1980) "Calibration of response-type road roughness measuring systems." National Cooperative Highway Research Program Report, No. 228, Washington, D.C.

Guerre, J., J. Groeger, S. Van Hecke, A. Simpson, G. Rada, and B. Visintine (2012) "Improving FHWA's Ability to Assess Highway Infrastructure Health – Pilot Study Report." FHWA-HIF-12-049. Federal Highway Administration, Washington, D.C.

Haas, R. and W. R. Hudson (1978) "Pavement management systems." McGraw-Hill, New York, NY.

Haas, R., W. R. Hudson, and J. P. Zaniewski (1994) "Modern pavement management." Krieger Publishing Company, Malabar, FL.

Haider, S. and M. Dwaikat (2011) "Estimating Optimum Timing for Preventive Maintenance Treatment to Mitigate Pavement Roughness." *Transportation Research Record,* 2235: 43–53.

Hall, K. and C. Muñoz (1999) "Estimation of present serviceability index from international roughness index." *Transportation Research Record*, 1655: 93–99.

Hall, K., C. Correa, and A. Simpson (2003) "Performance of Flexible Pavement Maintenance Treatments in the Long-Term Pavement Performance SPS-3 Experiment." *Transportation Research Record*, 1823: 47–54.

Hastings, W. K. (1970) "Monte Carlo Sampling Methods Using Markov Chains and Their Applications." *Biometrika*, 57, 97-109.

Highway Research Board (HRB) (1962) "The AASHO Road Test." Special Report No. 61A – E, Highway Research Board National Academy of Science, National Research Council, Washington, D.C.

Hong, F. and J. A. Prozzi (2006) "Estimation of Pavement Performance Deterioration Using Bayesian Approach." *Journal of Infrastructure Systems*, 12(2): 77–86.

Hong, F. and J. A. Prozzi (2010) "Roughness Model Accounting for Heterogeneity Based on In-Service Pavement Performance Data." *Journal of Transportation Engineering*, 10.1061/(ASCE) 0733-947X(2010)136:3(205): 205–213.

Hong, F. and J. A. Prozzi (2014) "Pavement Deterioration Model Incorporating Unobserved Heterogeneity for Optimal Life-Cycle Rehabilitation Policy." *Journal of Infrastructure Systems*, 10.1061.

Horne, W. B. and R. C. Dreher (1963) "Phenomena of pneumatic tire hydroplaning." NASA TN D-2056, National Aeronautics and Space Administration, Washington, D.C.

Huang, Y. H. (1993) "Pavement analysis and design." Prentice-Hall, Englewood Cliffs, NJ.

Huang, Y., P. Hempel, and T. Copenhaver (2009) *A Rut Measurement System Based on Continuous Transverse Profiles from a 3-D*. Research and Development Project Report. Texas Department of Transportation. Austin, TX.

Hudson, W. R., R. Haas, and W. Uddin (1997) "Infrastructure Management: Integrating Design, Construction, Maintenance, Rehabilitation, and Renovation." McGraw-Hill. ISBN 0070308950.

Henderson, J. and O. Lemon (2008) "Mixture model POMDPs for efficient handling of uncertainty in dialogue management." *Proceedings of the 46th Annual Meeting of*

the Association for Computational Linguistics on Human Language Technologies: Short Papers (pp. 73-76). Association for Computational Linguistics.

Jedidi, K., H. S. Jagpal, and W. S. DeSarbo (1997). "Finite-mixture structural equation models for response-based segmentation and unobserved heterogeneity." *Marketing Science*, 16(1), pp.39-59.

Knaus, J. (2015) *snowfall: Easier cluster computing (based on snow)*. R package version 1.84-6.1. https://CRAN.R-project.org/package=snowfall

Laurent, J., J. F. Hébert, D. Lefebvre, and Y. Savard (2012) "3D laser road profiling for the automated measurement of road surface conditions and geometry." 7th RILEM Int. Conf. on Cracking in Pavements, Springer, Netherlands.

Li, H. and K. Yamanishi (2003) "Topic analysis using a finite mixture model." *Information processing & management*, 39(4), pp.521-541.

Li, Z. (2005) *A Probabilistic and Adaptive Approach to Modeling Performance of Pavement Infrastructure*. Doctoral Thesis. Department of Civil, Architectural, and Environmental Engineering, The University of Texas at Austin, Austin, TX.

Lunn, D., D. Spiegelhalter, A. Thomas, and N. Best (2009) "The BUGS project: Evolution, critique and future directions." *Statistics in medicine*, 28(25), pp.3049-3067.

Luo, Z. and Y. Chou (2006) "Pavement condition prediction using clusterwise regression." *Transportation Research Record,* 1974: 70–77.

Luo, Z. and H. Yin (2008) "Probabilistic analysis of pavement distress ratings with the clusterwise regression method." *Transportation Research Record,* 2084: 38–46.

LTPP InfoPave (2015) "Standard Data Release." Available online at: http://www.infopave.com/Data/StandardDataRelease/ (last accessed on 07/15/15).

Madanat, S. M., S. Bulusu, and A. Mahmoud (1995) "Estimation of infrastructure distress initiation and progression models." *Journal of Infrastructure Systems*, 1(3): 146–150.

Madanat, S. M., M. Karlaftis, and P. McCarthy (1997) "Probabilistic infrastructure deterioration models with panel data." *Journal of Infrastructure Systems*, 10.1061/(ASCE)1076-0342(1997)3:1(4): 4–9.

McGhee, K. H. (2004) "Automated Pavement Distress Collection Techniques." Transportation Research Board. National Cooperative Highway Research Program (NCHRP) Synthesis 334. Washington, D.C.

McLachlan, G. and D. Peel (2004). *Finite mixture models*. John Wiley & Sons.

Metropolis, N., A. W. Rosenbluth, M. N. Rosenbluth, A. H. Teller, and E. Teller (1953) "Equation of state calculations by fast computing machines." *The journal of chemical physics*, 21(6), pp.1087-1092.

Miller, J. S. and W. Y. Bellinger (2003) "Distress Identification Manual for the Long-term Pavement Performance Program." Fourth Revised Edition, FHWA-RD-03-031, Office of Infrastructure Research and Development, Federal Highway Administration.

Morian, D. A., S. D. Gibson, and J. A. Epps (1998) "Maintaining Flexible Pavements – The Long-Term Pavement Performance Experiment SPS-3 5-Year Data Analysis." Report No. FHWA-RD-97-102. Federal Highway Administration, Office of Infrastructure Research and Development, Washington, D.C.

Morian, D. A., G. Wang, D. Frith, and J. B. Reiter (2011) "Analysis of Completed Monitoring Data for SPS-3 Experiment." Transportation Research Board 90th Annual Meeting, Washington, D.C.

Ng, M. W., Z. Zhang, and S. T. Waller (2011) "The Price of Uncertainty in Pavement Infrastructure Management Planning: An Integer Programing Approach." *Transportation Research Part C: Emerging Technologies*, 19(6): 1326–1338.

National Oceanic and Atmospheric Administration (NOAA) (2016) *1981-2010 U.S. Climate Normals*, Database [ftp://ftp.ncdc.noaa.gov/pub/data/normals/1981-2010/]. Accessed on 01/22/2016

O'Brien, L. G. (1989) "Evolution and benefits of preventive maintenance strategies." Transportation Research Board. National Cooperative Highway Research Program (NCHRP) Synthesis 153. Washington, D.C.

Onar, A., F. Thomas, B. Choubane, and T. Byron (2006) "Statistical mixed effects models for evaluation and prediction of accelerated pavement testing results." *Journal of Transportation Engineering*, 10.1061/(ASCE)0733-947X (2006)132:10(771): 771–780.

Orthmeyer, R. (2007) "States Take a Smoother Route." *Roads & Bridges*, 45(8).

Paterson, W. D. O. (1987) "Road deterioration and maintenance effects: models for planning and management." The Highway Design and Maintenance Series, The John Hopkins University Press, Baltimore, Maryland.

Pederson, N. J. (2007) "Pavement Lessons Learned from the AASHO Road Test and Performance of the Interstate Highway System." *Transportation Research Circular E-C118*. Transportation Research Board, Washington D.C.

Peng, B., Y. Jiang, and Y. Pu (2015) "Review on Automatic Pavement Crack Image Recognition Algorithms." *Journal of Highway and Transportation Research and Development (English Ed.)*, 10.1061/JHTRCQ.0000435: 13–20.

Peshkin, D. G., T. E. Hoerner, and K. A. Zimmerman (2004) "Optimal timing of pavement preventive maintenance treatment applications." National Cooperative Highway Research Program (NCHRP) Report 523. Washington, D.C.

Pierce, L. M., M. Fisher, and S. Aref (2012) "Field Validation of Procedures for Collecting Images of Pavement Surfaces for Distress Detection and for Transverse Pavement Profile Data Collection." *Unpublished*.

Plummer, M., N. Best, K. Cowles, and K. Vines (2006) "CODA: Convergence Diagnosis and Output Analysis for MCMC." *R News*, vol 6, 7-11

Prozzi, J. A. and S. M. Madanat (2000) "Analysis of Experimental Pavement Failure Data using Stochastic Duration Models." *Transportation Research Record,* 1699.

Prozzi, J. A. (2001) *Modeling Pavement Performance by Combining Field and Experimental Data*. Doctoral Dissertation. University of California, Berkeley, CA.

Prozzi, J. A. and S. M. Madanat (2003) "Incremental Nonlinear Model for Predicting Pavement Serviceability." *Journal of Transportation Engineering*, 129(6): 635–641.

Prozzi, J. A. and S. M. Madanat (2004) "Development of Pavement Performance Models by Combining Experimental and Field Data." *Journal of Infrastructure Systems*, Vol. 10, No. 1, March 1.

Proïa, F., A. Pernet, T. Thouroude, G. Michel, and J. Clotault (2016) "On the characterization of flowering curves using Gaussian mixture models." *Journal of theoretical biology*, 402, pp.75-88.

Queiroz, C., R. Haas, and Y. Cai (1994) "National economic development and prosperity related to paved road infrastructure." *Transportation Research Record,* 1455. ISSN: 0361-1981.

R Core Team (2016) "R: A language and environment for statistical computing." R Foundation for Statistical Computing, Vienna, Austria. URL https://www.R-project.org/.

Roberts, F. L., P. S. Kandhal, E. R. Brown, D. Y. Lee, and T. W. Kennedy (1996) "Hot Mix Asphalt Materials, Mixture Design and Construction." Second edition, National Asphalt Pavement Association Research and Education Foundation, Lanham, MD.

Roberts, G.O., A. Gelman & W. R. Gilks (1997) "Weak Convergence and Optimal Scaling of Random Walk Metropolis Algorithms." *The Annals of Applied Probability*, vol. 7, no. 1, pp. 110-120.

Saliminejad, S. and N. Gharaibeh (2013) "Impact of Error in Pavement Condition Data on the Output of Network-Level Pavement Management Systems." *Transportation Research Record: Journal of the Transportation Research Board*, (2366), pp.110-119. Washington, D.C.

Sayers, M. W., T. D. Gillespie, and C. A. V. Queiroz (1986) "The international road riding quality experiment: Establishing correlation and a calibration standard for measurements." Technical Paper 45, World Bank, Washington, D.C.

Sayers, M. W. and S. M. Karamihas (1998) "The little book of profiling." Transportation Research Institute, University of Michigan.

Serigos, P. A., M. R. Murphy, and J. A. Prozzi (2014a) "Evaluation of Rut-Depth Accuracy and Precision Using Different Automated Measurement Systems." *Journal of Testing and Evaluation,* 43, No. 1: 149–158.

Serigos, P. A., P. Karki, Z. Zhang, and J.A. Prozzi (2014b) "Impact of Upgrading Distress Measurement System on Assessed Pavement Network Condition*", 93rd Annual Meeting of Transportation Research Board Compendium of Papers*, Washington, D.C.

Serigos, P. A., K. Chen, A. de Fortier Smit, M. R. Murphy, and J. A. Prozzi (2015) "Automated Distress Surveys: Analysis of Network Level Data (Phase III)." Report No. FHWA/TX-15/0-6663-3. Center for Transportation Research, Austin, Texas.

Serigos, P. A., J. A. Prozzi, A. de Fortier Smit, and M. R. Murphy (2016a) "Evaluation of 3-D Automated Systems for the Measurement of Pavement Surface Cracking." *Journal of Transportation Engineering*, 05016003.

Serigos, P. A., M. Y. Kim, and P. Buddhavarapu (2016b) "Assessment of the Effectiveness of Preventive Maintenance Treatments on Flexible Pavement using Censored Regression", Second Place winner paper in the Graduate Category of the Fifteenth

International Contest on LTPP Data Analysis. Accepted for publication by the FHWA. *In press*

Shahin, M. Y. and S. D. Kohn (1979) "Development of a pavement condition rating procedure for roads, streets, and parking lots." Technical Report. Construction Engineering Research Laboratory. Springfield, VA.

Shirazi, H., R. L. Carvalho, M. Ayres Jr., and O. I. Selezneva (2010) "Statistical Analysis of LTPP SPS-3 Experiment on Preventive Maintenance of Flexible Pavements." First International Conference on Pavement Preservation, Newport Beach, CA.

Simpson, A. L. (2001) *Measuring of Rutting in Asphalt Pavements*. Doctoral Thesis. Department of Civil, Architectural, and Environmental Engineering, The University of Texas at Austin, Austin, TX.

Small, K. A. and C. Winston (1988) "Optimal highway durability." *American Economic Review*, 78(3): 560–569.

Smadi, O. (2004) "Quantifying the benefits of pavement management." 6th International Conference on Managing Pavements: The Lessons, the Challenges, the Way Ahead. Conference Proceedings. Brisbane, Queensland, Australia.

Smith, R. E., M. I. Darter, and S.M. Herrin (1979) "Highway Pavement Distress Identification Manual." FHWA-RD-79-66. Federal Highway Administration, Washington, D.C.

Spiegelhalter, D. J., N. G. Best, B. P. Carlin, and A. Van Der Linde (2002) "Bayesian Measures of Model Complexity and Fit", *Journal of the Royal Statistical Society. Series B (Statistical Methodology)*, vol. 64, no. 4, pp. 583-639.

Stampley, B. E., B. Miller, R. E. Smith, and T. Scullion (1995) "Pavement Management Information System Concepts, Equations, and Analysis Models." Texas Department of Transportation Report No. TX-96-1989-1.

Texas Department of Transportation (TxDOT) (2009) "Pavement Management Information System Rater's Manual FY 2010." Texas Department of Transportation, Austin, Texas.

Texas Department of Transportation (TxDOT) (2014a) "Pocket Facts." Accessed on https://ftp.dot.state.tx.us/pub/txdot-info/gpa/pocket_facts.pdf (last accessed on 06/07/16).

Texas Department of Transportation (TxDOT) (2014b) *Standard Specifications for Construction and Maintenance of Highways, Streets, and Bridges*. Maintenance Division. Austin, Texas.

Texas Department of Transportation (TxDOT) (2016). *Statewide Planning Map*. Accessed on 01/22/2016. http://www.txdot.gov/inside-txdot/division/transportation-planning/maps/statewide-planning.html.

Timm, D. H. and J. M. McQueen (2004) "A study of manual vs. automated pavement condition surveys." Auburn University, Auburn, AL.

Timm, D. H., S. Tisdale, and R. Turochy (2005) "Axle Load Spectra Characterization by Mixed Distribution Modeling." *Journal of Transportation Engineering*, 10.1061/(ASCE)0733-947X(2005)131:2(83), 83-88.

Wang, K. C. P. (2000) "Designs and Implementations of Automated Systems for Pavement Surface Distress Survey." *Journal of Infrastructure Systems*, ASCE, Vol. 6, No.1.

Wang, K. C. P. (2011) "Elements of automated survey of pavements and a 3D methodology." *Journal of Modern Transportation*, 19(1): 51–57.

Wang, K.C. and O. Smadi (2011) "Automated imaging technologies for pavement distress surveys." *Transportation Research E-Circular E-C156*. Transportation Research Board, Washington, D.C.

Wang, K. C. P., Q. J. Li, G. Yang, Y. Zhan, and Y. Qiu (2015) "Network level pavement evaluation with 1 mm 3D survey system." *Journal of Traffic and Transportation Engineering (English Edition)*, 2(6): 391–398.

Wedel, M. and W. A. Kamakura (2012) *Market segmentation: Conceptual and methodological foundations* (Vol. 8). Springer Science & Business Media.

Wix, R. and R. Leschinski (2012) "Cracking – a Tale of Four Systems." 25th ARRB Conference – Shaping the Future: Linking Policy, Research and Outcomes, Perth, Australia.

Yoder, E. J. and M. W. Witczak (1975) "Principles of pavement design." Second Edition, John Wiley & Sons.

Zaniewski, J. P. and B. C. Butler (1985) "Vehicle Operating Costs Related to Operating Mode, Road Design, and Pavement Condition." *Measuring Road Roughness and Its Effects on User Cost and Comfort*, ASTM STP 884: 127–142. American Society for Testing and Materials, Philadelphia, PA.

Zhang, W. and P. Durango-Cohen (2014) "Explaining Heterogeneity in Pavement Deterioration: Clusterwise Linear Regression Model." *Journal of Infrastructure Systems*, 10.1061/(ASCE)IS.1943-555X.0000182, 04014005.

Zhang, Z., W. R. Hudson, and R. Haas (1999) "Applied Asset Management." Chapters 1 to 4. Unpublished manuscript. Copyright 1999 by the authors.